

RECEPTOR FOR ADVANCED GLYCATION END-PRODUCTS: EXPRESSION AND
SIGNALING

by

Julia V. Gefter

MD in Biophysics, 2nd Moscow Medical Institute (Pirogov's)

Submitted to the Graduate Faculty of the
School of Medicine in partial fulfillment
of the requirements for the degree of
Doctor of Philosophy

University of Pittsburgh

[2009]

UNIVERSITY OF PITTSBURGH

SCHOOL OF MEDICINE

This dissertation was presented

by

Julia V. Gefter

It was defended on

May 12, 2009

and approved by

Dr. Robert Bowser

Dr. Mitchell P. Fink

Dr. Yoram Vodovotz

Committee Chair: Dr. Tim Oury

Dissertation Advisor: Dr. Russell L. Delude

© by Julia V. Geftter

2009

ASSESSMENT OF THE ANTI-INFLAMMATORY EFFECTS OF ENONE-CONTAINING COMPOUNDS IN THE CELL-BASED NF- κ B REPORTER SYSTEM.

ASSESSMENT OF THE TISSUE- AND CELL-SPECIFIC EXPRESSION AND SIGNALING OF RECEPTOR FOR ADVANCED GLYCATION END-PRODUCTS

Julia V. Gefter, M.D.

The NF- κ B transcription factor family plays a central role in many aspects of the immune response, and activation of this family of transcription factors has been shown to trigger many disease processes. Thus, the ability to modulate NF- κ B activity may be an attractive way to treat these diseases. We used an *in vitro* cell-based assay to test potential NF- κ B inhibitors by measuring their effect on IL-1 β -induced expression of the NF- κ B dependent intracellular adhesion molecule-1 (ICAM-1, CD54). We tested ethyl pyruvate, a novel anti-inflammatory drug candidate, and the ability of related compounds to block activation of NF- κ B activity by measuring the expression of CD54 on U373 cells exposed to IL-1 β . 4-hydroxyphenylpyruvic acid was the best inhibitor of CD54 upregulation. These studies show the ease of using an endogenous reporter gene (i.e., CD54) and FACS analysis to rapidly characterize the relative efficacy of pharmacologic inhibitors. A second completely unrelated topic of the dissertation dealt with the receptor for advanced glycation end-products (RAGE). RAGE is thought to be important in a variety of pathological conditions, including diabetes, sepsis, atherosclerosis, renal diseases, hypertension and Alzheimer's disease. However, RAGE proximal signaling events are still unclear. We were able to establish that original RAGE, sequenced from bovine lung, is only present in the lung. This observation was based on antibody specificity, Northern blotting and N-glycosylation analysis. One of the antibodies that we used (H-300, Santa Cruz, CA) was very selective for lung RAGE and not cross-react with other RAGE isoforms. Only lung RAGE had a transcript size of 1.4 kb as determined by Northern blot and only lung RAGE was N-

glycosylated. Non-lung tissues and cell lines appeared to express their own unique RAGE isoforms. In addition, we established that previously described endogenous soluble RAGE (esRAGE) does not contain any of the canonical RAGE epitopes, but includes sequence encoded in intron 9. Signaling studies with pro-inflammatory stimuli in mouse lung slices of wild-type and knockout mice revealed the importance of RAGE in LPS and IL-1 β -induced inflammatory response, but not when reported RAGE ligands, including AGEs, HMGB1 and S100B, were applied.

TABLE OF CONTENTS

PREFACE.....	XV
1.0 INTRODUCTION.....	1
1.1 SCREENING OF ANTI-INFLAMMATORY PROPERTIES OF ENONE CONTAINING COMPOUNDS	2
1.1.1 The NF-κB pathway in inflammation.....	2
1.1.2 The enone moiety may react with the thiol groups of NF-κB.....	4
1.2 RECEPTOR FOR ADVANCED GLYCATION END PRODUCTS (RAGE).....	6
1.2.1 RAGE tissue-specific expression	9
1.2.2 RAGE isoforms	10
1.2.3 RAGE signaling in cell physiology	14
1.2.4 Role of RAGE in inflammatory cell recruitment	17
1.2.5 RAGE studies in animals	18
1.2.6 The role of sRAGE in disease	19
1.3 SUMMARY AND CONCLUSIONS	20
2.0 CHAPTER TWO – USING <i>IN VITRO</i> CELL-BASED SYSTEMS TO ASSAY ENONE-CONTAINING ANTI-INFLAMMATORY DRUGS.....	22
2.1 ABSTRACT.....	22

2.2	RESULTS	23
2.2.1	Establishing a cell-based U373 reporter cell line to screen compounds for NF-κB inhibitory activity	23
2.2.2	Using the clonal U373 human astrocytoma cell line in the screening of the enone-containing compounds	25
2.2.3	Using RAW 264.7 murine macrophage-like cell line for further testing the enone-containing compounds	27
2.2.4	pHPP inhibited LPS-induced IL-6 secretion in LPS-stimulated RAW 264.7 cells	29
2.3	DISCUSSION	30
3.0	CHAPTER THREE - COMPARISON OF DISTINCT PROTEIN ISOFORMS OF THE RECEPTOR FOR ADVANCED GLYCATION END-PRODUCTS EXPRESSED IN TISSUES AND CELL LINES	33
3.1	ABSTRACT	33
3.2	RESULTS	34
3.2.1	<i>In silico</i> analysis of RAGE mRNA expression	34
3.2.2	Northern blot analysis of RAGE isoforms expression	36
3.2.3	H-300 and N-16 recognize distinct RAGE epitopes that are only present together in RAGE protein isoforms expressed in lung	37
3.2.4	Mouse lung RAGE isoforms	40
3.2.5	RAGE isoforms in mouse cell lines	43
3.2.6	Protein N-glycosylation of RAGE protein isoforms	44

3.2.7	Non-pulmonary cells transfected with the lung RAGE cDNA express and N-glycosylate the canonical pulmonary membrane RAGE protein isoform	46
3.2.8	Pulmonary cell lines transfected with full-length RAGE express mRNA but no detectable protein	46
3.2.9	Lung RAGE is N-glycosylated in mouse, human, rat and cow	47
3.2.10	Mouse thyroid expresses the same RAGE isoforms as lungs	48
3.3	DISCUSSION	49
4.0	CHAPTER FOUR – RESPONSE TO THE RAGE LIGANDS IN VARIOUS TISSUES AND CELL LINES.....	57
4.1	ABSTRACT.....	57
4.2	RESULTS	58
4.2.1	“RAGE” ligands do not activate NF- κ B in A549, HMEC-1 and HMEC-1 transfected with the full-length RAGE	58
4.2.2	“RAGE” ligands alter MCP-1 mRNA expression in the HMEC-1 cell line: S100B induces and HMGB1 suppresses it	59
4.2.3	Anti-RAGE antibody (N-16) inhibits MCP-1 upregulation by post-induction repression.....	60
4.2.4	“RAGE” ligands failed to stimulate A549 and HEK 293 cell lines.....	61
4.2.5	“RAGE” ligands fail to stimulate mouse lung slices (MLS), but RAGE is important in the inflammatory response to LPS and IL-1 β	62
4.2.6	Mouse lung slices from RAGE knockout mice express less IL-6 and MCP-1 mRNA after LPS stimulation.....	63
4.3	DISCUSSION.....	65

5.0	CHAPTER FIVE – SUMMARY AND CONCLUSIONS	68
6.0	CHAPTER SIX – FUTURE DIRECTIONS.....	75
6.1	‘CANONICAL’ RAGE EXPRESSION MECHANISMS.....	75
6.1.1	Lung-derived cell lines cannot express canonical RAGE	75
6.1.2	Identifying RAGE isoform mRNA via Northern blot and cDNA library screening	79
6.1.3	Utilizing primary type 1 alveolar cell lines from wild-type and RAGE knockout mice to characterize cell line RAGE.....	80
6.1.4	Lung and thyroid specific transcription factors could drive canonical RAGE mRNA expression	81
6.1.5	Determine X-RAGE sequence	83
6.2	RAGE SIGNALING.....	84
6.2.1	RAGE ligand signaling in cell lines.....	84
6.2.2	Canonical RAGE signaling in MLS.....	85
7.0	CHAPTER SEVEN - MATERIALS AND METHODS	88
7.1	REAGENTS	88
7.2	CELL LINES	88
7.3	CELL-BASED ASSAY FOR STUDYING THE RELATIVE PHARMACOLOGY OF THE ANTI-INFLAMMATORY DRUGS.....	90
7.4	TESTED COMPOUNDS	91
7.5	FLOW CYTOMETRY ANALYSIS	91
7.6	PHARMACOLOGIC ANALYSIS USING FACS ANALYSIS	92
7.7	PROTEIN N-GLYCAN REMOVAL.....	92

7.8	WESTERN BLOTTING.....	93
7.9	ANIMAL AND HUMAN TISSUES.....	94
7.10	MOUSE LUNG SLICES.....	95
7.11	PRIMARY LUNG CELL CULTURE.....	95
7.12	NORTHERN BLOT ANALYSIS.....	96
7.13	PURIFICATION AND MASS SPECTRAL ANALYSIS OF MOUSE LUNG RAGE ISOFORMS.....	97
7.14	REAL-TIME REVERSE TRANSCRIPTASE-PCR ANALYSIS.....	98
7.15	ANALYSIS OF MOUSE CYTOKINE MRNAS.....	99
7.16	ELECTROPHORETIC MOBILITY SHIFT ASSAY (EMSA).....	99
	APPENDIX A.....	101
	APPENDIX B.....	102
	APPENDIX C.....	104
	BIBLIOGRAPHY.....	106

LIST OF TABLES

Table 1. Splice map of different RAGE variants detected in human lung and human primary aortic smooth muscle cells (AoSMC) cDNA.....	12
Table 2. Relative number of EST clones per million identified in tissue and species-specific databases (129). Table was last updated on 10/06/08.....	35

LIST OF FIGURES

Figure 1. Schematic representation of NF- κ B activation.....	3
Figure 2. Hypothetical reaction of ethacrynic acid with sulfhydryl groups to form a thiol adduct (23).....	5
Figure 3. Schematic representation of RAGE.....	8
Figure 4. FACS enriched U373 cell population stimulated with IL-1 β	24
Figure 5. FACS enriched clonal U373 NF- κ B reporter cell lines.	24
Figure 6. Graded IL-1 β -induced CD54 cell surface expression on the bulk sorted population of U373 cells as measured by FACS analysis.....	25
Figure 7. pHPP exhibits the best inhibitory properties on CD54 cell surface expression after IL-1 β stimulation in bulk sorted population of U373 cells.....	26
Figure 8. Effect of graded concentrations of compounds of interest on NO \cdot release by LPS-stimulated RAW 264.7 cells.	28
Figure 9. Real time quantitative RT PCR analysis showing iNOS expression after 18 hour incubation with LPS in the presence of the graded concentrations of the indicated drugs in RAW 264.7 cells.	29
Figure 10. Effect of graded concentrations of compounds of interest on IL-6 by LPS-stimulated RAW 264.7 cells.....	30
Figure 11. Northern blot analysis of mouse tissues and cell lines.....	37

Figure 12. Western blots showing RAGE isoforms expressed in various mouse tissues.....	38
Figure 13. α -esRAGE antibody failed to detect canonical RAGE bands in Western blot analysis but detected numerous bands of various mobilities.....	39
Figure 14. Western blots analysis of mouse pulmonary RAGE isoforms expressed following injection of C57BL6 mice with 2 mg/kg of LPS at the times indicated (time course).....	41
Figure 15. Purification and confirmation that xRAGE is an authentic RAGE isoform.	42
Figure 16. Comparative Western blot analysis of representative established mouse cell lines....	43
Figure 17. Mouse deglycosylation pattern of RAGE isoforms.....	45
Figure 18. Comparative deglycosylation analysis of the mouse lung lysate.	45
Figure 19. Lung-derived cell lines transfected with full-length RAGE do not express canonical RAGE protein.	47
Figure 20. Comparative deglycosylation analysis of human and bovine tissues.....	48
Figure 21. Comparative deglycosylation analysis of RAGE isoforms from mouse thyroid and lung.	49
Figure 22. Cartoon showing positions of the N, H and ES immunogens used to generate the antisera.....	50
Figure 23. NF- κ B activation in sample cell lines.	59
Figure 24. MCP-1 mRNA dose response to increasing concentrations of S100B (A) and HMGB1 (B).	60
Figure 25. Anti-RAGE antibody (N-16) inhibits MCP-1 mRNA upregulation by S100B and IL-1 β (A) as measured by MCP-1 mRNA increase (real time RT-PCR) in HMEC-1 cells.....	61
Figure 26. MCP-1 expression in A549 cells in response to the “RAGE” ligands.....	62

Figure 27. MCP-1 expression in mouse lung slices (MLS) following exposure to pro-inflammatory factors in wild type and RAGE knockout mice.	63
Figure 28. Luminex™ cytokine assay in MLS.	64
Figure 29. Molecular structure of the enone forming compounds (A,B,C) and one compound that does not isomerize to an enone (D).....	1

PREFACE

I'd like to thank my mentor, Russell Delude, for his guidance and understanding and for bringing me as a scientist to the place where I am right now. I learned resilience, patience and honesty, a lot of it. I want to thank my committee, Dr. Oury, Dr. Bowser, Dr. Fink, Dr. Vodovotz, their suggestions made my work so much more interesting. I want to thank Dr. Fink for finding time for me in his busy out of state schedule. I want to thank my family, here and in Russia, for the support they gave me during my time here. My sister and my mother were very supportive. I am glad I managed to impress my daughter Alissa; it is not easy to impress teenagers. Mark was wonderful and very supportive even in the times when I was ready to give up. I also want to thank people in my lab, Meaghan, Hanna, Katie, and everyone who left the lab. I always got help when I needed it. I want to thank Dr. Phillips who always encouraged me. My poodle Duke was always by my side when I was working at home.

1.0 INTRODUCTION

Inflammation is involved in a variety of processes in health and disease. In general, a controlled inflammatory response could be beneficial, but a chronic and/or dysregulated response may be detrimental. An unbalanced response may lead to septic shock, cancer, allergies, and many other detrimental effects (1-3).

In order to manage unbalanced inflammation, more diverse pharmacological approaches offering better targeting and/or specificity are needed. This dissertation consists of several interrelated projects relevant to the mechanisms and treatments of inflammation. Our first focus was on the use of the enone-containing compounds (unsaturated compounds consisting of a conjugated system of an alkene and a ketone) to modulate the inflammatory response. These studies were based on the hypothesis that the enone can modify cysteine residues in NF- κ B, a central inflammation-associated transcription factor. This modification interferes with DNA binding and expression of endogenous NF- κ B-dependent genes. We made use of a clonal astrocytoma cell line to compare efficacy of different enone containing compounds to decrease activation of the endogenous CD54 gene, also known as ICAM-1 (inter-cellular adhesion molecule 1). Our second focus was studying the expression of tissue- and cell line-specific isoforms of the receptor for advanced glycation end-products (RAGE), a protein that is thought to play a role in inflammation. Finally, our third focus was examining several RAGE ligands in signaling experiments in cell lines and in mouse lung slices.

1.1 SCREENING OF ANTI-INFLAMMATORY PROPERTIES OF ENONE CONTAINING COMPOUNDS

1.1.1 The NF- κ B pathway in inflammation

The NF- κ B transcription factor family plays a central role in many aspects of the immune response, and activation of this family of transcription factors has been shown to underlie many disease processes including AIDS, atherosclerosis, asthma, arthritis, cancer, diabetes, inflammatory bowel disease, muscular dystrophy, stroke, and viral infections (4). Thus, the ability to modulate NF- κ B activity is attractive in terms of possible therapeutic approaches. Originally identified as a transcription factor involved in the activation of the κ light chain genes in B lymphocytes (5), NF- κ B is now known to be controlled by over 150 stimuli and to regulate the expression of more than 150 genes (6). Members of the Rel/NF- κ B transcription factor family include p50, p65 (RelA), c-Rel, p52, and RelB, which is represented by multiple splice variants (7). In resting cells, homo- or heterodimeric forms of NF- κ B exist in the cytoplasm in an inactive form due to binding by an inhibitory protein called I κ B (8). Following exposure of cells to an appropriate pro-inflammatory stimulus (e.g., IL-1 β), I κ B is phosphorylated and targeted for ubiquitination and subsequent proteasomal degradation (9, 10) (Fig. 1). Phosphorylation, release, and degradation of I κ B permits translocation of NF- κ B into the nucleus where it can bind to *cis*-acting elements in the promoter regions of various NF- κ B-responsive genes. Different dimer

combinations could serve as transcriptional repressors or activators and have different affinity and specificity for NF- κ B binding sites. p50/p65 heterodimer was studied the most.

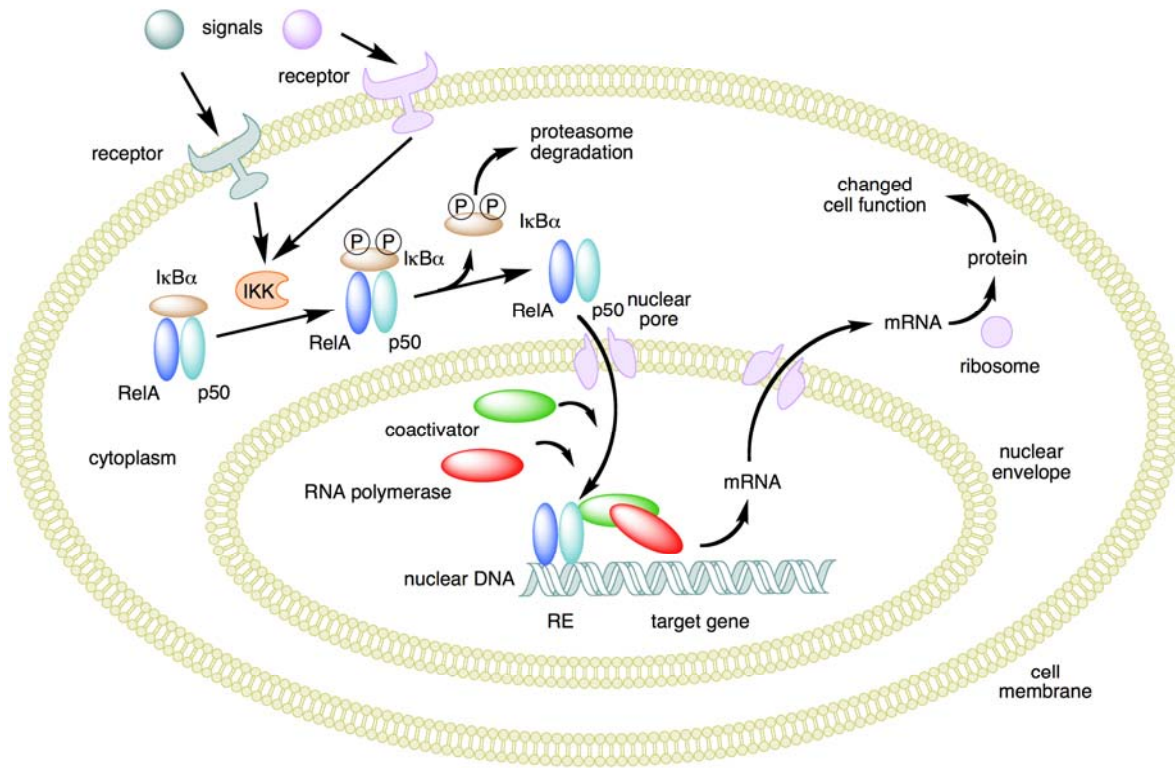


Figure 1. Schematic representation of NF- κ B activation.

In this figure, the NF- κ B heterodimer between RelA and p50 is used as an example. While in an inactive state, NF- κ B is located in the cytosol complexed with the inhibitory protein I κ B α . A variety of extracellular signals can activate the enzyme I κ B kinase (IKK). IKK, in turn, phosphorylates the I κ B α protein, which results in ubiquitination of I κ B α and degradation of I κ B α by the proteasome. Released NF- κ B is then translocated into the nucleus where it binds to specific sequences of DNA called response elements (RE). The DNA/NF- κ B complex then recruits other proteins, such as co-activators and RNA polymerase, which transcribe downstream DNA into mRNA, which, in turn, is translated into protein, resulting in a change of cell function (11).

1.1.2 The enone moiety may react with the thiol groups of NF- κ B

Ethyl pyruvate was first studied as a derivative of sodium pyruvate which has been shown to preserve organ function *in vivo* (12-14). However, sodium pyruvate is unstable in the aqueous solutions forming parapryuvate and pyruvate hydrate (15). Sims *et al.* used the ethyl ester of pyruvic acid, ethyl pyruvate, because it was expected to be more stable in aqueous solution compared to pyruvic acid. Interestingly, ethyl pyruvate was far more protective in a rat intestinal ischemia model when compared to sodium pyruvate (16).

Ethyl pyruvate exhibits anti-inflammatory activity in many *in vitro* and *in vivo* assays. Pyruvic acid and sodium pyruvate, which are structurally similar to ethyl pyruvate, have been reported to scavenge reactive oxygen species (ROS). But Sappington *et al.* showed that even short transient exposure to ethyl pyruvate was enough to provide protection against cytomix-induced hyperpermeability in immunostimulated Caco-2 human enterocyte-like cells. Ethyl pyruvate was washed off the cells extensively several hours before pro-inflammatory stimulation. This would prevent ROS scavenging activity suggesting that other mechanisms exist (17). However, it is still possible that the cells rapidly internalize ethyl pyruvate and it would not be removed by cell washing. Further research is needed to eliminate this possibility.

ROS are considered to be a major cause of intracellular damage associated with inflammatory conditions (18). Glutathione (GST) is an essential tri-peptide with the side chain sulfhydryl residue that protects cells against free radical damage; the GST redox status of the cells is crucial for various biochemical events, including inflammation (19). GST levels have been reported to diminish in response to TNF α and glucocorticoids (dexamethasone) (20). So it is reasonable to suggest that oxidizing drugs like ethyl pyruvate and derivatives would be

inactive in the reducing healthy cell environment with plenty of GST around. But in the inflammation when GST is depleted they would be able to interact with NF-κB. Numerous studies have shown that NF-κB DNA-binding activity is inhibited by oxidizing agents or electrophilic compounds that can react with thiols (21), suggesting that one or more reduced cysteine residues in NF-κB are critical for its activation. Compounds containing the electrophilic “enone” moiety may cause modification of the thiol groups in proteins (22, 23) via a Michael-type addition reaction. This is shown for ethacrynic acid in the following figure:

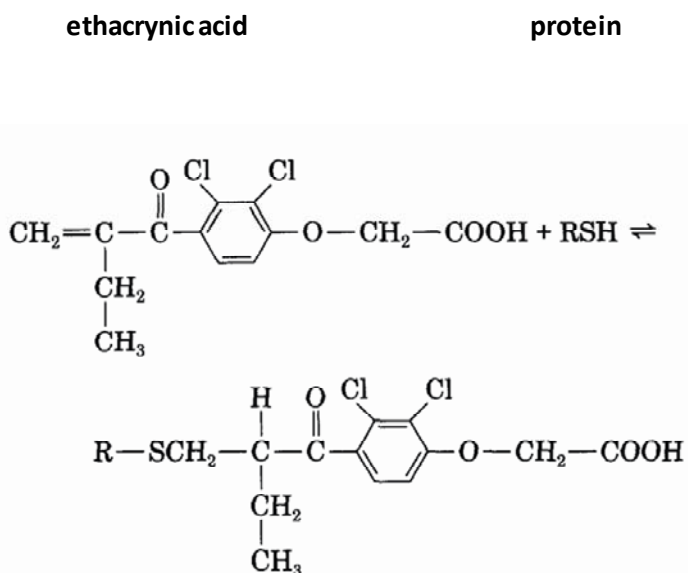


Figure 2. Hypothetical reaction of ethacrynic acid with sulfhydryl groups to form a thiol adduct (23).

This notion is supported by data in a brief report published several years ago by Brennan and colleagues where they show that thiol modifying compounds inhibited NF-κB activation in several cell lines (24). Another group of compound, the sesquiterpene lactones, is known to act this way. They inhibit NF-κB activation by alkylating a critical cysteine residue (Cys³⁸) in the p65 subunit of NF-κB (25-27). Data from our laboratory suggest that ethyl pyruvate can also

inhibit p65 DNA binding by modifying Cys³⁸ (28), and ethacrynic acid can modify Cys³⁸ in p65 and another cysteine-containing residue in p50 (29). Han et al. compared DNA binding of wild-type and mutant p65 (Cys³⁸ → Ser and Cys³⁸ → Ala). Ethyl pyruvate inhibited binding by the wild-type and alanine-substituted p65 mutant; however, it failed to inhibit binding of Cys³⁸ → Ser mutant. Ethyl pyruvate could also inhibit basal p65 DNA binding in unstimulated RAW 264.7 cells which is consistent with interfering with binding itself and not with activation steps of this transcription factor. In addition, ethyl pyruvate did not affect IκBα and IκBβ degradation (28). Thus, it is reasonable to hypothesize that compounds containing an electrophilic enone moiety may modify critical thiol residues in NF-κB.

Therefore, we compared several compounds that contain or lack an enone moiety for their ability to inhibit NF-κB-dependent activation. We chose cell surface expression of the inflammation marker CD54 in U373 astrocytoma cell line as was described before (30). We selected and cloned cells that had minimal basal expression of the marker and maximum expression upon pro-inflammatory stimulation (IL-1β). It is important to realize that actual modification of NF-κB transcription factors by the drugs themselves has not been formally shown.

1.2 RECEPTOR FOR ADVANCED GLYCATION END PRODUCTS (RAGE)

RAGE is involved in promoting recruitment and activation of inflammatory cells (31, 32), cell adhesion and spreading (33), stimulating cell migration (34, 35), and upregulation of pro-inflammatory cytokine production (36). RAGE was first identified as an advanced glycation end-products (AGE) - binding protein present in bovine lung protein extracts (37) which was

subsequently shown to bind a variety of ligands including amyloid- β peptide and β sheet fibrils (38), members of a small Ca^{2+} -binding protein family called S100/calgranulins (39), and HMGB1, a DNA-binding protein (also called amphoterin) (40). The RAGE extracellular domain sequence encodes one “V”-type Ig domain followed by two “C”-type Ig domains (41). RAGE ligands were shown to compete for binding to the V-type Ig domain of RAGE using radioligand-binding assays (39, 42). RAGE has also been shown to be a counter-receptor for the β 2-integrin Mac-1, (CD11b/CD18) mediating leukocyte recruitment and adhesion to sites of inflammation (32). Mac-1 interaction is enhanced by S100B (32) and by HMGB1 (31). These findings emphasize the importance of RAGE during acute inflammatory response involving neutrophil recruitment and activation.

Recently, RAGE was added to the group of pattern-recognition receptors (PRRs), which are expressed by cells to identify pathogen-associated molecular patterns (PAMPs), based on its ability to interact with several classes of molecules, rather than individual ligands, and to amplify the inflammatory response (43, 44).

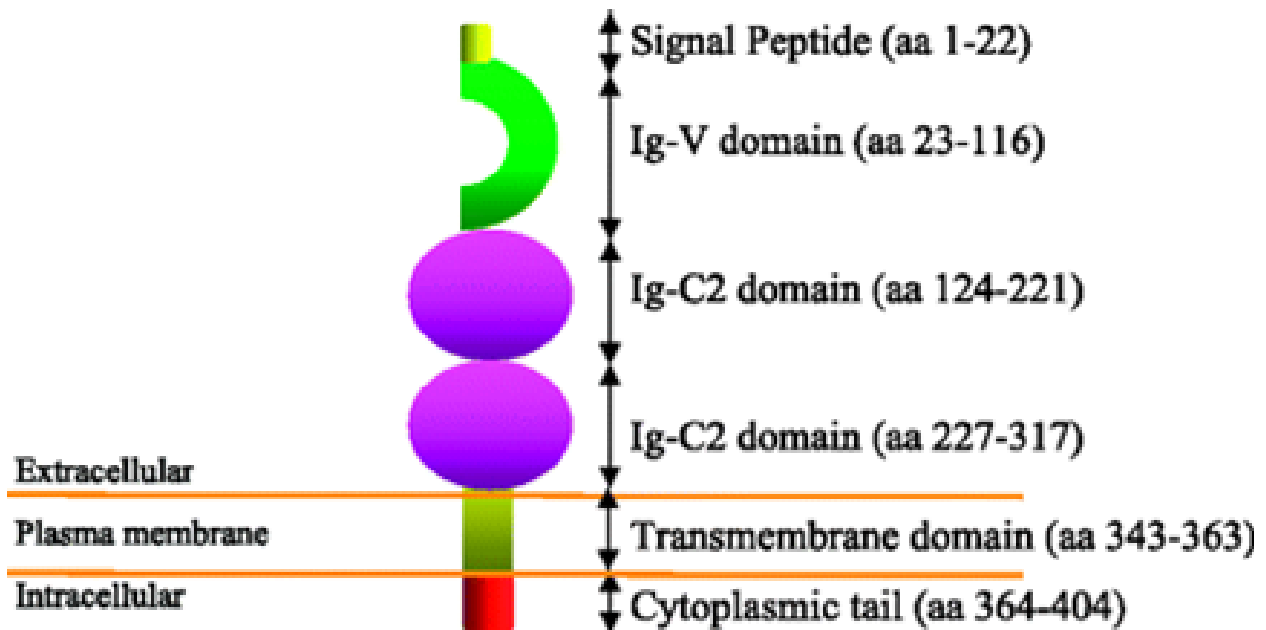


Figure 3. Schematic representation of RAGE.
Domains of RAGE are shown with corresponding amino acid numbers (45).

Given the large number of apparent RAGE-ligands, it is not surprising that RAGE has been implicated in the pathogenesis of a variety of human diseases including Alzheimer’s disease, diabetes mellitus, severe sepsis, hemorrhagic shock, rheumatoid arthritis, cancer and inflammatory bowel disease (reviewed in ref 46, 47). Schmidt et al. developed two-hit model of vascular perturbation mediated by RAGE. First hit includes increased expression of RAGE and RAGE ligands, therefore resulting in a constant state of activation; a superimposed stimulus such as an inflammatory response, tissue damage or ischemia leads to the constant state of vascular dysfunction and tissue damage rather than restoring of homeostasis (41).

RAGE has also been shown to play an important role in the natural aging process. Inflammation, through generation of reactive oxygen species (ROS), oxidative stress and inflammatory cytokines, increases generation of AGEs and decreased anti-AGE defense leading to accumulation of AGEs. Adhesion molecules attract inflammatory cells; NFκB activation itself

up-regulates RAGE expression in turn amplifying inflammation and making it chronic. Eventually tissue damage becomes irreversible (47).

1.2.1 RAGE tissue-specific expression

RAGE was partially sequenced after it was first purified from bovine lung protein extracts as lung was an excellent source of endothelial cell AGE-binding activity (48); consequently RAGE mRNA was demonstrated to be highly expressed in lungs (49). Interestingly, later studies revealed that RAGE in the lung was localized to the epithelial rather than endothelial cells. Although RAGE mRNA levels were reported to be the highest in type II alveolar epithelial cells in rat by *in situ* hybridization (50), most researchers, including us, view lung RAGE as an exclusive type I alveolocyte marker which is not present in type II cells or endothelial cells (51-54). Shirasawa et al. and Fehrenbach et al. utilized immunoelectron microscopy and showed lung RAGE expression exclusively in type I alveolar cells. Dahlin et al. identified the differentially expressed genes in freshly isolated rat type I and type II alveolocytes. This was done by creation of an mRNA subtraction library and confirmed the results by Northern blotting; RAGE was found to be expressed in type I cells (53).

The RAGE promoter sequence contains two apparently functional NF- κ B binding sites (55). Full-length RAGE is considered to be a pro-inflammatory factor as it is able to trigger NF- κ B signaling. This results in the up regulation of full-length RAGE as well as other factors in response to ligand binding to RAGE receptor and to general inflammatory stimuli (LPS, IL1- β etc.). According to our unpublished observations, cultured cells transfected with canonical RAGE up regulate their RAGE protein expression in response to IL-1 β and LPS. sRAGE is

believed to be a decoy receptor only able to bind the ligands and therefore is an anti-inflammatory factor.

RAGE expression is tightly regulated at different levels depending on the tissue and condition (healthy or diseased) of the cell. It is highly expressed in embryo and is downregulated in adult tissues. The known exceptions are lung, muscle and skin (33, 56, 57). RAGE is abundantly expressed in lungs of humans, dogs (58, 59), rats (51) and mice (60, 61). Reportedly, RAGE expression could be induced in generalized pathological conditions (inflammation) (57, 62) and lung diseases such as idiopathic pulmonary fibrosis (60, 63).

Studying RAGE expression is particularly difficult because it has overlapping sequence with the gene of pre-B-cell leukemia homeobox 2 (PBX2), a transcription factor implicated in the development of pre-B cell leukemia, on the chromosome 6 (-1204-507). PBX2 in turn has a pseudogene copy on chromosome 3 (64). The shared sequence between two genes has to be taken into account when studying gene expression/polymorphism using RT-PCR analysis because of the possibility of false positive PCR analysis. PCR primers should be designed to avoid the shared sequences between RAGE and PBX2.

1.2.2 **RAGE isoforms**

Multiple RAGE isoforms are reported to arise through alternative splicing and/or proteolysis. The first RAGE isoform identified, often referred to as “full-length” RAGE, is a type-Ia transmembrane protein with a cleavable signal peptide, an NH₂-terminal oriented towards the extracellular space, a single transmembrane domain and an intracellular COOH-terminal. The NH₂-terminal of the mature peptide contains one variable-type and two distally located constant-type Ig domains that are required for ligand binding. The COOH-terminal consists of 43 amino

acids and does not appear to contain significant homology to known functional protein domains. The cytosolic tail is thought to be essential for RAGE intracellular signal transduction following receptor engagement (65, 66).

Mouse lung was reported to express two major RAGE protein isoforms including the full-length transmembrane RAGE isoform and a soluble RAGE (sRAGE) (61). In addition, Harashima et al. identified endogenous soluble RAGE carboxyl-truncated isoform (esRAGE) in the mouse lung and other organs (brain, kidney and small intestine) (67). Human esRAGE and an amino-truncated transmembrane isoforms have been previously described by Yonekura et al. (68) in cultured human endothelial cells and pericytes together with a full-length transmembrane RAGE isoform. Interestingly, sRAGE is thought to be produced by proteolytic cleavage and esRAGE appeared to arise through alternative splicing (61, 67). Proteolysis is thought to require matrix metallo-proteinase-9 (61) and/or ADAM metalloproteinases, in particular ADAM 10 (69, 70). Ding and Keller (71, 72) reported the existence of at least six RAGE isoforms detected in human brain using RT-PCR: a full-length isoform, an isoform lacking the carboxyl-terminus, two soluble protein isoforms, and two N-truncated isoforms. Schlueter et al. (73) used RT-PCR to demonstrate that three sRAGE isoforms were present in human lung, lymph node, breast carcinoma and myometrium. Park et al. (74) described another soluble RAGE isoform, Δ^8 -RAGE, which was detected in human astrocytes and peripheral blood mononuclear cells (PBMCs). It lacks exon 8 of the original transcript and contains an early stop codon in exon 10 resulting from frameshift. Malherbe *et al.* cloned and analyzed yet another soluble RAGE, hRAGEsec, which lacks 19 amino acids corresponding to the membrane-spanning domain. It was confirmed to be expressed in brain and appears to be a decoy receptor for β -amyloid

precursor protein (75). All soluble RAGE isoforms are believed to act as decoy receptors diminishing pro-inflammatory effects of the full-length receptor.

Hudson *et al.* (45) recently published a summary of different RAGE isoforms as detected by RT-PCR (presented in table 1). The work was based on the analysis of RAGE mRNA transcripts in human lung and in human primary aortic smooth muscle cells (AoSMCs). In addition to the ‘classical’ full-length transmembrane RAGE mRNA they identified a range of RAGE RNA splice variants including 3 previously described isoforms and 10 novel isoforms. They were unable to confirm 6 previously reported isoforms. Tissue and cell lines expressed different relative amounts of each RAGE transcript. Half of the detected mRNA transcripts possessed premature termination codons and were targeted for degradation. Although, polyadenylation sites were identified in the untranslated region of these amplified cDNA, polyadenylation of the RNAs themselves has not been proven. So the presence of mature mRNA for the splice variants discovered in this study has never been confirmed and it is reasonable to suggest that some or all mRNA transcripts were not translated into proteins. In the next step authors generated isoform-specific antibodies for the newly discovered RAGE proteins. However, instead of using the cell lines that were initially utilized for mRNA analysis they transfected HEK293 cell line with the cDNAs and used antibodies to probe for the transfected and not endogenous RAGE. This

Table 1. Splice map of different RAGE variants detected in human lung and human primary aortic smooth muscle cells (AoSMC) cDNA.

Previously identified variants detected here are shown in blue, novel variants in red, and other variants not detected in this study in green (45).

Schematic of RAGE splice form	Previous nomenclature	Name (HUGO terminology)	Target of NMD pathway	Genbank entry no.
	RAGE	RAGE	No	AY755619
	esRAGE C-truncated RAGE sRAGE sRAGE2	RAGE_v1	No	AY755620
	Nt-RAGE N-RAGE N-truncated RAGE	RAGE_v2	Yes	DQ104254
	Δ ⁸ -RAGE	RAGE_v3	Yes	DQ104253
	(Exon 3 splice difference seen in hRAGEsec with exon 8 removal)	RAGE_v4	No	DQ104252
	Not previously detected	RAGE_v5	No	AY755621
	Not previously detected	RAGE_v6	No	AY755622
	Not previously detected	RAGE_v7	Yes	DQ104251
	Not previously detected	RAGE_v8	Yes	EU117141
	Not previously detected	RAGE_v9	Yes	AY755623
	Not previously detected	RAGE_v10	No	AY755628
	Not previously detected	RAGE_v11	Yes	AY755626
	Not previously detected	RAGE_v12	Yes	AY755625
	Not previously detected	RAGE_v13	No	AY755627
	sRAGE1	RAGE_v14	Yes	AF536236
	sRAGE3	RAGE_v15	Yes	AF537303
	hRAGEsec	RAGE_v16	No	AJ133822
	NtRAGE ^Δ	RAGE_v17	Yes	Ding <i>et al.</i> (16)
	sRAGE ^Δ	RAGE_v18	No	Ding <i>et al.</i> (16)
	RAGE ^Δ	RAGE_v19	No	Ding <i>et al.</i> (16)

approach raised the question of very existence of the endogenous RAGE isoforms which was just discovered in the first part of the study.

The authors made a huge effort in cataloguing RAGE isoforms but the following questions still remain: 1. What different RAGE proteins are expressed in different tissues/cell lines? 2. What factors contribute to RAGE processing including RNA splicing and proteolysis? 3. What is the difference between the various RAGE isoforms in terms of ligand binding and signaling? 4. What is the significance of particular RAGE isoforms in health and disease? 5. What is the proportion of RAGE isoforms at the site of inflammation?

1.2.3 **RAGE signaling in cell physiology**

RAGE was discovered based on its high affinity for AGEs and is thought to be more of an accidental receptor for (76) since AGEs have at least eight other receptors and RAGE has multiple ligands. It shares structural homology with other Ig-like receptors (such as ICAM-1) and could very well be functionally similar acting as an adhesion molecule.

Although RAGE was first discovered as a protein that binds AGEs (48), and studies have convincingly shown that AGEs bind to RAGE in a dose-dependent manner, there have been reports showing either a lack of signaling induced by AGEs (77-80) or negative (anti-inflammatory) responses (81, 82). Several reports question the ability of RAGE to effect transmembrane signaling events in response to known RAGE ligands including AGEs although confirming binding affinity of AGEs to RAGE (77, 78). There are many reports stating that AGEs signal through RAGE but in at least some of them the strong possibility exists that the AGEs used in some experiments have been contaminated with proinflammatory bacterial products; many of the studies did not use proper controls.

Another issue arises from studies of diabetes. Increased serum glucose leads to glycation of extracellular proteins. Those become irreversibly oxidized and are thought to bind to and activate RAGE. Most RAGE-expressing organs (lung, muscle and skin) do not seem to be affected by diabetes, the pathology related to AGEs. If AGEs were actually capable of triggering a pro-inflammatory response through RAGE, those organs would be expected to have more diabetes-related problems (83).

Strong arguments have been made against RAGE involvement with dietary AGEs which are generated in the Maillard reaction the same way AGEs are made in biological systems. The Maillard reaction involves reducing sugars that modify proteins thus changing their properties. The relationship between dietary AGEs and AGEs in biological systems is still unclear (84). Dietary AGEs would have to be digested in the gastrointestinal tract and be absorbed into the blood stream, at which point the AGEs might not be able to activate RAGE. Maillard reaction products of low molecular weight are unlikely to interact with RAGE - high molecular weight proteins are unlikely to enter the blood stream. They would be toxic through RAGE-independent mechanisms (84). In regards to endogenous proteins, only a small fraction of them are glycosylated and they contain too few modifications per protein, which could be insufficient for RAGE binding. In addition, the AGEs would have to compete with other RAGE ligands, and the concentrations of those (S100 proteins and HMGB1) would prevail under inflammatory conditions as they are released locally from activated cells (83).

The exact mechanisms involved in RAGE-mediated cell signaling remain to be elucidated. RAGE signaling is thought to follow binding of the ligand to the receptor and to employ the mitogen activated protein (MAP) kinase ERK 1/2 (p44/p42), stress-activated protein (SAP) kinases p38 and JNK, and the downstream NF- κ B signaling cascades (66, 85-87). There is

a single report suggesting that the RAGE intracellular domain interacts with ERK 1/2 directly (88) when using recombinant full-length RAGE expressed in the cell lines that do not normally express the full-length RAGE. This result is questionable since it has not been repeated since the original publication.

Recently, there have been studies indicating that RAGE-binding ligands may in fact utilize non-RAGE receptors, at least in part, to induce signal transduction. In turn, every RAGE ligand has been shown to bind a unique non-RAGE receptor(s) and/or binding partner(s). AGEs bind SR-A (class A scavenger receptor types I and II) and SRB, CD36, SR-BI (scavenger receptor class B type-I), galectin-3, LOX-1 (lectin-like Ox-LDL receptor-1), HA-SR (hyaluronan scavenger receptor, and RAGE. Additionally, it binds to an unidentified non-RAGE receptor in A549 cells (89, 90). By means of a RAGE-independent mechanism, S100B exhibits myogenic differentiation and apoptotic effects on cells (91, 92). The role of RAGE in amyloid- β peptide toxicity has been questioned (93); recent studies suggest that HMGB1 binds to and signals through Toll-like receptors 2 and 4 (94, 95) to the exclusion of RAGE and TLR9 (96). It appears that not only RAGE has multiple potential ligands, but each of those ligands has targets in addition to RAGE.

Despite tremendous efforts in the field, mechanisms involved in diversity of RAGE signaling in response to individual ligands still remains unclear. There is also a question of the contribution of different RAGE isoforms to the signaling events resulting in observed pathologies. On one hand, there is a number of RAGE isoforms expressed in different tissues, and on the other hand, there are many putative RAGE downstream signaling cascades. RAGE protein is upregulated in inflammation but the proportion of each RAGE isoform (full-length vs. soluble) is unknown. As stated before, the relative contribution to RAGE signal transduction by

the various isoforms remains to be determined. There are no studies addressing RAGE signaling specific to inflammation, tumorigenesis, diabetes, etc.

As for the inhibiting RAGE signaling in order to diminish inflammation, there are some concerns that in fact NF- κ B activation is necessary to mount an effective immune response to invading pathogens. RAGE knockout mice have diminished immune response which could harm immune defense to some extent (97). Therefore the use of anti-RAGE directed therapies should be approached with caution.

1.2.4 **Role of RAGE in inflammatory cell recruitment**

In addition to the ‘classical’ RAGE-binding partners (AGEs, β -sheet fibrils, S100B and HMGB1), RAGE, along with ICAM-1, was shown to be a counter receptor for β 2-integrins Mac-1 and, to a lesser extent, for p150, 95 (32). Direct interaction between RAGE and Mac-1 was shown in a purified system using transfected cells and *in vivo* (in mice) (32). sRAGE, anti-Mac-1 antibody and anti-ICAM-1 antibody were used as negative controls. Interestingly, classical RAGE ligands, namely S100B and HMGB1, augmented RAGE binding to Mac-1 promoting leukocyte recruitment (31, 32, 44). While RAGE expression in healthy organs, except for lung, is thought to be very low, it is reported to become upregulated in inflammation and at places where RAGE ligands accumulate (41, 55, 98). It is particularly important in diabetic vasculature in the presence of AGEs (99). AGEs are thought to mediate the inflammatory response and increase vascular permeability that contributes to diabetic vasculopathy, while RAGE modulates leukocyte adhesion, recruitment, and extravasation. sRAGE could be a therapeutic drug of choice in this model (32, 44).

1.2.5 RAGE studies in animals

In animal studies, RAGE knockout mice were found to be less susceptible to diabetic nephropathy, atherosclerosis, and inflammation (reviewed in (100)). Since sRAGE is generally viewed as a decoy molecule, it was used to treat different pathological conditions.

Administration of sRAGE was found to be beneficial in tumor treatment (40), diabetic atherosclerosis (101), and diabetic wound healing (102). It also protected myocardium from ischemic damage (103) and preserved intestinal barrier after hemorrhagic shock (104).

Surprisingly, sRAGE had an advantageous effect in the cecal ligation and puncture model of polymicrobial peritonitis in mice when administered to RAGE knockout mice compared with wild-type mice (105). This may be explained by the ability of sRAGE to bind potential RAGE ligands in the absence of the RAGE receptor which is helpful because RAGE ligands have pro-inflammatory effects thus modulating inflammatory process.

RAGE is highly expressed in the lung therefore it was predicted to play a role in the lung disease pathogenesis. In, in bleomycin mouse model of idiopathic pulmonary fibrosis authors observed loss of membrane and sRAGE, which was predicted to have beneficial effects; sRAGE was predicted to have beneficial effects (63). In an asbestos model, both RAGE isoforms were also downregulated, but in addition, RAGE knockout animals spontaneously developed pulmonary fibrosis. The disease is enhanced in the RAGE knockout mice in an asbestos-induced model of fibrosis compared with wild-type littermates (60). Those studies suggest protective role of RAGE in the pulmonary fibrosis. It is not clear that RAGE is detrimental in pathological conditions. It could also be associated with the protective immune response.

1.2.6 The role of sRAGE in disease

Uchida et al analyzed BAL fluids and found that soluble RAGE (sRAGE) could be a selective marker of type I cells damage in acute lung injury.

Soluble RAGE isoforms (including sRAGE, esRAGE, Δ^8 -RAGE and others) are thought to act as decoy molecules that bind RAGE ligands without triggering signal transduction. Mouse sRAGE has been shown to be a result of proteolysis (61), and human sRAGE is considered to be a product of alternative splicing. Endogenous soluble RAGE (esRAGE) was discovered by reverse transcribing mRNA library from human microvascular endothelial cells and pericytes, amplifying and sequencing resulting cDNA clones (106). esRAGE is generated by alternative splicing and contains 5' part of intron 9 and not exon 10 which encodes transmembrane domain. Multiple reports have been published concerning the plasma level of esRAGE isoforms in diabetes (107), atherosclerosis (108), renal diseases (109), hypertension (110) and Alzheimer's disease (111).

It appears that circulating levels of soluble RAGE isoforms, in general, were associated with a lower risk of complications, better prognosis and, in a few studies, lower mortality. Yamagishi et al.(112) reported that circulating esRAGE levels positively correlated with the serum level of AGEs in non-diabetic subjects; Tan et al. made the same observation in subjects with type 2 diabetes (113). In some cases, however, sRAGE indicated a poor prognosis. For instance, in septic patients, esRAGE levels were elevated in comparison with healthy controls, and non-survivors had higher levels of sRAGE compared to survivors (114). In addition, sRAGE levels in type 2 diabetic patients were shown to positively correlate with important markers of inflammation such as tumor necrosis factor (TNF) $-\alpha$ and monocyte chemoattractant protein 1 (MCP-1), making it of interest as a possible biomarker of vascular injury (115).

It is unclear if those levels could be viewed as prognostic markers of the disease or rather as a defense mechanism against the pathological condition (116). In other words, sRAGE could indicate a reaction of the organism to the pathological condition and/or a protective mechanism to minimize this condition. Further studies are necessary to understand the place of sRAGE in the development of the disease, including longitudinal ones, where RAGE is measured over a period of time along with other parameters/markers.

sRAGE has been considered as a candidate for a biomarker for acute lung injury, especially for patients on with mechanical ventilation. It is unclear however whether sRAGE blood levels rise as a result of injured lungs or as a part of an anti-inflammatory response (117).

1.3 SUMMARY AND CONCLUSIONS

Inflammation plays an important role in the interactions of the organism with the environment. The NF- κ B family of transcription factors is a major part of the inflammatory response. In the first part of this dissertation we screened enone-containing compounds for their abilities to modulate the inflammatory response. This was based on the hypothesis that the compounds modify NF- κ B therefore preventing it from binding to DNA. In the second part we evaluated RAGE protein isoforms expressed in cell lines and tissues. Scientific publications report multiple RAGE isoforms; most of them however were discovered by RT-PCR. Very little is known about RAGE protein isoforms, sequences, locations and functions. We used molecular biology tools available to us to address those questions which are undoubtedly important in RAGE-related pathologies and treatments. We also attempted to summarize cellular responses to RAGE ligands (AGEs, HMGB1 and S100B).

2.0 CHAPTER TWO – USING *IN VITRO* CELL-BASED SYSTEMS TO ASSAY ENONE-CONTAINING ANTI-INFLAMMATORY DRUGS

2.1 ABSTRACT

We showed that exposing the human U373 astrocytoma cell line to IL-1 β increased the surface expression of intracellular adhesion molecule-1 (ICAM-1; CD54). However, when the bulk population of U373 cells (stock obtained from the American Type Culture Collection) was exposed to IL-1 β , only 50-60% of the cells appeared to express CD54. We used fluorescence activated cell sorting (FACS) to enrich for CD54-expressing cells following exposure to IL-1 β . Six clonal cell lines were obtained and found to express CD54 in a higher percentage of cells (70-98%) compared to the bulk population. However, some of these clones were also found to express slightly elevated baseline levels of CD54 compared to the non-sorted population. We used the protease inhibitor N-tosyl-L-phenylalanine chloromethyl ketone (TPCK) to block proteasome activity and this almost completely blocked upregulation of CD54 expression in these cells, which is consistent with the dependence of CD54 expression on NF- κ B activation. The sorted cell line was in screening substances for anti-inflammatory and, more specifically, NF- κ B blocking activity. We utilized this endogenous NF- κ B reporter system to study the relative efficacy of several compounds that have similar chemical properties to ethyl pyruvate, a promising new candidate compound for the treatment of a variety of systemic and localized

inflammatory diseases. We discovered that the endogenous metabolite para-hydroxyphenyl pyruvate was more potent than ethyl pyruvate. These studies show the value of using U373 cells as a reporter cell line for studying the relative pharmacology of anti-inflammatory drugs that work by blocking the activation of NF- κ B. Utilizing an endogenous reporter gene (i.e., CD54) as a read out may have certain advantages over other engineered NF- κ B-dependent reporter systems.

2.2 RESULTS

2.2.1 **Establishing a cell-based U373 reporter cell line to screen compounds for NF- κ B inhibitory activity**

The U373 human glioblastoma astrocytoma cell line was used for these experiments because it has low background expression levels of CD54 which increased with IL-1 β stimulation. Approximately 60% of all cells became CD54 positive upon stimulation with the pro-inflammatory factor. We wanted to enrich the parental population for IL-1 β -responsive cells so we stimulated the bulk cell population with IL-1 β and stained the cells for CD54 expression, and sorted them with a fluorescence activated cell sorter (FACS) selecting for the CD54 expressing cells. The sorted cells were plated on a T25 tissue culture flask and allowed to expand. They were cloned using cloning cylinders and assayed, along with the bulk population, for both background and stimulated expression of CD54. The percent stimulation for the bulk population and for the individual clones was determined (Fig. 4, 5). For the experiments, we used the bulk cell population as well as individual clones that became more than 90% CD54 positive following

exposure to IL-1 β . We generated a calibration curve of increasing IL-1 β concentrations vs. increasing expression of CD54 (Fig. 6). As a control for the system, we used the protease inhibitor N-tosyl-L-phenylalanine chloromethyl ketone, (TPCK), which blocks proteasome activity and thus almost completely abolished upregulation of CD54

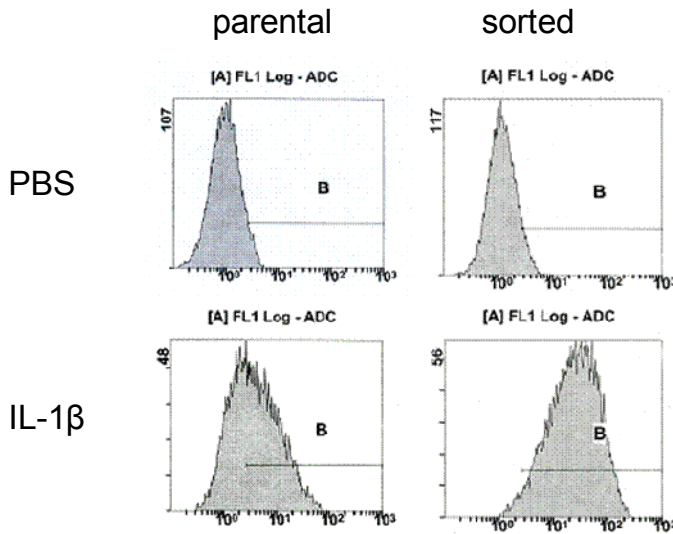


Figure 4. FACS enriched U373 cell population stimulated with IL-1 β . 96.3% cells express CD54 vs. 59.8% in the parental population. Histograms show results of stimulating parental and sorted U373 reporter cell lines.

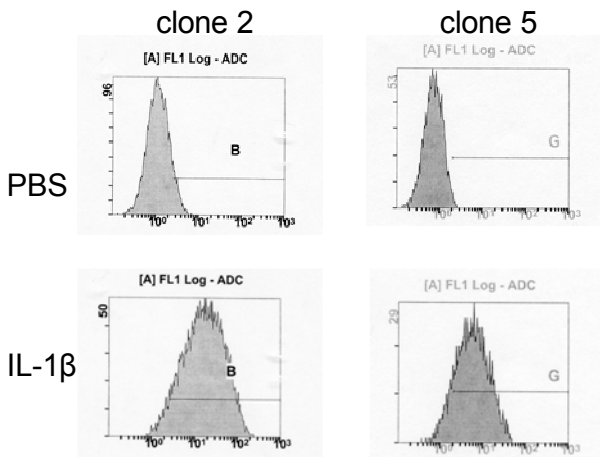


Figure 5. FACS enriched clonal U373 NF- κ B reporter cell lines. Histograms show results of stimulating two clonal U373 reporter cell lines stimulated with 10 ng/ml IL-1 β .

expression in these cells (data not shown), confirming the dependence of CD54 expression on NF- κ B activation. TPCK is a serine protease inhibitor that has been shown to inhibit NF- κ B activation by blocking I- κ B phosphorylation and subsequent degradation via proteasome (118). Our *in vitro* system was ready to screen NF- κ B inhibitors. The definite advantage of this *in vitro* cell system is the endogenous origin of the readout protein (CD54).

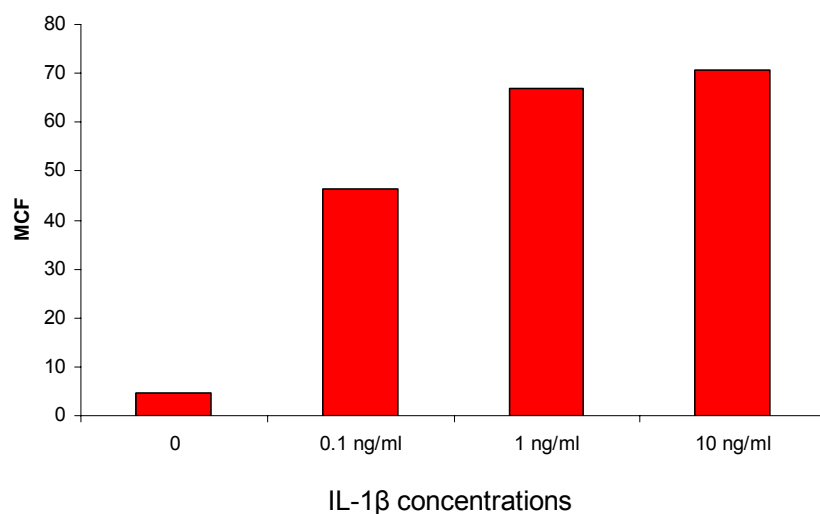


Figure 6. Graded IL-1 β -induced CD54 cell surface expression on the bulk sorted population of U373 cells as measured by FACS analysis.

Cells were stimulated with the indicated concentrations of IL-1 β and stained as described in Methods. After evaluating percentage stimulation of the sorted cells we performed calibration curve of the graded IL-1 β concentrations vs. CD54 expression. We were able to show that mean channel fluorescence (MCF) increased from 2.4 with no stimulation to 6.8 with upon stimulation with 10 ng/ml IL-1 β . The results are representative of 2 different experiments.

2.2.2 Using the clonal U373 human astrocytoma cell line in the screening of the enone-containing compounds

To screen the enone-containing compounds, we grew sorted U373 cells in the 6-well dishes, treated them with the indicated compound and stimulated them with IL-1 β the next day. CD54 surface expression was assayed 18 h later. In this experiment, the groups consisted of: unstained cells, stained unstimulated cells, stained stimulated cells and stained stimulated cells treated with

the compound of interest. Percent inhibition for each compound was determined by comparing the mean channel fluorescence (MCF) of cells stimulated with IL-1 β with the MCF of cells pretreated with the drug of interest prior to stimulation with IL-1 β . We compared the ability of ethyl pyruvate (ET), sodium pyruvate (SP), para-hydroxyphenyl pyruvate (pHPP) and benzoyl formate (BF) to inhibit CD54 expression. The results are presented in Fig. 7.

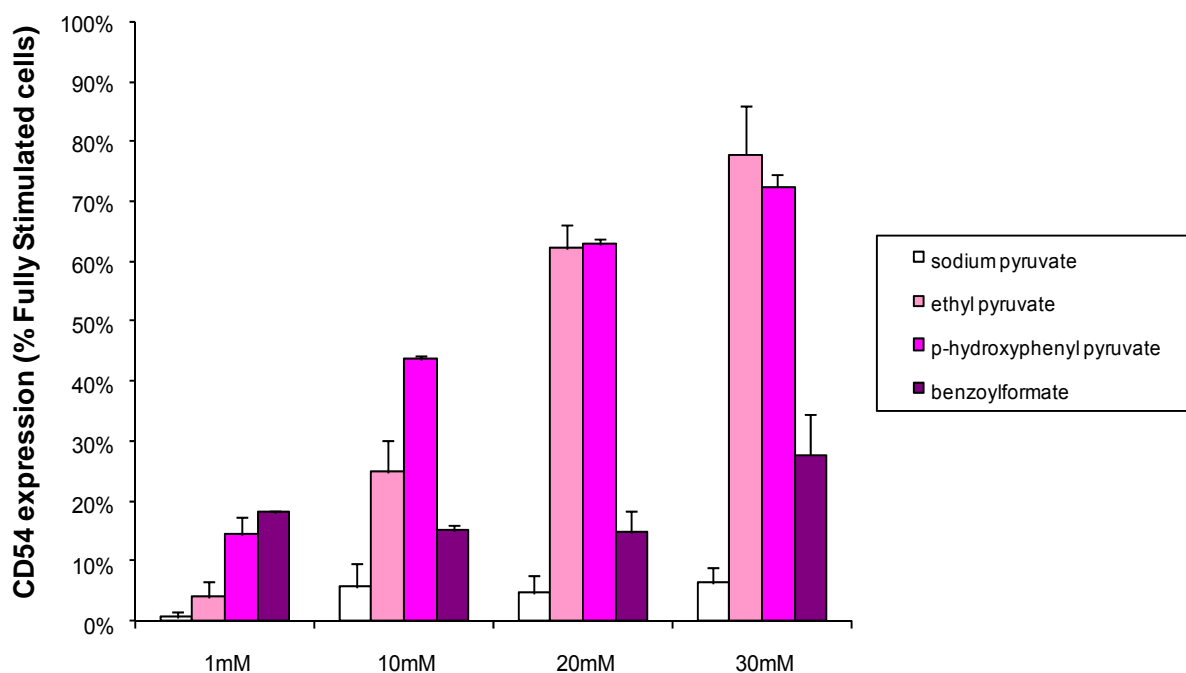


Figure 7. pHPP exhibits the best inhibitory properties on CD54 cell surface expression after IL-1 β stimulation in bulk sorted population of U373 cells. CD54 was measured by FACS analysis. Percent inhibition is determined from mean channel fluorescence as described in Methods. Results are presented as means \pm SD (N=4 per conditions).

All compounds were tested at 4 concentrations (1, 10, 20 and 30 mM). EP and pHPP exhibited comparable abilities to inhibit CD54 expression. However, pHPP worked better than ethyl pyruvate at the 10 mM concentration. SP had no significant effect on CD54 expression and BF exhibited a minimal effect that did not increase with increasing concentration. In this experiment, we demonstrated that the U373 human astrocytoma cell line can be used as a test

system for potential anti-inflammatory drugs and that it is responding to anti-inflammatory agents in a dose-dependent manner. It allowed us to compare enone-containing compounds for their anti-inflammatory activity using endogenously expressed protein (CD54) as readout.

2.2.3 Using RAW 264.7 murine macrophage-like cell line for further testing the enone-containing compounds

Since NF- κ B is thought to play a role in inflammation, we further tested our compounds using the mouse macrophage-like RAW 264.7 cell line. RAW cells are very sensitive to bacterial lipopolysaccharide (LPS), producing a variety of cytokines and nitric oxide (NO \cdot) in an NF- κ B-dependent manner. Tested drugs downregulated LPS-induced inflammatory responses (namely, IL-6 production, iNOS upregulation, and NO \cdot production) following the same trend they demonstrated during primary screening in U373 cells (i.e. pHPP>EP>BF).

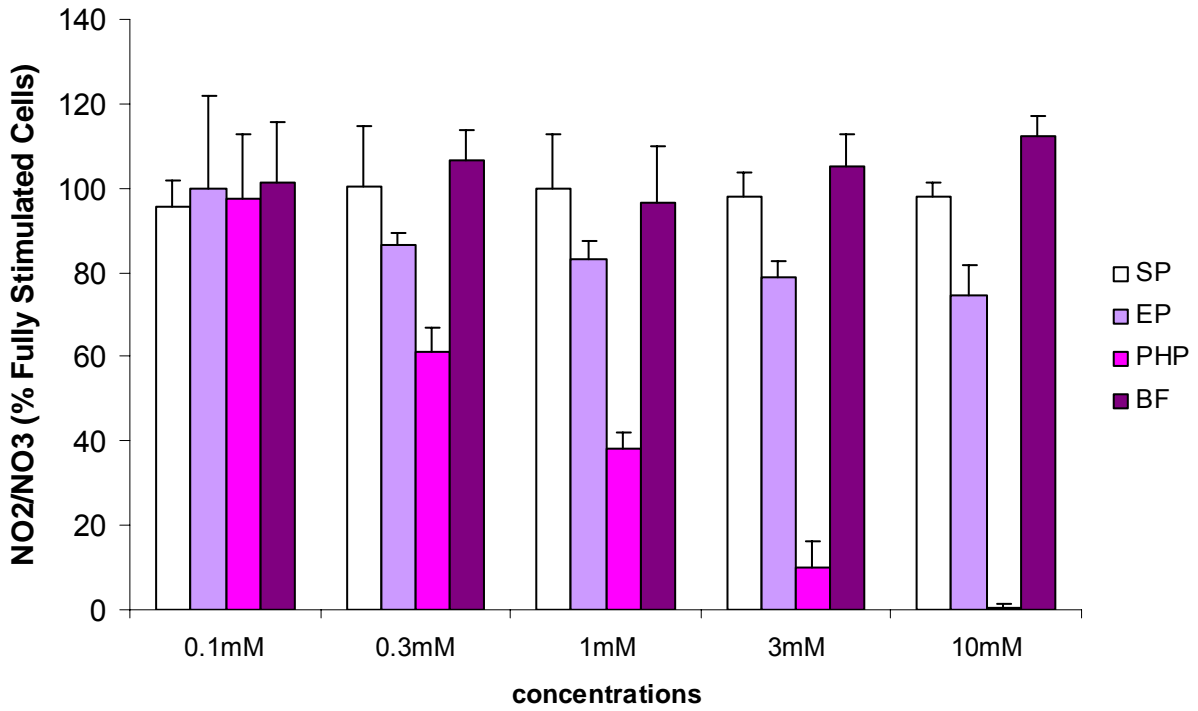


Figure 8. Effect of graded concentrations of compounds of interest on NO[•] release by LPS-stimulated RAW 264.7 cells.

The cells were stimulated with LPS (10 ng/ml) for 18 h later supernatants were assayed for IL-6 and nitrite concentration using commercially available kits. Results are presented as means±SD (N=4 per conditions).

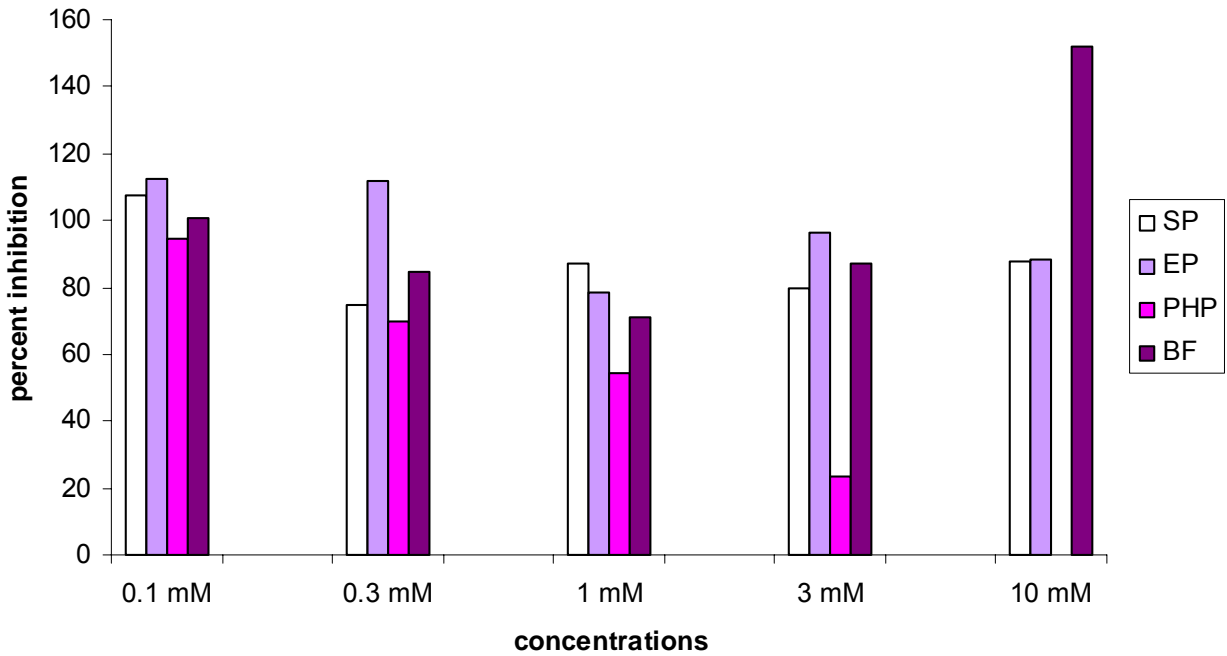


Figure 9. Real time quantitative RT PCR analysis showing iNOS expression after 18 hour incubation with LPS in the presence of the graded concentrations of the indicated drugs in RAW 264.7 cells. The experiment was performed in duplicates.

Ethyl pyruvate downregulated pro-inflammatory gene expression in various experimental models (119-122). In this experiment, we tested SP, BF, EP and pHPP at 5 graded concentrations. Ethyl pyruvate and pHPP inhibited NO \cdot production and iNOS steady-state mRNA levels (Fig. 8, 9). Under the tested conditions, pHPP appeared to be the most active compound. It showed the greatest inhibition, even in lower doses (1 mM), while the higher doses brought iNOS down to baseline levels. Oxalpropionate and ethyl pyruvate also exhibited substantial iNOS-inhibiting activity at the higher doses. The ability of pHPP to inhibit inflammatory markers at lower doses could be beneficial for decreasing toxicity.

2.2.4 pHPP inhibited LPS-induced IL-6 secretion in LPS-stimulated RAW 264.7 cells

RAW cells were treated with 10 ng/ml LPS in the absence or presence of graded concentrations of the tested compounds. Cell culture supernatants were tested for IL-6 18 hours after LPS treatment. pHPP demonstrated the best IL-6 inhibiting activity at the 3 mM concentration. When used at 10 mM, pHPP inhibited IL-6 below baseline. Oxalpropionate and ethyl pyruvate showed less inhibition when used at the higher concentrations (Fig. 10).

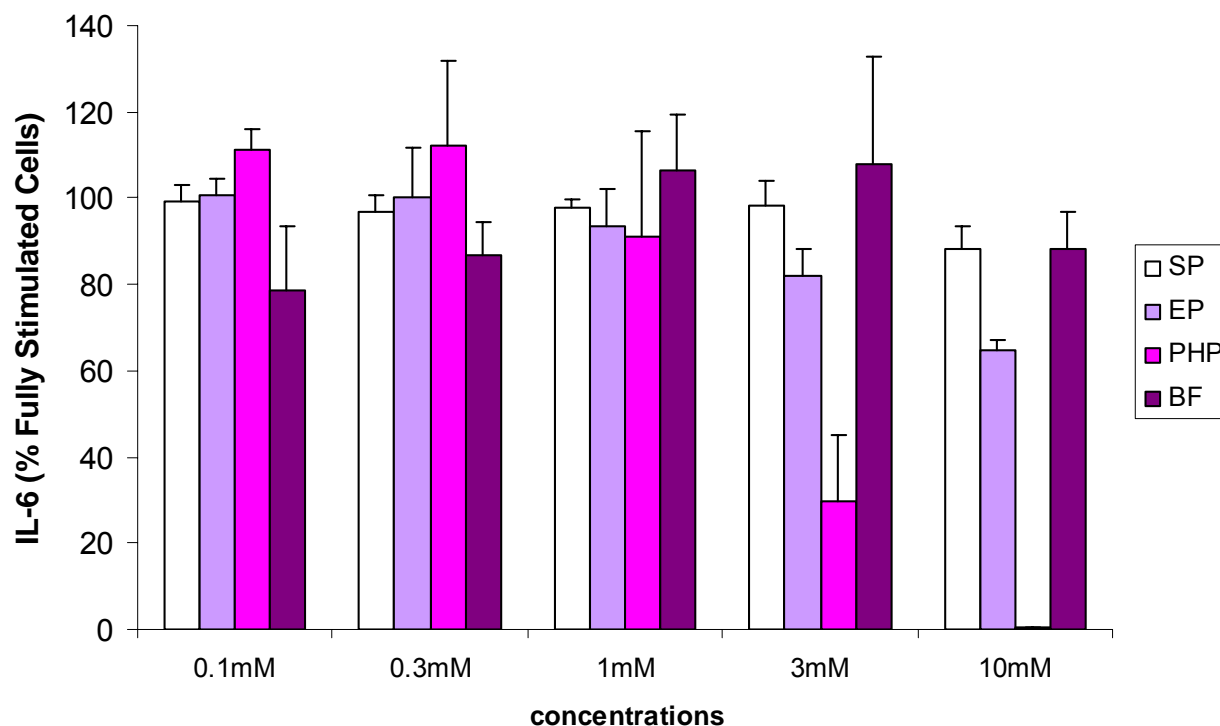


Figure 10. Effect of graded concentrations of compounds of interest on IL-6 by LPS-stimulated RAW 264.7 cells.

The cells were stimulated with LPS (10 ng/ml) for 18 h later supernatants were assayed for IL-6 and nitrite concentration using commercially available kits. Results are presented as means±SD (N=4 per conditions).

2.3 DISCUSSION

First, we established a cell-based *in vitro* system for testing potential anti-inflammatory compounds containing an enone structure. U373 cells were enriched using a FACS and cloned to create a cell population with a low background CD54 expression and high expression upon stimulation with IL-1 β . After the *in vitro* cell-based system was established, we performed tests which showed that the cells responded to IL-1 β stimulation in a dose-dependent manner and that the proteasome inhibitor TPCK, which blocks I κ -B degradation, completely abolished IL-1 β stimulated CD54 upregulation. In this way, we confirmed that the system was indeed NF- κ B dependent. Then, we were able to utilize the system for testing of ethyl pyruvate and related enone-containing anti-inflammatory compounds, which were shown to work in various *in vivo*

and *in vitro* systems (28, 123). Pyruvate is a part of intermediary metabolism and is considered to be an endogenous scavenger of reactive oxygen species (ROS) (124, 125). However, use of pyruvate in a biological system is limited by its poor stability in aqueous solutions (15). Eventually, ethyl pyruvate was proven to be more effective than pyruvate in *in vivo* and *in vitro* models (16, 126). Therefore we tested anti-inflammatory effects of ethyl pyruvate and related compounds. Our results showed that pHPP was the most potent drug along with ethyl pyruvate. Sodium pyruvate and benzoyl formate exhibited no NF- κ B blocking activity. pHPP demonstrated anti-inflammatory effects in lower doses than ethyl pyruvate, which made it potentially a better candidate as a drug. This is also supported by the fact that pHPP is an endogenous catabolite of trypsin.

After we tested enone-containing compounds in our newly developed system, we used another cell line - RAW 264.7 murine macrophage-like cells. RAW 264.7 are routinely used in the lab to test anti-inflammatory compounds; they produce various cytokines in response to LPS in a dose-dependent manner. We assayed iNOS expression using real-time RT PCR and we also collected supernatants to assay for NO \cdot production and IL-6 secretion. In agreement with the U373 data, pHPP was the most effective drug in suppression of LPS-stimulated iNOS mRNA expression, followed ethyl pyruvate (Fig. 9). These data were closely followed by NO \cdot production (Fig. 8) and IL-6 secretion (Fig. 10) where pHPP was again the most effective drug. Taken together, our results suggest that pHPP could be as effective, if not more, as ethyl pyruvate.

As mentioned before, the mechanisms of the enone-containing anti-inflammatory compounds could be explain, at least in part, by modification of thiol residues on the p65 subunit of NF- κ B decreasing its DNA-binding activity (28). Ethyl pyruvate has been shown to affect p65

basal binding in resting cells and it does not interfere with I κ B degradation (28). These findings are consistent with the compound interfering with p65 DNA binding directly and not with the NF- κ B activation steps. Recently, our lab obtained data confirming that pHPP inhibits activation of NF- κ B using EMSA analysis (Meaghan E. Killeen, unpublished results). Further work to confirm modification of NF- κ B by pHPP is currently awaiting funding. Pyruvate derivatives may also inhibit activation of NF- κ B by scavenging ROS (126). In addition ethyl pyruvate was shown to inhibit lipid peroxidation *in vitro* (127) and *in vivo* (128). pHPP is the first intermediate in tyrosine catabolism: it is converted to homogentisic acid, which is oxidized to maleylacetoacetate (MAA); maleylacetoacetic acid isomerase (MAAI) catalyzes the isomerization of MAA to fumarylacetoacetate, which is converted to fumarate and acetoacetate. This makes pHPP a suitable carbon source which could be important in inflammation when the energy sources are deprived.

Regardless of the underlying mechanism, further studies of the ability of pHPP to treat experimental inflammation seem warranted. Studies in a rat profound hemorrhagic shock (HS) model have shown that pHPP is superior to EP in extending survival time in the absence of resuscitation.

3.0 CHAPTER THREE - COMPARISON OF DISTINCT PROTEIN ISOFORMS OF THE RECEPTOR FOR ADVANCED GLYCATION END-PRODUCTS EXPRESSED IN TISSUES AND CELL LINES

3.1 ABSTRACT

The receptor for advanced glycation end-products (RAGE) is expressed as numerous protein isoforms. Northern blotting, immunoblotting and sensitivity to N-glycanase digestion were used to survey RAGE isoforms expressed in cell lines and mouse tissues to obtain a comprehensive view of the RAGE expressome. Pulmonary RAGE mRNA (1.4 kb) was smaller than cell line and tissue RAGE mRNA (6 kb-10 kb). Three anti-RAGE antibodies that recognize three distinct RAGE epitopes were used for these studies (N-16, H-300 and α ES; see Fig. 21). Lung expressed four predominant protein isoforms with apparent molecular masses of 57.4, 52.6, 45.1 (N-16/H-300) and 25 kDa (α ES), and three less abundant isoforms at 46.9, 52.5 and 54.2 kDa (α ES). These isoforms were expressed exclusively in lung, heart, ileum and kidney as a 44.0 kDa isoform (N-16), while aorta and pancreas expressed a 53.3 kDa isoform (α ES). Each of these isoforms were absent in tissue extracts prepared from RAGE^{-/-} mice. Cell lines expressed a 70 kDa isoform and a subset expressed a 30 kDa isoform (α ES). Lung RAGE appeared to contain two N-linked glycans, whereas tissue and cell line RAGE isoforms were completely insensitive to PNGase F digestion. Thus, numerous RAGE protein isoforms are detected in tissues and cell

lines. Canonical transmembrane and soluble RAGE appear to be expressed solely in lung (N-16/H-300). Non-pulmonary tissues and cell lines, regardless of the source tissue, both expressed distinct RAGE protein isoforms containing the N-terminally located N-16 epitope or the α ES RAGE epitope encoded by alternate exon 9, but not the H-300 epitope. Cell lines, of both pulmonary and non-pulmonary origins, were able to express pulmonary RAGE mRNA (1.4 kb) upon transfection with an expression plasmid containing the pulmonary full-length cDNA. However, only non-pulmonary cell lines (HEK 293 and HMEC-1) were able to express full-length RAGE protein (H-300 antibody-positive, PNGase-sensitive). Lung-derived cell lines, including human A549, CaLu-3, and rat R3/1 failed to express canonical RAGE protein in spite of the fact that they expressed the transfected canonical RAGE mRNA at levels equal to HEK 293 and HMEC-1. After evaluating a mouse EST (expressed sequence tags) database, we analyzed RAGE expression in the mouse thyroid. We confirmed that mouse thyroid expressed the same RAGE isoforms as lungs. They were H-300 antibody-positive and PNGase-sensitive. Thyroid however expressed only a small fraction of the RAGE protein levels expressed in lung.

3.2 RESULTS

3.2.1 *In silico* analysis of RAGE mRNA expression

We examined RAGE mRNA expression by comparing the relative abundance of ESTs in various human, mouse and rat tissues using the Gene Expression Omnibus repository at the National Center for Biotechnology Information (129) and the results are summarized in Table 2. Most notable is the over-representation of RAGE ESTs present in the lung of all three species.

This trend is also obvious in other mammalian species, but the analysis here is limited to human, mouse and rat. Only mouse thyroid expressed more RAGE transcripts than lungs. This information is not shown in an attempt to catalog the RAGE transcriptome, but it is included to highlight the notable exceptions where RAGE transcripts are expected but not well represented (e.g., brain 71, 72).

Table 2. Relative number of EST clones per million identified in tissue and species-specific databases (129). Table was last updated on 10/06/08.

<i>H. sapiens</i>		<i>M. musculus</i>		<i>R. norvegicus</i>	
lung	139	thyroid	899	lung	682
ear	61	lung	110	thymus	245
connective tissue	26	mammary gland	3	placenta	46
heart	22	adipose tissue	0	eye	32
lymph node	21	blood	0	brain	16
eye	18	bone marrow	0	adipose tissue	0
mammary gland	12	brain	2	connective tissue	0
thymus	12	connective tissue	0	dorsal root ganglion	0
ovary	9	dorsal root ganglion	0	endocrine	0
stomach	10	embryonic tissue	0	gastrointestinal tract	0
pancreas	9	eye	0	genitourinary	0
intestine	4	female genital	0	head and neck	0
prostate	5	gastrointestinal tract	0	heart	0
testis	6	head and neck	0	liver	0
bladder	0	heart	0	muscle	0
blood	0	inner ear	0	pancreas	0
bone marrow	0	limb	0		
brain	0	liver	0		
kidney	0	lymph node	0		
liver	0	muscle	0		
lymph	0	pancreas	0		

muscle	0	prostate	0		
nerve	0	skin	0		
parathyroid	0	spinal cord	0		
skin	0	spleen	0		
small intestine	0	sympathetic ganglion	0		
spleen	0	testis	0		
thyroid	0	thymus	0		
trachea	0	urinary	0		
vascular	0	vascular	0		
whole brain	0	vesicular gland	0		

3.2.2 Northern blot analysis of RAGE isoforms expression

Northern blot analysis was performed to compare the size of RAGE transcripts expressed in various cell lines and tissues (Fig. 11). Total RNA was hybridized using an *in vitro* transcribed full-length human RAGE cRNA probe. Distinctly different hybridization patterns were observed when comparing lung, liver, brain, and pancreas. Lung expressed a major band of approximately 1.4 kb and another much less prominent band of approximately 3.5 kb. One predominant band of approximately 6 kb was present in liver extracts. Two bands of higher mobility were also present, but they did not seem to correspond to the same size bands present in lung at the resolution achieved using agarose gels. Mouse brain expressed very low levels of what appear to be the 1.4 and 3.5 kb RAGE transcripts present in mouse lung but their presence is much less convincing. No bands were detected in pancreases that were homologous to the human mRAGE probe at the hybridization stringency used for these studies.

Northern blot analysis of several human and mouse cell lines generated a common transcript pattern (Fig. 11B). Each cell line expressed an approximately 6 kb transcript of similar size to the

transcript observed in mouse liver. Cell lines also expressed a longer transcript that is also detectable in mouse lung at approximately 10 kb. We compared HEK293 cells transfected with RAGE cDNA with HEK293 transfected with the empty vector (Fig. 11C). RAGE-transfected cells obtained lung size transcript (1.4 kb) while still expressing the endogenous ones.

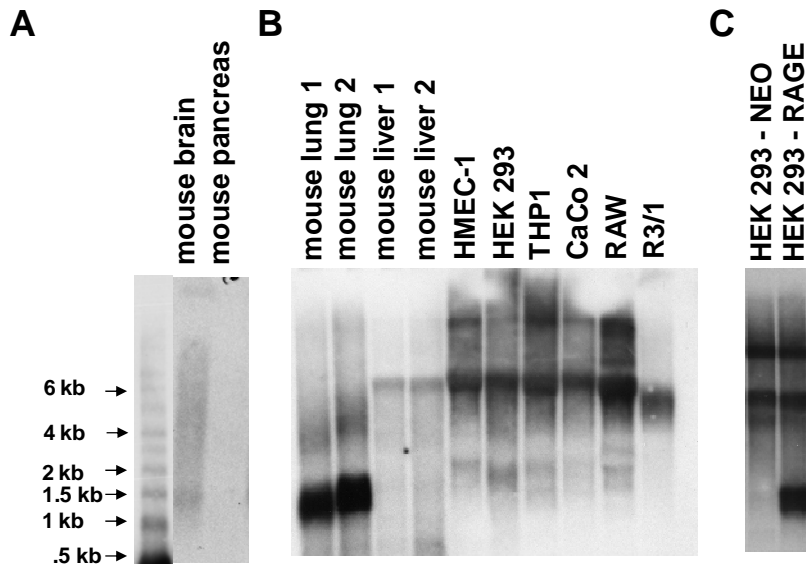


Figure 11. Northern blot analysis of mouse tissues and cell lines.

Radiolabeled full-length cRNA was hybridized to size-fractionated total RNA on nylon filters. In mouse lung RAGE transcript was approximately 1.4 kb. Other tissues and cell lines expressed larger transcripts ranging from 4 to 10 kb (B). HEK293 transfected with the full size RAGE also express 1.4 kb isoform (C). This blot is representative of at least 3 experiments.

3.2.3 H-300 and N-16 recognize distinct RAGE epitopes that are only present together in RAGE protein isoforms expressed in lung

We compared the ability of two commercially available α -RAGE antisera to detect RAGE protein expression in various mouse tissues. H-300 and N-16 (Figs. 12A & 13B, respectively) each recognized bands in mouse lung lysate with apparent molecular masses of 57.4, 52.6 and 45.1 kDa. H-300 failed to detect RAGE in other tissues, even after overexposing the film (not shown). In contrast, N-16 also detected a 51.2 kDa band in liver extract (Fig. 12B), and longer

exposures detected a 40 kDa band in heart and kidney extracts and an additional 34.5 kDa band in kidney extracts (Fig. 17). GAPDH is used as a loading control (Fig. 12C). Clearly, the lung isoform possesses all the epitopes that are believed to be in the RAGE protein, whereas other tissues only have the N-16-positive sequence. Thus, H-300 and N-16 clearly recognize different epitopes.

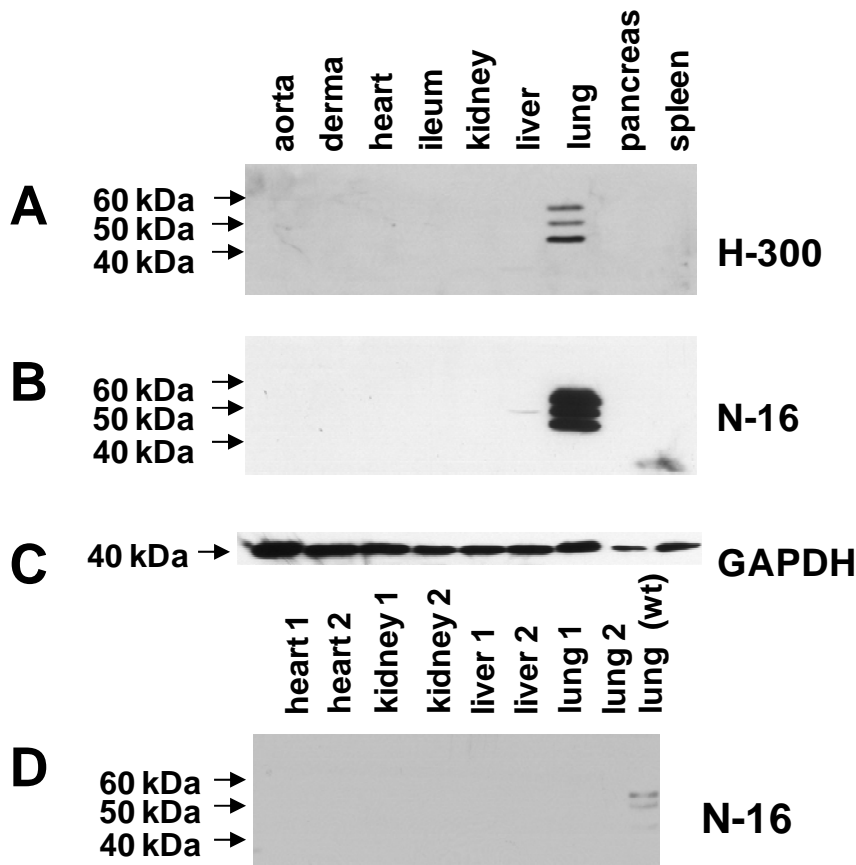


Figure 12. Western blots showing RAGE isoforms expressed in various mouse tissues.

Equal amounts of protein (20 μ g/lane, 10 μ g/lane for the lung lysate) were fractionated using reducing SDS-PAGE. H-300 and N-16 antibodies recognize the three major RAGE isoforms expressed in mouse lung lysate (A and B). H-300 only detected the mouse lung isoforms while N-16 recognized a single band in liver on this exposure. GAPDH was used as loading control (C). Western blot of the RAGE knockout mice probed with the N-16 antibody was used as a negative control (D). Wild type mouse lung (1 μ g/lane) was used as a positive control. This blot is representative of at least 3 experiments.

The α ES polyclonal antiserum was raised against a unique peptide present in the esRAGE sequence that is not present in the transmembrane pulmonary RAGE isoform (106). This

antiserum detected four bands in lung protein extract with apparent molecular masses of 44.0, 46.9, 52.5 and 54.2 kDa and a more intense band of approximately 25 kDa (Fig. 13A). α ES detected numerous RAGE isoforms with various sizes that appear to be expressed in a tissue-specific manner. Aorta expressed a strongly staining 53.3 kDa isoform that also appears to be the major RAGE isoform in pancreas and derma. α ES also detected poorly resolved bands in aorta and derma in the 47 – 49 kDa region of the gel. Kidney and liver express unique proteins at 40.0 kDa and 56.8 kDa. Liver also expressed 58.6 kDa and 54.2 kDa isoforms that were detected by

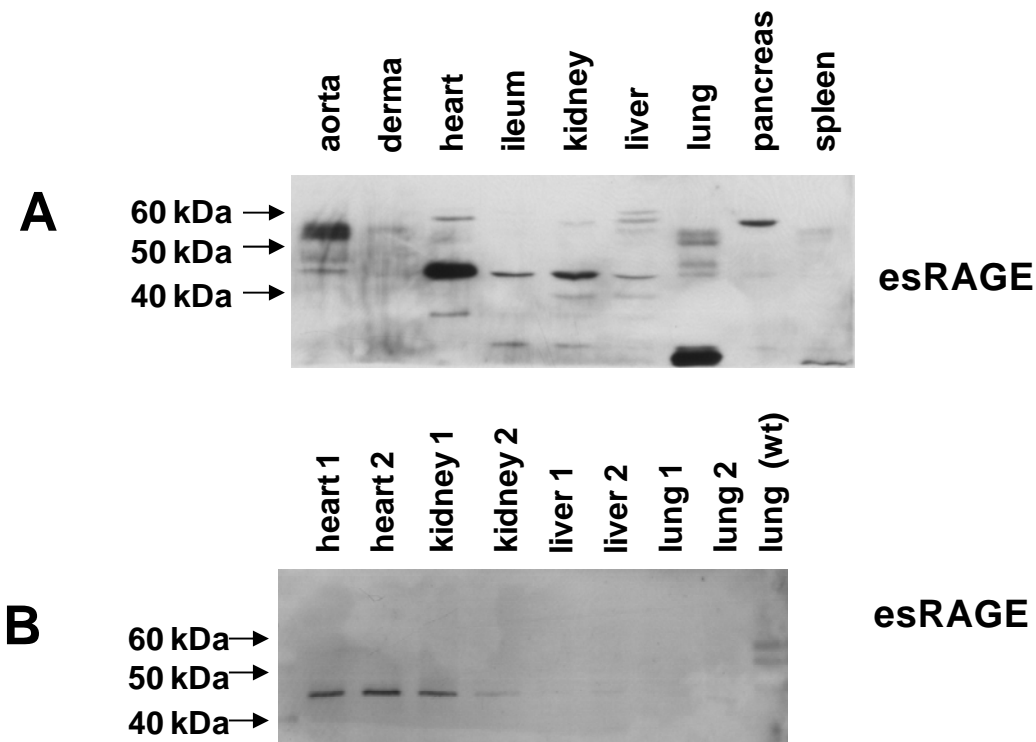


Figure 13. α -esRAGE antibody failed to detect canonical RAGE bands in Western blot analysis but detected numerous bands of various mobilities.

Western blot analysis showing RAGE protein in the engineered RAGE $-/-$ mice was used as a negative control. Each organ is represented by two different mice. Both blots were probed with the anti-esRAGE antibody. Each lane contained 20 μ g of total protein. This blot is representative of at least 3 experiments.

α ES. All tissues, except spleen, express a 45kDa α ES band. It is important to note that none of the bands recognized with the α ES antiserum were also recognized by either the N-16 or the H-300 antisera.

We prepared and analyzed protein extracts from tissues obtained from engineered RAGE^{-/-} mice (105, 130-132) kindly provided by Dr. Oury. H-300 (data not shown) and N-16 failed to detect proteins in any of the tissues obtained from knockout mice (Fig. 12D). Most of the bands recognized by α ES in RAGE^{+/+} tissue extracts were absent in extracts from RAGE^{-/-} tissue (Fig. 13A&B). However, α ES detected a 44.0 kDa protein in heart and kidney extracts obtained from RAGE^{-/-} mice. Lung and liver extracts from RAGE^{-/-} mice did not contain the 44.0 kDa protein. The relative reduction in the expression of this protein in heart and kidney suggests that some of the signal in wild-type mice represents a unique esRAGE isoform, but this will need to be confirmed using higher resolution studies.

3.2.4 Mouse lung RAGE isoforms

We refer to the 57.4, 52.6 and 45.1 kDa proteins recognized by N-16 in lung lysate as xRAGE, membrane (m)RAGE, and soluble (s)RAGE, respectively. Expression of the xRAGE isoform increased following injection of mice with endotoxin (2 mg/kg, given by ip injection; Fig. 14). Mice injected with saline vehicle typically expressed low to undetectable amounts of the xRAGE protein isoform in the lung. We used the method described by Hanford et al. (61) to confirm that both xRAGE and mRAGE were membrane bound and sRAGE was not (data not shown).

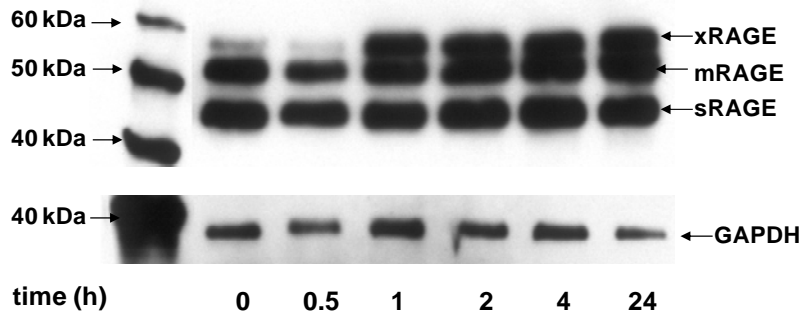


Figure 14. Western blots analysis of mouse pulmonary RAGE isoforms expressed following injection of C57BL/6 mice with 2 mg/kg of LPS at the times indicated (time course).

10 µg of total protein were fractionated per lane using reducing SDS-PAGE and GAPDH was used as loading control. This blot is representative of at least 3 experiments.

Mass spectroscopy (MS) was used to confirm that the inducible 57.4 kDa protein is a RAGE protein isoform. xRAGE was captured from mouse lung protein lysate using a DEAE Sepharose column as was done previously (48, 61) (Fig. 15A). Analysis of column fractions by Western blotting with N-16 demonstrated enrichment of xRAGE and mRAGE in Step II. These fractions were pooled and subjected to affinity chromatography on concanavalin A lectin agarose and Mono Q anion exchange beads. The highly enriched proteins were size-fractionated using SDS-PAGE (Fig. 15B) and subjected to in-gel trypsin digestion. MALDI-TOF MS spectral analysis of xRAGE (Fig. 15C) identified eight peptide fragments resulting in 22% sequence coverage based on the pulmonary mRAGE protein sequence (Fig. 15D). Identical peptides were obtained from the mRAGE MS analysis (data not shown). No information was obtained concerning the apparent molecular mass difference between the xRAGE and mRAGE isoforms.

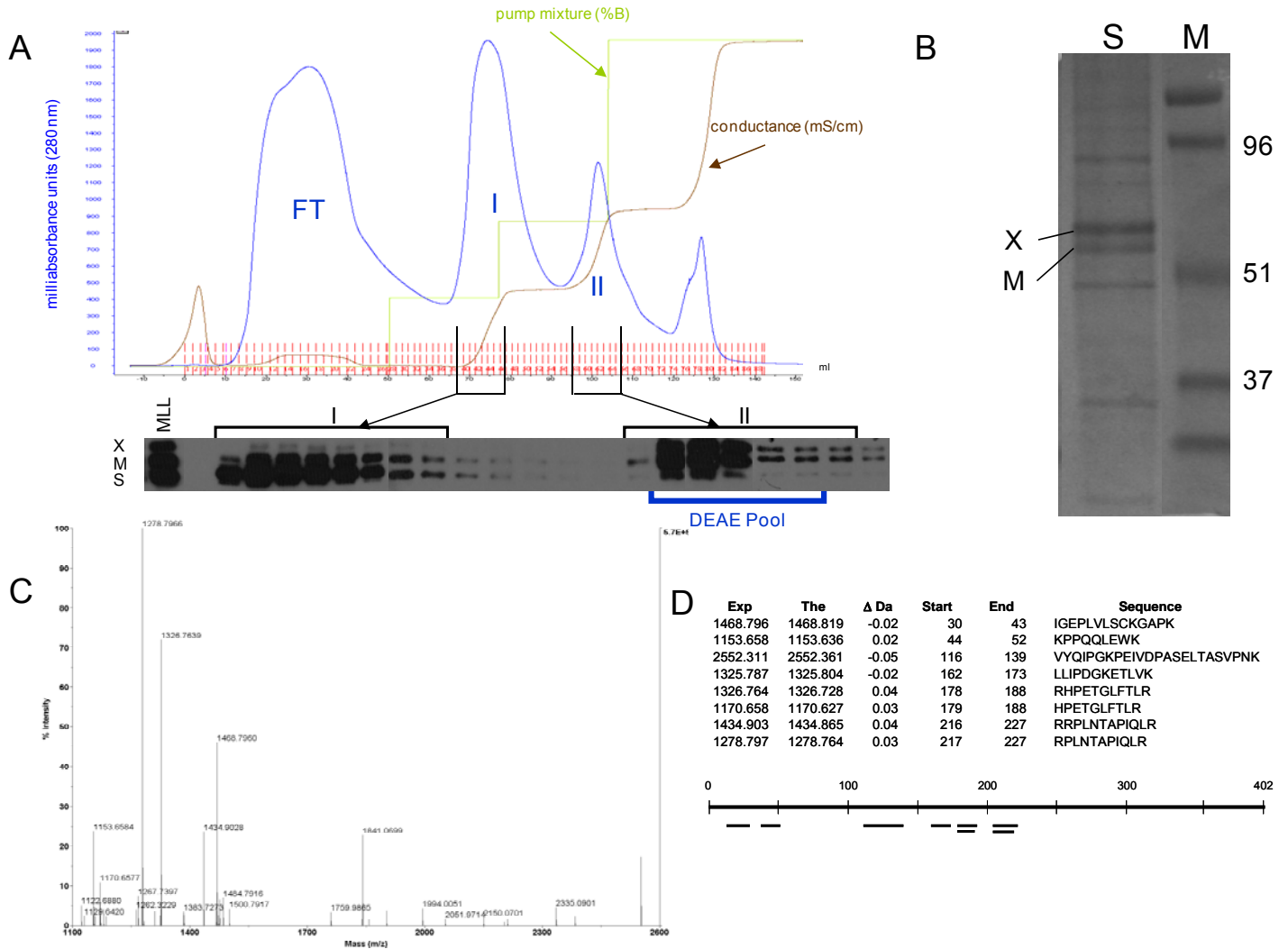


Figure 15. Purification and confirmation that xRAGE is an authentic RAGE isoform.

Lungs were prepared from 6 endotoxemic mice and lysed using RIPA buffer. This was diluted 1:1 in Buffer A (20 mM Tris, pH 7.5, 50 mM NaCl, 1% CHAPS, and 1 mM DTT) and applied to a DEAE Sepharose CL4B column (40 ml). Proteins were step eluted with 220 mM NaCl (Step I) and 460 mM NaCl (Step II) (A). xRAGE was detected in fractions by Western blotting and was enriched in Step II. This material was bound to a concanavalin A agarose column (10 ml), washed extensively until the eluent was within 2% of baseline absorbance, and eluted with 15 ml of 0.5 M methylmannopyranoside. The eluted material was concentrated and size-fractionated using SDS-PAGE (B). The xRAGE band was excised, subjected to in gel digestion with trypsin. Mass spectra were obtained (C) that contained several peptides (D) encoded by the mouse RAGE gene.

3.2.5 RAGE isoforms in mouse cell lines

Protein extracts were prepared from several mouse-derived cell lines including enterocyte-like CMT-93, pneumocyte-like LA-4, renal mesangial-like MES-13, pulmonary fibroblast MLF, embryonic kidney epithelial NIH 3T3, macrophage-like RAW 264.7 and adrenal cortical Y1 cells. Equal amounts of protein were subjected to Western blot analysis (Fig. 16). Mouse lung lysate is included for comparison. N-16 detected a single 50 kDa band in CMT-93 cells while the other cell lines were negative for N-16 staining. H-300 antibody failed to detect any bands in any of these cell lysates (data not shown). α ES antibody detected an approximately 43.2 kDa isoform in each cell line. All cell lines, except Y1 adrenal cells, also expressed an esRAGE isoform with apparent molecular weight of 69.4 kDa. Additional lighter bands were also apparent in several cell lines.

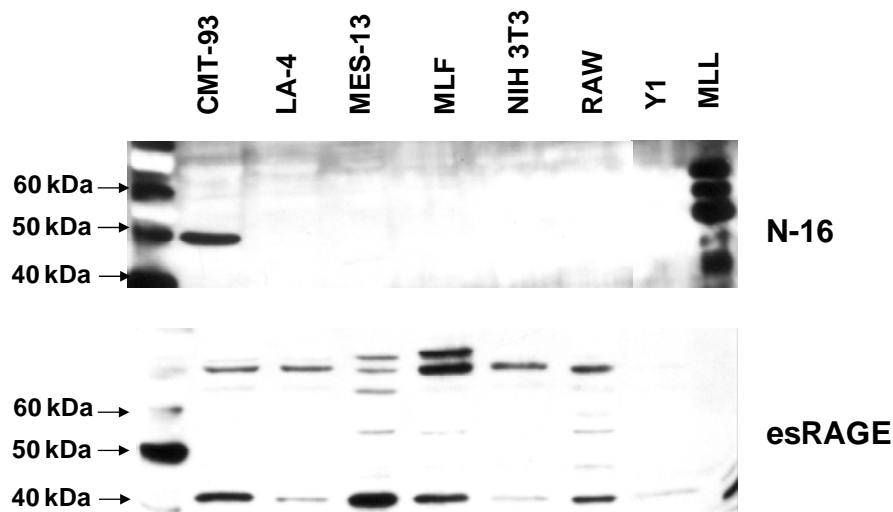


Figure 16. Comparative Western blot analysis of representative established mouse cell lines.

Cell lysates prepared in RIPA buffer were resolved on the SDS-PAGE gel system and probed with the indicated antibody. This blot is representative of at least 3 experiments.

3.2.6 Protein N-glycosylation of RAGE protein isoforms

The primary mouse RAGE sequence predicts two N-glycosylation sites, and this was confirmed experimentally for the lung canonical transmembrane (49) and soluble (61) RAGE isoforms. PNGase F digestion was used to compare N-glycosylation of various RAGE protein isoforms. xRAGE, mRAGE and sRAGE isoforms expressed in mouse lung lysate showed increased mobility on SDS-PAGE of approximately 3.4 kDa following PNGase F treatment (Fig. 17). This difference is consistent with the removal of two N-linked glycans of approximately 1.7 kDa each. RAGE isoforms identified in non-lung tissues using N-16 (Fig. 17) and α ES (Fig. 18) were insensitive to PNGase F digestion. This is important as these bands are not present in tissues from RAGE knockout mice (see Fig. 12) which supports our contention that non-lung tissues express a RAGE isoform with a distinct protein sequence compared to canonical pulmonary-thyroid RAGE. The implications of this for ligand recognition and subsequent signal transduction remain to be determined. RAGE isoforms detected with N-16 in human HEK 293 (Fig. 18), A549 and HMEC-1 (data not shown) cell lysates were insensitive to PNGase F digestion, suggesting that they were not N-glycosylated. In support of this finding, RAGE from the human enterocyte-like Caco-2 cell line was similarly not N-glycosylated (133).

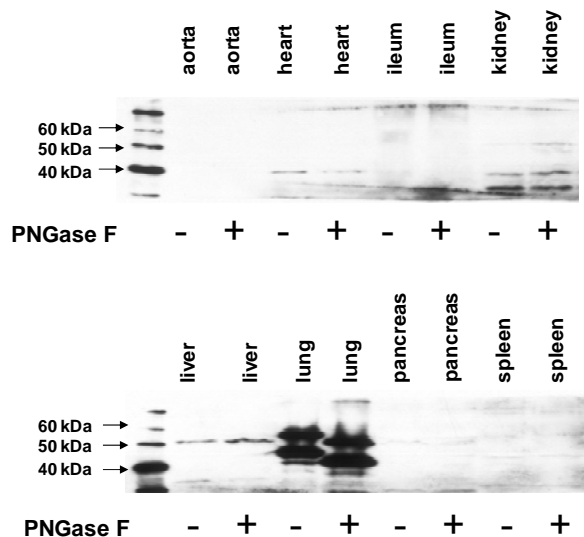


Figure 17. Mouse deglycosylation pattern of RAGE isoforms.

Mouse tissues indicated were homogenized in RIPA buffer and subjected to PNGase F digestions followed by Western blot analysis. Digested samples were run alongside with the undigested protein lysates. We used 25 μ g per lane for all the tissues except for the lung where we used 12 μ g. N-16 antibody was used to probe the membrane. This blot is representative of at least 3 experiments.

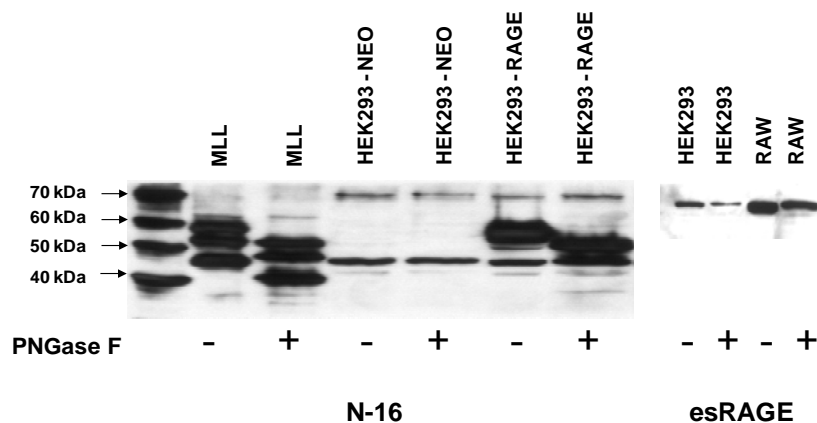


Figure 18. Comparative deglycosylation analysis of the mouse lung lysate.

HEK293 and HEK293 transfected with full-length RAGE. Control and PNGase digested samples were subjected to Western blot analysis. Notice that PNGase F does not affect migration of the endogenous RAGE band in both HEK293 and HEK293 transfected with the full-length RAGE. Transfected RAGE protein migrated similarly to the lung isoform. N-16 antibody was used to probe the membrane. This blot is representative of at least 3 experiments.

3.2.7 Non-pulmonary cells transfected with the lung RAGE cDNA express and N-glycosylate the canonical pulmonary membrane RAGE protein isoform

Transient transfection of HEK 293 (Fig. 18) and HMEC-1 (data not shown) cells with a human mRAGE cDNA expression vector (106) caused accumulation of a transcript the size of the predominant RAGE mRNA species expressed in mouse and human lung. Transfection with the empty vector was used as a negative control. Expression of the endogenous cell line RAGE transcripts did not change in transfected cells (Fig. 11). Transfected HEK 293 cells expressed a protein with the same mobility as pulmonary mRAGE (Fig. 18). Ectopically expressed pulmonary mRAGE was sensitive to digestion with PNGase F, increasing protein mobility by approximately 3.4 kDa. Expression of the endogenous cell line RAGE isoform that is detected with N-16 remained unchanged following exposure to PNGase.

3.2.8 Pulmonary cell lines transfected with full-length RAGE express mRNA but no detectable protein

We transfected three lung-derived cell lines (A549, CaLu-2, R3/1) with the full-length RAGE cDNA plasmid. Although their RAGE mRNA levels were significantly elevated (data not shown), we failed to detect any full-length RAGE protein (Fig. 19). Endogenously expressed RAGE protein isoforms remain unchanged.

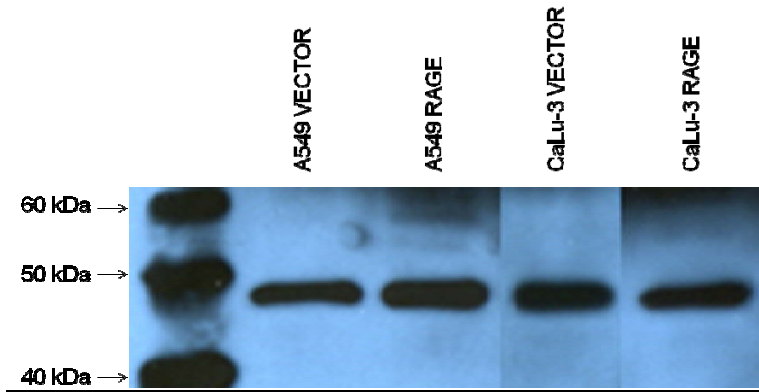


Figure 19. Lung-derived cell lines transfected with full-length RAGE do not express canonical RAGE protein. A549 and CaLu-3 cell lines were transfected according to the protocol. The cells express cell line endogenous RAGE isoform which stays unchanged after transfection. This blot is representative of at least 3 experiments. Western blot was used to access RAGE protein expression in 48 h.

3.2.9 Lung RAGE is N-glycosylated in mouse, human, rat and cow

N-glycosylation of lung RAGE is also found in human, cow and rat (Fig. 20 and unpublished observations). We performed a comparative deglycosylation analysis of RAGE isoforms in the above species. In mouse, rats and cows, only lung RAGE had two N-glycans, isoforms from other tested organs had none; in human lung RAGE could have three N-glycans and other tissues appear to have 1. Taken together our data suggest that lung RAGE differs from RAGE in other tissues in different species.

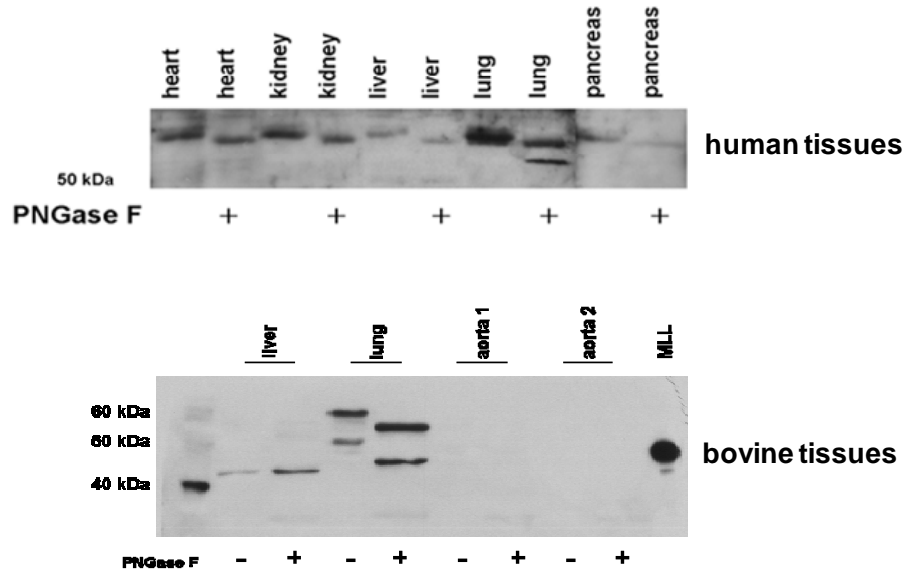


Figure 20. Comparative deglycosylation analysis of human and bovine tissues.

Control and PNGase F digested samples were subjected to Western blot analysis. Lung RAGE isoforms appeared to have more N-glycans in human and to be the only N-glycosylated isoform in cow. N-16 antibody was used to probe both membranes. This blot is representative of 2 independent experiments.

3.2.10 Mouse thyroid expresses the same RAGE isoforms as lungs

In Section 3.2.1, we showed that mouse thyroid expressed far more RAGE EST transcripts than lung. This, however, was true only for the mouse. Human and rat tissues did not follow the same trend. We analyzed mouse RAGE isoforms from thyroid in terms of antibody reactivity and PNGase sensitivity. To our surprise, we confirmed that mouse lung and thyroid indeed expressed the same RAGE isoforms. This finding was based on the antibody reactivity (H-300 antibody only identifies pulmonary RAGE) and PNGase sensitivity (Fig. 21). The same thyroid RAGE isoforms were also detected by N-16 antibody (data not shown). Thyroid, however, expressed far less RAGE protein than could be predicted from the EST transcript database (compare Table 2 and Fig. 21).

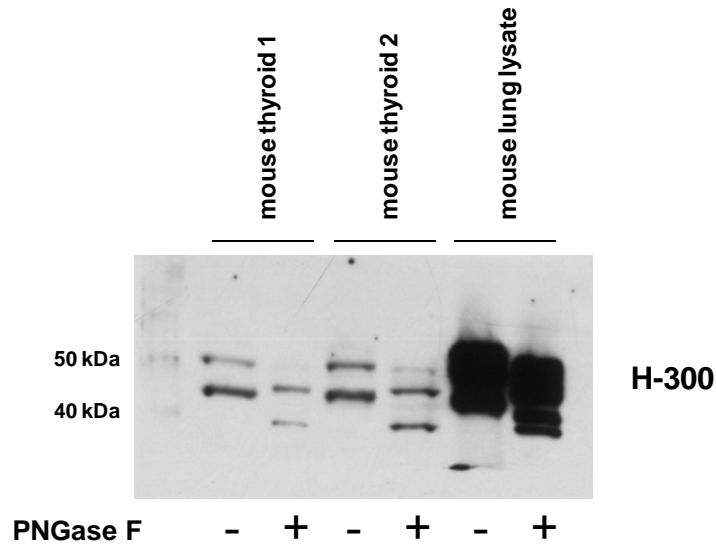


Figure 21. Comparative deglycosylation analysis of RAGE isoforms from mouse thyroid and lung. Control and PNGase F digested samples were subjected to Western blot analysis. Thyroid and lung RAGE isoforms appeared to have very similar sizes and N-deglycosylation patterns. Those are also only two on known to us organs that can be recognized by H-300 antibody which was used to probe the membrane. This blot is representative of 2 independent experiments.

3.3 DISCUSSION

Several conclusions can be drawn from these findings. First, of the tissues examined, lung expressed the highest levels of RAGE mRNA and protein. Second, in mice, the canonical transmembrane RAGE isoform (mRAGE) that was originally identified by Schmidt and colleagues in bovine lung extracts appears to only be expressed in lung and is detected by both H-300 and N-16. Third, transfection of cells with a pulmonary mRAGE cDNA expression vector permitted expression of an N-glycosylated pulmonary RAGE isoform (Figs. 10 & 17) showing that these cells are capable of protein N-glycosylation. This is important since the endogenous cell line RAGE isoforms were not N-glycosylated. Fourth, the RAGE-gene encoded α ES epitope was absent in RAGE^{-/-} mice and was expressed in all tissues examined. However, the α ES

epitope is not detectable in RAGE protein isoforms containing an N-16 or H-300 epitope, as is predicted by published mRNA sequences (67, 106) and Fig. 22. The inclusion of intron 9 in the esRAGE mRNA was predicted to result in early translation termination due to an in frame STOP codon. Therefore, these authors have assumed incorrectly that sequence upstream of the α ES epitope is the same as canonical RAGE.

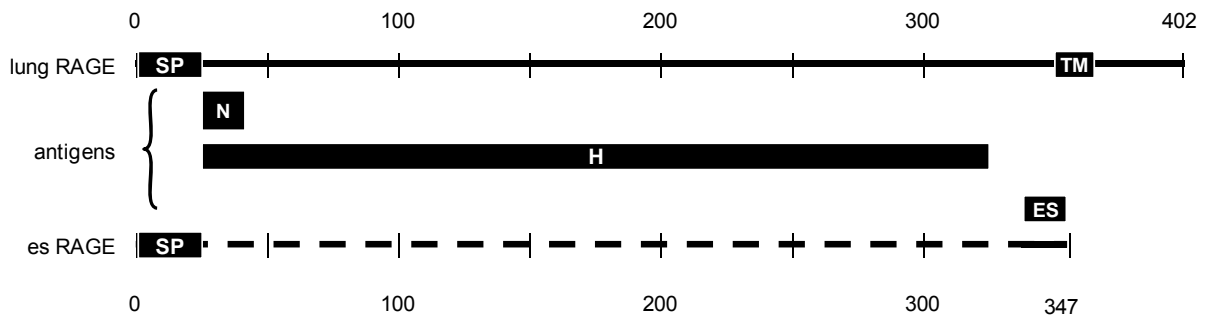


Figure 22. Cartoon showing positions of the N, H and ES immunogens used to generate the antisera.

While the canonical RAGE protein sequence is well established our data suggest that epitopes in N and H peptides are only co-expressed in lung RAGE isoforms. RAGE isoforms containing only the N epitope were identified. ES RAGE protein isoforms were detected but they were not co-expressed with the N or H epitopes as was proposed (67, 106). SP and TM stand for signal peptide and transmembrane domain, respectively.

The consequences of these studies are apparent when one considers them in light of data reported in the original manuscript by Schmidt and colleagues (48). An AGE-binding assay using newborn calf aortic endothelial cells was employed to assay fractions for the presence of AGE-binding proteins. Given that lung is about 50% endothelial cells and 50% epithelial cells (134), bovine lung served as a logical source material for their needs. A novel 35 kDa AGE-binding protein was identified using NH₂-terminal Edman degradation. Reverse translation of this sequence facilitated the cloning of the bovine cDNA which encodes a 44 kDa protein (GenBank NP_776407, refs 48, 49). The discrepancy between the predicted molecular weight is rather large and was not simply a resolution artifact of the gels. Subsequent studies by others

clearly show that the major site of expression of RAGE in lung is type I epithelial cells (33, 53). The bovine RAGE isoforms reported in studies of type I cells by Schmidt and colleagues are probably homologous to those recognized in Western blots of mouse, human and cow lung probed with H-300 (Fig. 12A&21). Figure 3A of reference 1 shows AGE-binding activity of fractions eluting from a hydroxylapatite column. Fractions with the highest AGE-binding activity were further purified for sequence analysis. This represented only 10% of the total AGE-binding activity applied to the column. We feel a significant proportion of the AGE-binding activity that did not co-elute with the 35 kDa bovine RAGE represents, at least in part, the N-16 and esRAGE isoforms expressed at significantly lower levels in the numerous additional cell types present in the lung. Thus, it is entirely possible that the AGE-binding activity present on the endothelial cells used in the identification of pulmonary mRAGE was actually a related esRAGE isoform. Alternatively, it may also be the bovine homologue of the non-N-glycosylated isoform recognized at low levels by N-16 that runs at 48 kDa in human cell lines and in the CMT-3 murine cell line. Additional studies are warranted to answer this important question.

Numerous esRAGE isoforms expressed in mouse lung may actually be expressed by a variety of cells including type I cells, alveolar macrophages and endothelial cells of smaller branching arteries and other components of the pulmonary tree. Our studies of mouse (Fig. 17) and human aorta and HMEC-1 cells (135) failed to detect the N-glycosylated mRAGE isoform that appears to be exclusively expressed in lung and thyroid. However, RAGE-gene derived protein isoforms that arise through alternative splicing of exon 9 which encodes the “es” epitope in mouse and human (106) are clearly present in mouse aorta and HMEC-1 cells.

We have seen that most cell lines express a cell line isoform of RAGE as determined by Northern (Fig. 11) and Western blotting (Figs. 6 & 8 and ref 135) and do not express the

endogenous full-length isoform expressed predominantly in lung and to a lesser extent in thyroid. Thus, these cells are not RAGE-negative, so the value of establishing a RAGE signaling pathway using them is suspect. Only when lung RAGE cDNA was expressed in cultured cell lines did they express full-length RAGE, suggesting that a special cellular environment is required. Hypoxia could be one of the factors as it was shown to alter expression and phosphorylation of translation initiation factors in lung and enhance their affinity for inhibitory proteins (4E-BP1). This ultimately resulted in the diminished protein synthesis (136). Lung RAGE might require specific oxygen concentrations to be expressed. RAGE also might need lung-specific transcription activators. For instance, expression of two forkhead related activator proteins (FREAC-1 and 2) is restricted to lung and placenta. Promoters of lung-specific genes (surfactant proteins A, B, C, and the Clara cell 10 kDa protein (CC10)) contain potential binding sites for FREAC-1 and FREAC-2. In the experiments with the cell lines FREAC-1 and FREAC-2, FREAC-1 activated transcription of the lung-specific genes (137). Later we discuss TTF-1, which also appears to be lung and thyroid-specific. When non-lung cells are transfected with the lung-specific RAGE, they might also express downstream signaling molecules that are specific for the RAGE isoforms expressed in cell lines and might be missing some elements only expressed in type I pneumocytes *in situ*.

Additional support for our belief that the non-lung RAGE isoforms are RAGE is as follows. In mouse, organs expressing detectable RAGE protein other than lung included heart, kidney and liver (Figs. 2 & 8). To get blots to work we needed to decrease stringency by decreasing the Blotto concentration and using longer exposure times. This may create a problem with specificity, however these bands were absent on Western blot from RAGE knockout mice. Additional confirmation is needed in the form of protein primary sequence which is the focus of

future studies. esRAGE isoforms expressed in these tissues were not N-glycosylated. Moreover, when we analyzed extracts derived from RAGE knockout animals, we only detected a single protein band on Western blot using α ES, suggesting that all other bands on that gel were in fact derived from the RAGE gene.

Our results are clearly incongruous with numerous publications describing “RAGE” expression in multiple animal tissues. We feel a major reason for this discrepancy comes from the fact that investigators assayed RAGE expression using tissue immunostaining (138) and ELISA (139). Importantly, Western blotting was not used; therefore, no conclusions should be made concerning isoform size and the extent of N-glycosylation. More importantly, we have data that suggests that canonical RAGE is not expressed at all in non-lung/thyroid tissues during normal and inflamed states. This is however the point that many of these authors are trying to make (i.e. that “RAGE” is expressed). Immunostaining alone cannot distinguish between RAGE isoforms. Significant information was obtained in our Northern blot studies. Clearly different mRNAs encode the distinct RAGE isoforms in mouse lung and thyroid, non-lung, and cultured cells. In rats and dogs, full-length mRAGE is only present in the lung (50, 59). It appeared on the Northern blot as a clear 1.4 kb signal in mouse and human total RNA (Fig. 11). This band is clearly absent from non-lung tissues (thyroid was not tested) and all cell lines, and we feel it represents RNA encoding of the H-300 and N-16 epitopes of RAGE. These data also suggest that the other RAGE-gene derived protein isoforms are clearly encoded by distinctly different mRNA.

In mouse lung, in addition to the two pulmonary mouse RAGE isoforms, an isoform was observed, which we designated xRAGE, which is induced in mice injected with endotoxin. It appears at 1 h post-treatment and remains elevated until at least 24 h. We were unable to obtain

complete sequence coverage for the xRAGE isoform; yet we confirmed that this was indeed a RAGE isoform using MS. Several possibilities exist: first, xRAGE could represent cell population of RAGE precursor still carrying signal peptide; LPS could cause an increase in RAGE production due to NF- κ B activation and the cells don't process it fast enough. Second, RAGE might go through some post-translational modification(s) to become xRAGE. We don't think that it involves N-glycosylation, because all three RAGE isoforms carried 2 N-Glycans that were removed by PNGase F (Fig. 18). However, other post-translational modifications that were not addressed (acetylation, amidation at C-terminus, modification by covalent attachment of the small ubiquitin-related modifier (SUMO), and many others) are plausible. Such modification could serve as a part of inflammatory response of the cell. As of now, we know very little about the exact nature of xRAGE, further investigations are needed to better understand the regulation of its expression and the role in the lung.

We evaluated RAGE isoforms expressed in different tissues and cell lines. Mouse organs, other than the lung and thyroid, and cell lines expressed distinctive RAGE isoforms which are not N-glycosylated and most likely have different primary sequences. The same is true about human, cow and rat. The RAGE isoform expressed in a particular tissue or cell line appears to depend upon the cell type and the cellular microenvironment. The reasons why thyroid expresses the same RAGE isoform as lung are currently unclear as are the exact mechanisms underlying the regulation of RAGE protein expression in general. Taken together, the data indicate complex expression and kinetics of RAGE isoforms with the undetermined role for each one of them in ligand recognition and signaling.

Based on these observations, we hypothesize that lung- and thyroid-specific RAGE isoforms are different not only structurally, but also functionally. The selective and relatively high level of

mRAGE expressed in type 1 alveolocytes suggests an important and underappreciated role for these protein isoforms in pulmonary homeostasis. This is supported by the fact that RAGE-null animals are more susceptible to the idiopathic pulmonary fibrosis (60). RAGE was found to play a crucial role in cell attachment to the basement membrane through collagen IV (33). Furthermore, N-glycosylation, which is specific to the pulmonary and thyroid RAGE, is very important in ligand recognition (140). The lung tissue microenvironment is able to drive the specific splicing/proteolytic events that are required for specific lung RAGE isoform synthesis.

In conclusion, we attempted to make sense of the numerous studies of RAGE isoform expression that have been published to date; we investigated the topic using a broad approach to examine RAGE isoform expression. We were able to identify thyroid as an organ expressing the same RAGE isoforms as lung using EST database. Thyroid RAGE isoforms appear to have the same molecular weights and deglycosylation patterns (two N-glycans) as the pulmonary isoforms. The respiratory system, along with thyroid and other organs (pancreas, liver etc.), arises from the ventral foregut endoderm which differentiates into various epithelial cell types (141). In addition, lung and thyroid progenitors could be identified in embryo at day 9 (E9) by expression of thyroid Nkx2.1 expression. Nkx2.1 is also known as thyroid transcription factor 1 (TTF-1). Nkx2.1 knockout mice have lungs, but they are highly abnormal (142). They consist of cystic structures lined by columnar cells with scattered cilia similar to those found in proximal airways. So, Nkx2.1 was found to be crucial in distal (alveolar) airway development (142). Also, Nkx2.1 could play a role in the epithelial-mesenchymal interactions based on the finding that collagen type IV and several integrins were extremely deficient in the Nkx2.1-null animals (143). Interestingly, collagen IV was found to preferentially interact with RAGE proteins in the RAGE-transfected HEK 293 cells, making it crucial for cell spreading and morphology (33).

Nevertheless, thyroid RAGE isoforms are not expressed at the high lung levels despite the abundance of RAGE transcripts. Further investigations are needed to elucidate the significance of canonical RAGE in the tissue. We feel this “forest for the trees” view will be helpful in designing future studies of RAGE isoform expression in particular, as well as assist investigators in designing and interpreting studies of RAGE function in general.

4.0 CHAPTER FOUR – RESPONSE TO THE RAGE LIGANDS IN VARIOUS TISSUES AND CELL LINES

4.1 ABSTRACT

RAGE was purified and sequenced from bovine lung extract 17 years ago, but the exact mechanisms of its signaling are still unclear. It is thought to involve ERK-1/2 kinases, p38, SAPK/JNK kinases, rho-GTPases, phosphoinositide 3-kinases, JAK/STAT pathway, and NF- κ B (43). One publication reported direct binding of ERK to RAGE, however those observations were made in RAGE-transfected cells (88). There is a whole body of literature debating the signaling events taking place following stimulation with “RAGE” ligands. Some of these false positive effects are explained by not using the appropriate controls (BSA with AGEs) or contamination of the “RAGE” ligands with LPS. In our hands, the human microvascular endothelial cell line (HMEC-1) was responsive to the “RAGE” ligands S100B and HMGB1. S100B upregulated monocyte chemotactic protein 1 (MCP-1) expression whereas HMGB1 downregulated it in a dose-dependent manner. When applied together, HMGB1 abrogated S100B-mediated effects. This trend did not change when HMEC-1 were transfected with full-length RAGE. All other utilized cell types, including two lung-derived lines, did not respond to the “RAGE” ligands when we assayed for NF- κ B activation and MCP-1 expression. HEK 293 cells did not respond to “RAGE” ligands even after being transfected with the plasmid encoding

the full-length RAGE sequence. When we used mouse lung slices (MLS) as a system expressing canonical full-length lung RAGE, we did not register a response from the “RAGE” ligands using these same assays. However, RAGE expression seemed to be important for the inflammatory response caused by LPS and IL-1 β . When comparing MLS from RAGE knockout mice to the wild-type controls, LPS-induced MCP-1 expression was consistently higher in the wild-type mice. These didn’t seem to suggest that lung RAGE plays a role in the inflammatory response. We also concluded that in cell lines, “RAGE” ligands do not apparently signal through RAGE, but through other receptors.

4.2 RESULTS

4.2.1 “RAGE” ligands do not activate NF- κ B in A549, HMEC-1 and HMEC-1 transfected with the full-length RAGE

NF- κ B is believed to take part in RAGE signal transduction. Two cell lines available to us were tested. These were human A549 cells, which were derived from lung, and HMEC-1, a human microvascular endothelial cell line (144). Since we were unable to detect canonical RAGE when the full-size RAGE cDNA was transfected into lung-derived cell lines (Section 3.1.8), we only used transfected HMEC-1 cells for some studies. NF- κ B binding was analyzed upon application of ‘RAGE’ ligands including AGEs, S100B and HMGB1 to A549, HMEC-1 and HMEC-1 cells transfected with the full-length RAGE. IL-1 β was used as a positive control for the assay. We failed to observe increased NF- κ B binding when we applied “RAGE” ligands (Fig. 23). This was surprising since many publications suggest that a lot of cellular responses to RAGE ligands are

mediated, at least in part, by NF- κ B. When we exposed HMEC-1 cells to IL-1 β we observed nuclear translocation of NF- κ B, confirming the integrity of that pathway in these cells.

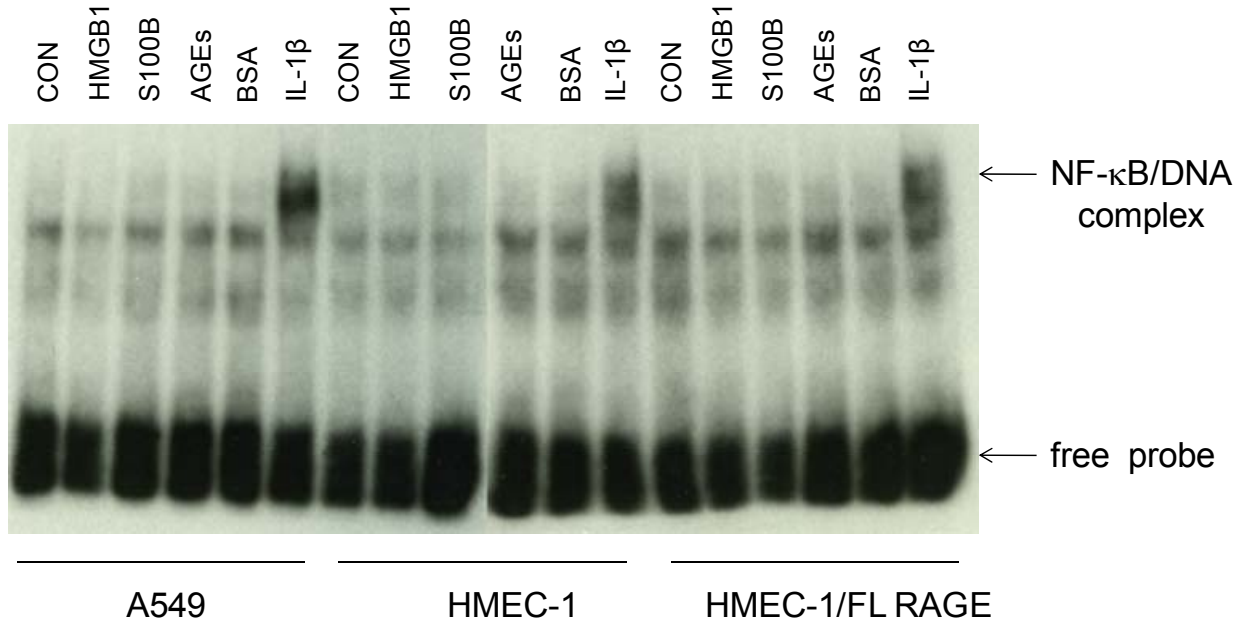


Figure 23. NF- κ B activation in sample cell lines.

EMSA was performed in A549 (lung-derived cell line) and HMEC-1 (non-lung derived cell line). HMEC-1 cells were transfected with the full-length RAGE and with the vector. A549 do not express full-length RAGE when transfected therefore transfected cells were not used (Section 3.1.8). Cells were assayed 30 min after stimulation. IL-1 β was used as a positive control. This blot is representative of 3 independent experiments.

4.2.2 “RAGE” ligands alter MCP-1 mRNA expression in the HMEC-1 cell line:

S100B induces and HMGB1 suppresses it

MCP-1 mRNA was reported to be induced by S100B in HMEC-1 cells using microarray analysis (78). We used S100B as well as HMGB1 and AGEs and measured MCP-1 mRNA as a readout. While we were unable to see any effect caused by AGEs, we registered a dose-dependent increase of MCP-1 mRNA induced by S100B. HMGB1 alone decreased MCP-1 basal levels. When added together, HMGB1 abrogated S100B-stimulated effects (Fig. 24).

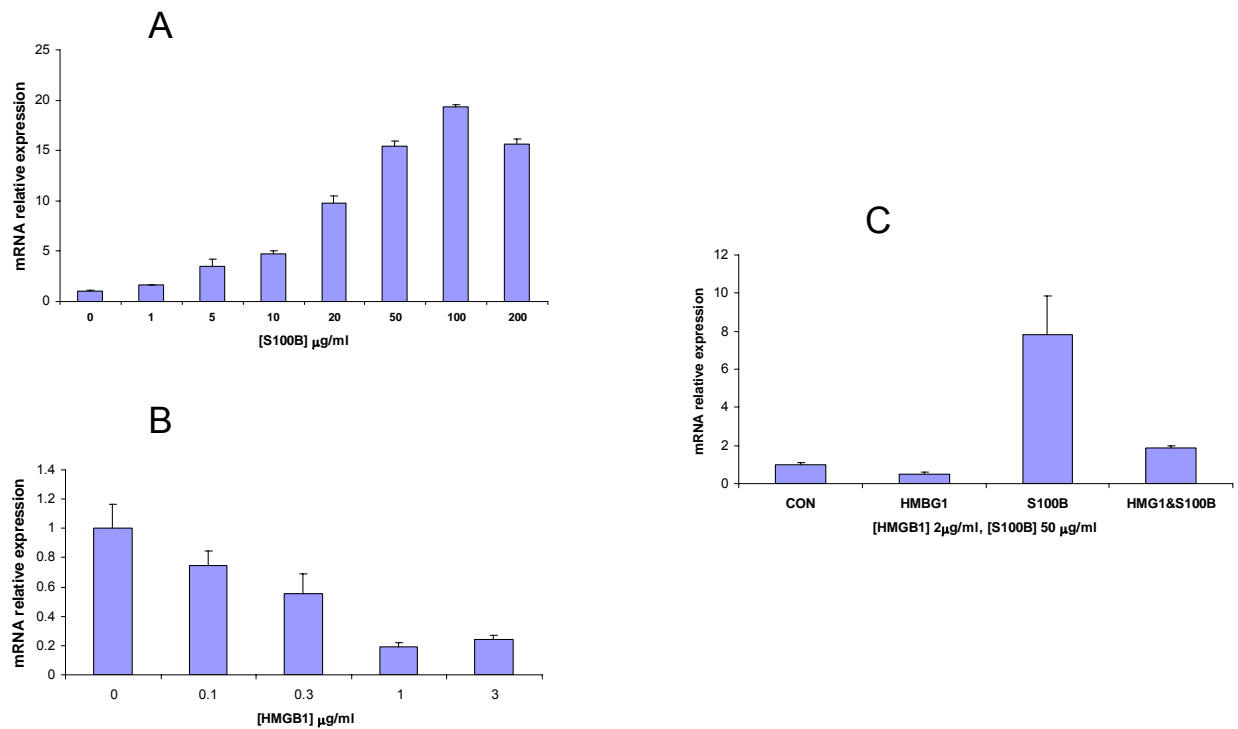


Figure 24. MCP-1 mRNA dose response to increasing concentrations of S100B (A) and HMGB1 (B). HMEC-1 cells were grown and stimulated as described. MCP-1 steady-state mRNA was measured in 18 h. using real time RT-PCR. Interestingly, HMGB1 appears to inhibit S100B induction of MCP-1 mRNA expression (C). Result are presented as means \pm SD (N=3).

4.2.3 Anti-RAGE antibody (N-16) inhibits MCP-1 upregulation by post-induction repression

HMEC-1 cells were pretreated with anti-RAGE antibody (N-16) for 10 min in an attempt to inhibit responses to S100B. When MCP-1 mRNA was measured using RT-PCR, no response was registered as a result of S100B treatment. This was also true for IL-1 β that was used as a positive control (Fig. 25A). In our hands anti-RAGE antibody was capable of inhibiting both S100B and IL-1 β responses despite the fact that IL-1 β is not a RAGE ligand. We then decided to

treat cells with anti-RAGE antibody alone to eliminate its direct effects on the cells (Fig. 25B). We registered MCP-1 response early (2 h), and it returned to baseline levels by 24 h time point. This is consistent with anti-RAGE antibody stimulating the cells by itself. We hypothesized that N-16 could cause dimerization of RAGE thus activating it. After the initial stimulation cells were not able to respond to other pro-inflammatory stimuli.

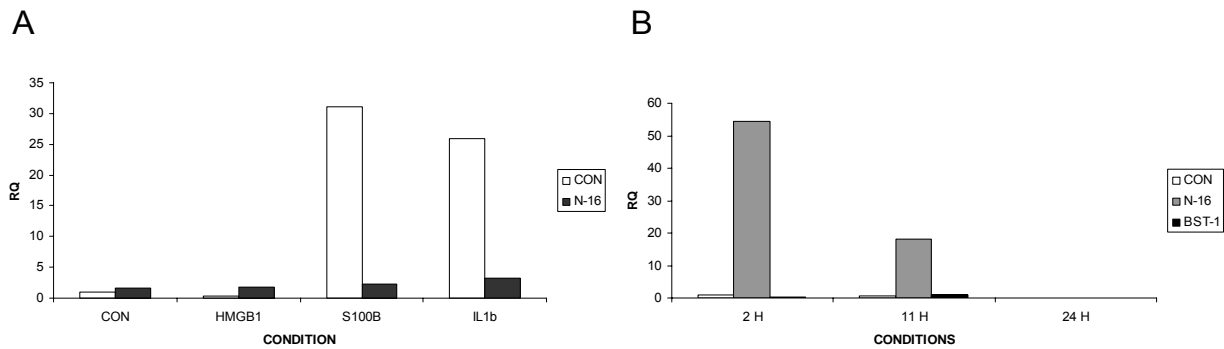


Figure 25. Anti-RAGE antibody (N-16) inhibits MCP-1 mRNA upregulation by S100B and IL-1 β (A) as measured by MCP-1 mRNA increase (real time RT-PCR) in HMEC-1 cells. HMEC-1 cells were pretreated with N-16 anti-RAGE antibody 10 min prior to applying RAGE ligands. MCP-1 mRNA was measured with real time RT PCR 18 h later as a respond (A). In B HMEC-1 cells are responding to N-16 antibody alone; BST-1 was used as an unrelated control. N-16-mediated response is completely gone by 24 h. This experiment was repeated twice.

4.2.4 “RAGE” ligands failed to stimulate A549 and HEK 293 cell lines

Since we were able to measure an affect caused by RAGE ligands in HMEC-1 cells, we sought to examine other cell types, especially those derived from lung. Lung appears to express the majority of RAGE as compared to other tissues, and the full-length RAGE isoform is unique to the lung (See Chapter 3). A549 is a human lung-derived cell type and HEK 293 is an epithelial type, derived from the human embryonic kidney. Both cell lines failed to express MCP-1 mRNA changes following stimulation with RAGE ligands, while IL-1 β , which was used as a positive control, induced MCP-1 expression (Fig. 26). Among all tested cell lines, including two derived

from lung, HMEC-1 was the only line that responded to “RAGE” ligands using NF- κ B or MCP-1 expression as read-outs.

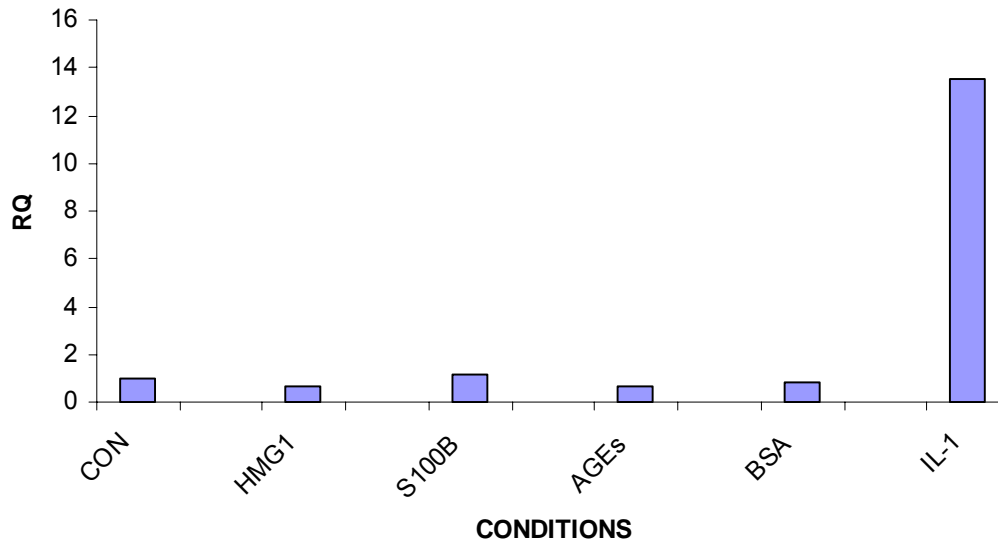


Figure 26. MCP-1 expression in A549 cells in response to the “RAGE” ligands.

A549 cells were grown and stimulated as described and assayed 18 h later. MCP-1 steady-state mRNA was measured 18 h later with the real time RT PCR. Experiment was done twice.

4.2.5 “RAGE” ligands fail to stimulate mouse lung slices (MLS), but RAGE is important in the inflammatory response to LPS and IL-1 β

In our experiments, we were unable to find a cell line or tissue other than lung that expresses the RAGE receptor originally sequenced from bovine lung (48) (See Chapter 3). Consequently, the MLS *in vitro* system was used to test “RAGE” ligands. MLS express lung RAGE *ex vivo* for at least a week (data not shown). As for HMEC-1 cells, we used MCP-1 as a readout. We were unable to measure any response to the “RAGE” ligands that were different in wild-type

compared to RAGE knockout mice. However, the inflammatory response to LPS and IL-1 β was consistently lower in the knockout animals compared to wild-type (Fig. 27). Based on this observation, we concluded that these ligands do not use RAGE receptor in this system. Complex inflammatory responses to LPS and IL-1 β , on the other hand, were not complete without RAGE.

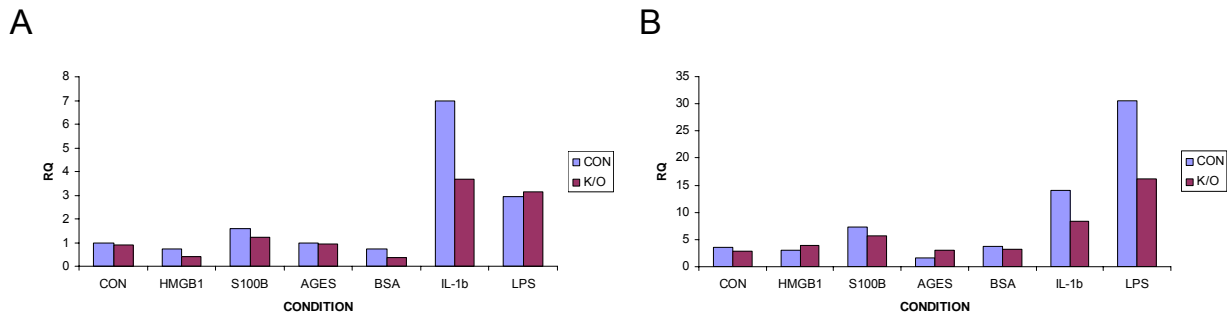


Figure 27. MCP-1 expression in mouse lung slices (MLS) following exposure to pro-inflammatory factors in wild type and RAGE knockout mice.

MCP-1 mRNA steady-state levels were measured with the real time RT PCR at 4 h (A) and 24 h (B). Experiment was repeated at least two times.

4.2.6 Mouse lung slices from RAGE knockout mice express less IL-6 and MCP-1 mRNA after LPS stimulation

In addition to real time RT-PCR we used the Luminex™ cytokine assay to measure levels of 20 cytokine mRNA per sample. Luminex™ technology does not require an amplification step. We wanted to compare cytokine expression of genes in wild-type and RAGE knockout mice in response to LPS. We analyzed mRNA levels at 24 h time point. IL-6 and MCP-1 mRNA were clearly different when comparing wild-type and knockout mice. It is possible that early responding cytokines (TNF α) were different as well; we are planning to analyze them in the future. In our hands two different assays (real time RT-PCR and Luminex™) showed differences in inflammatory response between wild-type and RAGE knockout mice. Further studies of signaling cascades are necessary.

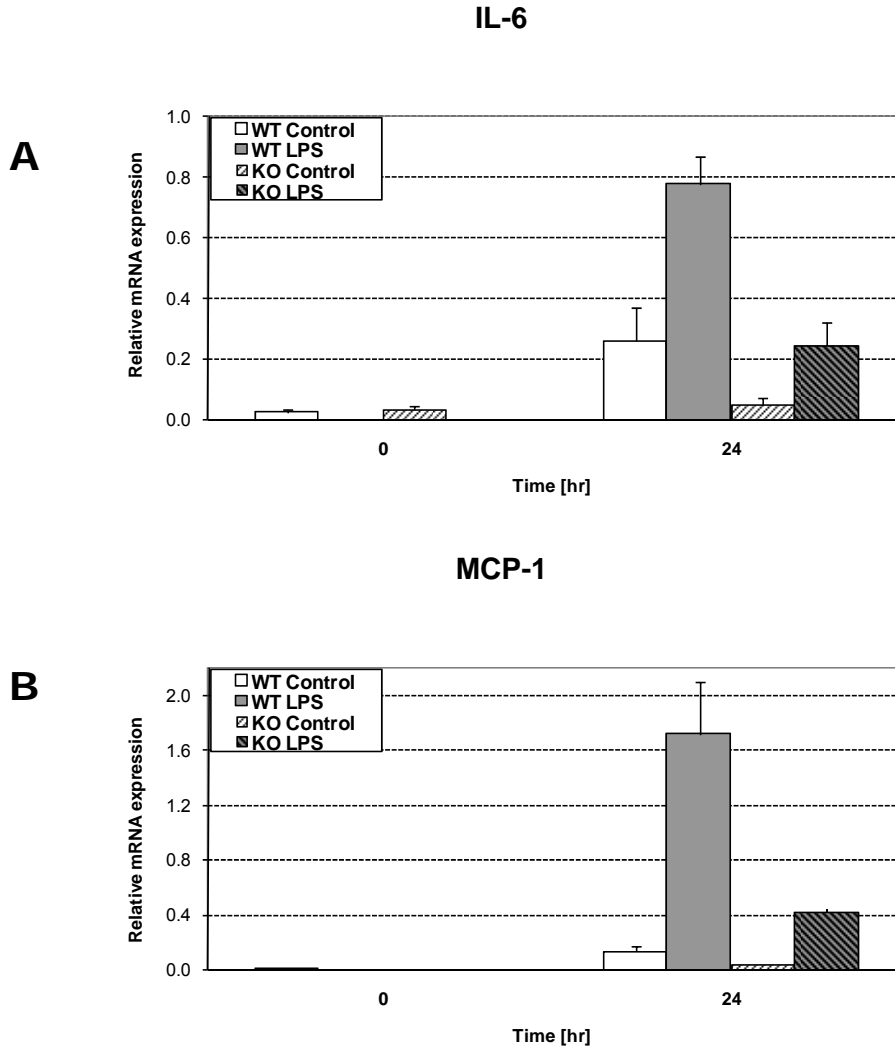


Figure 28. Luminex™ cytokine assay in MLS.

Mice were sacrificed by intraperitoneal injection of sodium pentobarbital, lungs were excised and MLS were prepared (see Methods). LPS was applied to the lung tissue cultures after 1 h in culture. MLS were lysed at 24 h and RNA was extracted according (see Methods). Each condition was assayed in triplicate. 100 µg of total RNA was assayed for inflammatory cytokines and chemokines using the BioSource International Mouse 20-plex Luminex™ beadset. The results were normalized to β-actin. IL-6 (A) and MCP-1 (B) mRNAs were different between wild-type and knockout mice. Results are presented as means±SD (N=4 per conditions).

4.3 DISCUSSION

Our signaling experiments do not cover all aspects of RAGE signaling. However, we tried to test most of the reported RAGE readouts. Among the cell lines tested, only HMEC-1 was responsive to S100B and HMGB1 in a dose-dependent manner when MCP-1 was used as a readout. At the same time, we failed to measure NF- κ B activation in those cells, so S100B and HMGB1 signaling appear to utilize NF- κ B. N-16 recognize a RAGE isoform in HMEC-1 so we tried to block signal with α RAGE antibody. The experiment produced the expected results for S100B but not for IL-1 β which does not signal through RAGE. It was therefore hypothesized that N-16 was stimulating cells by dimerizing the RAGE receptor and that this prevented them from responding to other pro-inflammatory stimuli, which is known as post-induction repression. When we exposed HMEC-1 cells to the anti-RAGE antibody, we saw a strong early response (MCP-1 mRNA) that completely disappeared by 24 h. We are planning digest N-16 RAGE antibody with papain to obtain monomeric Fab fragment antibody preparation. This would allow us see if the Fab fragment alone would cause cell activation. We don't expect to activate the cells because we will not dimerize RAGE receptor.

We will then crosslink antibody fragment with anti-Fab antibody and measure MCP-1 mRNA expression. We would expect constitutively increased MCP-1 expression with no impact from IL-1 β . Further experiment would be needed to clarify RAGE signaling cascade.

Although other cell lines appear to express a 'cell line' RAGE isoform, they do not respond to "RAGE" ligands when tested using accepted RAGE-dependent responses. Each "RAGE" ligand is able to bind receptors other than RAGE, so it is possible that S100B and HMGB1 employ other signal cascades in HMEC-1 cells.

Our laboratory has published data of CaCo-2 cells permeability and how HMGB1 affected it (145). CaCo-2 cells are grown on transwells and are commonly used as a model of intestinal permeability. It is widely used for drug absorption, metabolism and toxicity (146). As expected, HMGB1 increased permeability of CaCo-2 monolayers as measure by FD4 clearance. It also increased NO \cdot production in the cell supernatants. Anti-RAGE antibody (N-16) significantly reduced both effects of HMGB1. Unrelated antibody (raised against myosin light chain) did not have any effect on both permeability and NO \cdot production; however, IL-1 β positive control experiment was not done. Based on the HMEC-1 data we now think that anti-RAGE antibody could have prevented IL-1b hyperpermeability and NO \cdot production despite the fact that IL-1 β signaling has not been shown to depend on RAGE. We hypothesize that it could utilize the same mechanisms we discussed earlier (post-induction repression). It is important to use positive and negative controls in every experiment.

Further arguments of RAGE ligands not been able to signal through canonical RAGE come from the fact that MLS that express the lung RAGE isoform do not respond to “RAGE” ligands either. Although RAGE was convincingly shown to bind “RAGE” ligands, signaling events were always shown to be less credible (78). RAGE signaling is thought to be of a somewhat inflammatory nature, so LPS contamination of the ligand could mimic RAGE signaling, as it is viewed at the present time. A comparison of the response of wild-type and RAGE knockout MLS to general pro-inflammatory stimuli (LPS, IL-1 β) points to RAGE as an amplifying factor in the immune response as suggested (41). RAGE could interact with the pro-inflammatory factors released at the site of inflammation. However, it does not respond to AGEs, S100B and HMGB1 (Fig. 27). A more detailed study is needed to better define its role in this model as MLS

appear to be the only *in vitro* system that expressed full-length RAGE receptor at the lung microenvironment.

5.0 CHAPTER FIVE – SUMMARY AND CONCLUSIONS

RAGE was first purified and sequenced from bovine lung extract based on its specific interaction with AGEs (48). It belongs to the immunoglobulin family of cell surface receptors and in addition to AGEs binds HMGB1, S100/calgranulin protein family members, and amyloid- β peptides. RAGE is thought to be ubiquitously expressed with the higher levels expressed in the lung compared to other tissues that are thought to express “low” levels of RAGE. Ligand binding to RAGE is thought to trigger a whole range of cellular responses: generation of ROS and activation of NADPH (147), mitogen activated protein (MAP) kinase ERK 1/2 (p44/p42), stress-activated protein (SAP) kinases p38 and JNK, and the downstream NF- κ B signaling cascades (66, 85-87).

Our major conclusion of Chapter 3 states that originally sequenced pulmonary RAGE protein, referred to herein as canonical RAGE, is only expressed in lung and thyroid. Our data clearly indicate that non-lung organs and cell lines express distinct non-canonical isoforms of RAGE. Therefore, RAGE signaling studied in non-lung organs is suspect at best. However, general agreement that RAGE is ubiquitously expressed supports publication every year of a large number of research papers regarding the role of RAGE in organs including liver, pancreas, and heart. Canonical RAGE is not expressed in these organs, thus it cannot play a direct role in the pathologies of those organs.

Studies of RAGE signaling in cell lines are a major concern in light of our findings. Studies using wild-type or RAGE-transfected cell lines are suspect for two reasons. First, in wild-type cells what RAGE isoform if any is responsible for signaling observed. Second, can we expect cell lines to express lung-specific signaling components in a non-lung environment? Simply transfecting cells with full-length canonical RAGE cannot be expected to upregulate downstream signaling components. However, the majority of RAGE studies are performed in cell lines! We will try to clarify these issues using several examples of animal and cell studies below.

In 2005 Cataldegirmen and colleagues examined the role of RAGE in liver regeneration after massive liver injury (148). They observed better results in the RAGE knockout animals and when using anti-RAGE antibodies. Animals had better survival, better hepatocyte proliferation rates and more regeneration-promoting cytokines (TNF α , IL-6 and IL-10). However, the authors used RT-PCR and immunofluorescence in an attempt to establish RAGE expression in dendritic cells in the liver. Those two methods don't detect protein size or N-glycosylation state. These assays can therefore lead to false positives. We know that anti-RAGE antibodies see many non-canonical RAGE gene-derived isoforms that are present in non-lung tissues. However, their ligand binding and signaling have never been studied. We conclusively showed that pulmonary RAGE is not expressed by liver; other RAGE isoforms might be present. Interestingly, anti-RAGE antibodies or sRAGE increased survival of the animals, suggesting some other yet unidentified mechanisms that are involved. Raman et al. investigated the role of RAGE in pathogenesis of intestinal barrier dysfunction after hemorrhagic shock and reperfusion (HS/R) (104). These authors never even attempted to document the expression of RAGE in this tissue. Regardless, sRAGE treated mice and RAGE knockouts were protected from HS/R based on

bacterial translocation to mesenteric lymph nodes and ileal mucosal permeability to FITC-labeled dextran. In addition, IL-6 levels were higher and IL-10 levels were lower in the wild-type mice compared with the RAGE knockouts. Aleshin et al. evaluated the contribution of RAGE to myocardial injury (103). Although they used Western blot analysis to detect RAGE in the heart, the source anti-RAGE antibody was not specified, the apparent size of RAGE on the blot was not specified and degree of N-glycosylation was not addressed. Our data indicate that canonical pulmonary RAGE isoform is not expressed in the heart. However, their results also showed that RAGE knockout mice and mice treated with sRAGE were protected from ischemia-reperfusion damages. The role of RAGE was also studied in promotion of skin tumor development through sustained inflammation (149). These authors demonstrated that RAGE knockout mice were less prone to develop tumors; however, RAGE expression in the skin was shown only with immunofluorescence. It is common to study RAGE signaling in models that are not well defined. Researchers need to determine which RAGE isoform if any is responsible for RAGE signaling. If they use cells transformed with RAGE, then data should be confirmed in tissues expressing canonical RAGE (lung, thyroid).

In spite of the problems discussed above, sRAGE can still play protective role in various diseases involving non-lung tissues. That is consistent with the observation of Liliensiek and colleagues (150) where administered sRAGE reduced inflammation in both wild-type and RAGE knockout animals possibly based on its interaction with potential RAGE ligands that are capable of triggering inflammation without RAGE. When sRAGE, which is considered to be a decoy for all RAGE ligands, is artificially introduced into the system, it binds them and therefore serves as anti-inflammatory substance. Although sRAGE seems to be protective in most studies, adding it to the biological system is artificial. In fact, we have never detected sRAGE in serum from

normal or LPS exposed rodents or human (data not shown). Up to date there is no hard evidence that canonical sRAGE is ever in serum. Most authors seem to show Western blots of RAGE at best and the degree of N-glycosylation is never addressed. It is entirely possible however, that some tumors, especially of lung and thyroid origin, can express canonical RAGE with correct degree of N-glycosylation, and consequently be able to signal correctly as is seen in type 1 alveolocytes. This topic, though, has never been investigated.

It is important to address usage of anti-RAGE antibodies in treatment of experimental diseases (reviewed in 151). For example, as it was mentioned before, Cataldegirmen et al. used anti-RAGE antibody in their model of regeneration after liver injury. It appeared that in their study, anti-RAGE treatment had a positive effect on animal survival, liver regeneration and cytokine expression. Our data indicate that canonical RAGE is not expressed in liver. What mechanisms can explain how an anti-RAGE antibody can have an effect in the tissue that does not express canonical RAGE and therefore does not have a pathway? We have two possibilities: anti-RAGE antibody binds non-canonical RAGE isoform(s) expressed in the liver and either blocks the signaling or signals through RAGE and induces post-induction repression. The latter hypothesis comes from our experiments with anti-RAGE antibody (N-16) in HMEC-1 cells (4.2.3). Antibody initially activated the cells making them unresponsive to IL-1 β stimulation. This concept still needs further research which is described in the next section.

esRAGE was first discovered by Yonekura et al. (106). They amplified cDNA from microvascular endothelial cells and pericytes based on the assumption that it expresses part of intron 9 of canonical RAGE together with the usual 8 upstream exons. Intron 9 codes for the transmembrane part of RAGE protein therefore newly discovered isoform was considered soluble. Cheng et al. (138) performed an esRAGE profiling in human organs by

immunohistochemistry using the same antibody raised against esRAGE. They identified four types of staining with esRAGE antibody in different organs but failed to verify esRAGE protein size by Western blot and no N-glycosylation studies were done. Our studies indicate that esRAGE is of a different size and not N-glycosylated which is in disagreement with previous predictions made on cDNA sequence. esRAGE in mouse and human sera do not have the same size as canonical RAGE (our unpublished observations). In addition, anti-esRAGE antibody did not recognize the canonical RAGE isoform, but detected multiple bands of different sizes in mouse tissues (Fig. 13A). Since they were not detected in the RAGE knockout animals (Fig. 13B), we concluded that esRAGE also comes from the RAGE gene; however it does not share sequences encoding the N-16 and H-300 epitope presentation. The sequence and function of esRAGE are still under investigation, as is the source of this protein in serum.

In our research we established that thyroid and lung are the only tissues expressing canonical RAGE which correspond to 1.4 kb on Northern blot. It carries two N-glycans. We initially showed this in mice and have also obtained the same results in human and cow. N-glycosylation was shown to influence RAGE ligand binding (140). All analyzed cell lines, of lung and non-lung origin, express 2 bands of 6 and 10 kb. RAGE isoforms from them were not N-glycosylated. When we transfected cell lines with canonical RAGE cDNA-containing plasmid, we can see 1.4 band on the Northern blot. However, only non-lung originated cell lines are able to express canonical RAGE protein with 2 N-glycans. That finding can be explained in several ways: mRNA stability could be affected in the lung-derived cell lines, mRNA translation could be compromised at the initiation and/or elongation stages. Experiments necessary to address these issues are proposed in the next section.

We believe that RAGE is only expressed in lung and thyroid and that is where we should study canonical RAGE signaling. There is something particular about lung microenvironment that allows RAGE to be transcribed and translated into the protein. Once the cells are removed from the lung certain roadblocks appear that prevent RAGE from being made. These findings can be exploited to learn more about regulation of RAGE expression in particular and lung development biology in general.

We hypothesized that thyroid transcription factor 1 (TTF-1, Nkx2.1) is involved in RAGE mRNA production. In the early development thyroid and lung both rise from ventral foregut endoderm and are identified by TTF-1 by embryonic day 9. Moreover, TTF-1 is a necessary factor for the production of thyroglobulin (152). In addition, we were able to identify two TTF-1 sites on the RAGE promoter *in silico*. TTF-1 was shown to be expressed in the majority of the human lung cell lines (including A549) (153) and it could possibly affect canonical RAGE mRNA (1.4 kb). In addition, two other transcription factors expression, forkhead related activator 1 and 2 (FREAC-1 and 2), is limited to lung and placenta (137). We don't exclude however other factors that could be involved in 'canonical' RAGE expression.

We believe that for the reason stated above 'canonical' RAGE has never been studied in the 'native' lung environment. Therefore we developed an *in vitro* assay for RAGE signaling using mouse lung slices (MLS). They express RAGE and hopefully other necessary components for studying signaling. Initially, we used MCP-1 mRNA measured by real time RT PCR as readout (78). We were able to compare MLS from the wild-type mice and RAGE knockout mice to account for the differences in respond to the known RAGE ligands (AGEs, HMGB1 and S100B). Interestingly, MLS produced similar responses. We realized that when we studied RAGE in the only *in vitro* system canonical RAGE is expressed the response to the RAGE

ligands was absent. However, we observed differences in response to IL-1 β and LPS, with the MLS from the RAGE knockout mice having a weaker response. This was consistent with RAGE being a factor amplifying immune response (41). We then measured a whole panel of mouse cytokines by a different method (Luminex™) to confirm the results. LPS-induced IL-6 and MCP-1 mRNA levels were different between wild-type and RAGE knockout mice at 24 h time point.

In conclusion, canonical RAGE is only expressed in two tissues: lung and thyroid. Cell lines express a different RAGE isoform(s) that has never been characterized at the molecular level. MLS appear to be the only model allowing the study of canonical RAGE signaling in an *in vitro* system. Additional studies are needed to better understand the function of non-canonical RAGE isoforms. Ligands that bind to these proteins must be identified to allow further studies of signaling pathways they act on and their roles in disease processes.

6.0 CHAPTER SIX – FUTURE DIRECTIONS

6.1 ‘CANONICAL’ RAGE EXPRESSION MECHANISMS

6.1.1 Lung-derived cell lines cannot express canonical RAGE

Lung-derived cell lines transfected with canonical RAGE are not able to produce canonical RAGE protein even though they express mRNA of the correct size. We propose to perform a series of fusion experiments with RAGE-transfected HEK293 and non-transfected A549 cells. HEK293 cells will express RAGE detectable by fluorescence-activated cell sorting (FACS). If we stably transfect each cell line with a surface marker (CD2 or CD14 for example) we can follow each cell type through fusion. The goal is to use FACS to sort heterokaryotic cells (containing more than one nucleus) that express both CD2 and CD14. These cells will have cytoplasm and a nucleus from both parents. If the inability of A549 cells to express RAGE protein is dominant then the fused cells will not express RAGE protein. In this case, we predict that A549 cells express some factor(s) inhibiting translation of the transfected RAGE mRNA. Alternatively, RAGE protein may be rapidly degraded in A549 cells. This could be due to the expression of RAGE-specific microRNAs, small regulatory molecules that have been shown to inhibit protein expression. Although the exact mechanisms of their actions are not known, they have been shown to work by repressing translation and/or by promoting mRNA degradation

(154). In this case, microRNA expressed in lung-derived cells grown outside the lung would prevent transcription of the ectopically expressed RAGE mRNA. Those microRNAs would not be expected to be expressed in the lung or thyroid tissues *in situ*, but would be upregulated in lung-derived cell lines. Several other factors are known to inhibit translation initiation and elongation. Eicosapentaenoic acid, for example, has been shown to inhibit translation initiation through a range of processes leading to inhibition of eukaryotic initiation factor 2 (155).

If the fused cells resulting from transfected HEK293 and non-transfected A549 cells continue to express RAGE, it may be due to some deficiency in A549 cells that has been overcome by cytoplasm from HEK 293 cells. In other words, the phenotype of the A549 cells would be expected to be recessive. A549 cells may be deficient in transcription initiation and elongation factors that are lung and thyroid specific. In this case non-lung cell lines could express some other translation factors that are able to make up for its absence. It is also possible that RAGE protein is synthesized in A549 cells, but misfolded and targeted for rapid degradation. That could happen due to lack of correct chaperone or some other necessary factors. We expect that the opposite experiment (RAGE-transfected A549 cells fused with the non-transfected HEK293 cells) would give us similar results with expression of RAGE protein being dependent on whether the A549 or HEK293 cell phenotypes are recessive or dominant.

Once we know if the A549 phenotype is recessive or dominant we would proceed with studies to identify the factor or factors responsible for the differential expression of canonical RAGE protein in cell lines transfected with the RAGE cDNA. One possible approach involves the use of a rabbit reticulocyte lysate translation system for *in vitro* translation of canonical RAGE mRNA. To establish the system, we will first transcribe canonical RAGE mRNA *in vitro* using a plasmid containing the RAGE cDNA as a template. Then we will translate the mRNA

using the translation system and immunoblot to detect RAGE. After confirming this, we will add A549 and HEK293 cytosol to the translation system. These studies assume that the A549 cell phenotype is dominant. Therefore, we would expect A549 but not HEK293 cytosol to inhibit translation in a dose-dependent manner. Then, we will fractionate cell cytoplasm from those two cell lines and add different fractions from A549 cells (those that cannot make RAGE protein) and from HEK293 cells (those that are able to make RAGE protein) to the translation system and see if RAGE protein is made. Once we identify the inhibiting fraction we should work towards identifying the inhibiting component(s). When we identify the component(s), they should be verified in the translation system if they can inhibit translation when added alone.

If the A549 cell phenotype turns out to be dominant it would imply that those cells express some translation inhibiting factor. A random mutagenesis strategy can be used to screen for this factor using RAGE protein expression as a readout. We will subject RAGE transfected cells to ethyl methanesulfonate, a chemical mutagen (156), and use FACS sorting to select for RAGE protein expressing cells. Alternatively, a panning strategy with adsorbed anti-RAGE antibody and washes of increasing stringency could be also used to isolate mutants that express RAGE (157). If, on the other hand, the HEK293 cells possess the dominant phenotype, the same strategy could be used, only followed by screening for mutants that would permit RAGE protein expression.

One more approach for identifying factors crucial for RAGE protein expression will involve creating a subtraction cDNA library from A549 and HEK293 cells and HEK293 and A549. By doing so we would be able to identify candidate proteins that either inhibit RAGE protein translation or promote RAGE translation in A549 cells. This approach could be used in conjunction with the previous approaches, to help narrow the range of possible translation factors

or other genes that can be tested to reverse the mutant phenotype of cell lines created by method described in the previous paragraph.

Each of these approaches has associated strengths and limitations. The use of reticulocyte lysate to purify factors will identify proteins functionally but we may need to use translation systems made from either HEK293 or A549 cells rather than rabbit reticulocytes. Another possible drawback is that the factor may contain two distinct factors that could be separated during fractionating. Such an occurrence would greatly complicate this method.

The mutagenesis approach is straight forward and isolating mutants using these strategies has been done for a variety of eukaryotic cells (158, 159). The difficulty is identifying the mutated gene. In theory this can be accomplished by introducing an expression cDNA library and isolating cells with a restored phenotype (160).

The plasmid DNA can be isolated by growth in transformed bacteria. Once identified, the sequence of the endogenous cell line gene would be obtained to confirm the presence of a mutation in that gene. Finally, the substitution method will produce a set of cDNA that is expressed in one cell line vs. the other. These would represent candidate genes to rescue mutant phenotypes.

These experiments will help us to understand the mechanisms of RAGE expression and hopefully lead us to elucidating the mechanisms directing organ-specific expression of lung specific genes. This work could have implications for other diseases where errors in pulmonary differentiation are involved including cystic fibrosis and chronic pulmonary fibrosis.

6.1.2 Identifying RAGE isoform mRNA via Northern blot and cDNA library screening

In Section 3.2.2 we discussed RAGE and RAGE-related mRNA transcripts in various tissues and cell lines. These studies could be substantially improved by using RAGE knockout mice as negative controls for mouse organs. We were able to identify pulmonary RAGE isoforms in thyroid, so thyroid tissues should be added to the Northern blot panel. We used human probe to analyze RAGE mRNA from mouse tissues. Ideally, these studies should be repeated using a mouse cRNA probe. We expect thyroid to express the same mRNA transcript as lung and transfected cell lines (1.4 kb). It would be informative to use a probe that corresponds to the amino acids encoding the epitopes recognized by N-16 anti-RAGE antibody. This would presumably allow detection of messages for non-canonical RAGE isoforms that were observed using Western blot. The same experiments should be performed with a cRNA probe spanning the esRAGE intron 9 sequence to identify authentic esRAGE mRNA species. Studies performed by others (45, 106) in order to detect RAGE isoforms, utilized primers known to amplify canonical RAGE. We showed that N-16 and H-300 do not recognize esRAGE on the Western blot, therefore those exons cannot be not included in esRAGE sequence. Hudson et al. (45) cloned and sequenced RAGE isoforms based on the assumption that they included some exons from canonical RAGE. Both groups used a PCR amplification step with RAGE primers and later expressed newly discovered cDNAs in the HEK293 (45) and COS-7 (106) cell lines, permissive for expressing canonical RAGE. Lung cell lines do not express canonical RAGE protein in spite of expressing RAGE cDNA, so it is unclear if real tissues would inhibit expression of the other RAGE isoforms.

Instead, we propose to create a lung cDNA library with any commercially available kit (The SuperScript® Plasmid System, Invitrogen, CA, for example). We will take mRNA and reverse transcribe it with high efficiency RT transcriptase (SuperScript™ II RT for the Invitrogen kit). That would result in complete cDNA sequences that could be screen with N-16 and esRAGE sequences for the possible RAGE isoform candidates. This way we will not limit screening to the mRNA sequences located within canonical RAGE sequence and avoid errors introduced by the PCR amplification step.

Another way to identify protein RAGE isoforms will be to fluorescently label anti-RAGE antibody (or Fab fragments, described in details in section 1.2.1), bind them to the cell line and crosslink the antibody, isolate proteins from plasma membrane and run them on a 2-D gel. We will then visualize fluorescent spots, isolate them then sequence them by mass spectrometry analysis. This has the potential to identify RAGE gene encoded proteins expressed in cell lines.

6.1.3 Utilizing primary type 1 alveolar cell lines from wild-type and RAGE knockout mice to characterize cell line RAGE

We were not able to find a single cell line expressing canonical RAGE. Given that most RAGE signal transduction studies are performed in cell lines that do not express canonical RAGE protein, it seems appropriate to confirm that the bands recognized by N-16 and \square ES are shown to be generated from the RAGE gene. This can be done by growing primary cell lines (161) from different tissues obtained from both wild-type mice and RAGE knockout mice and comparing their RAGE protein expression. We will choose tissues representing different organs, including lung, liver, and intestine with and without transfection with large T antigen to immortalize the cells. We will use cell-specific marker to differentiate specific cell types.

Markers of mature hepatocytes, for instance, include albumin, glucose-6-phosphatase, tyrosine aminotransferase, cytochrome P450-3a, phosphoenolpyruvate carboxykinase and tryptophan 2,3-dioxygenase (162). Caveolin-1 and 2, T1 α , ICAM-1, connexin-43 could serve as markers for the type 1 alveolocytes (163). We expect to lose the expression of canonical RAGE in the cultures from wild-type mice. We also expect to lose all RAGE isoforms in the cell lines derived from the knockout animals. Cells derived from wild-type mice will probably lose their RAGE expression, but will likely express a cell line specific RAGE isoform. Cells grown from the RAGE knockouts will not have canonical RAGE and will not have cell line RAGE. By comparing two cell lines of the same tissue type from wild-type and knockout mice pair-wise on Western blot we will distinguish cell line mouse RAGE isoform(s) and will hopefully be able to obtain primary protein from them and sequence it. This set of experiments will help the field and speed future RAGE research.

6.1.4 Lung and thyroid specific transcription factors could drive canonical RAGE mRNA expression

While RAGE role and significance are studied extensively in different tissues, little is known about tissue-specific RAGE expression and the factors driving it. The question still remains: why lung-derived cell lines (A549 and CaLu-3) are not expressing RAGE mRNA while the lung tissue is the major RAGE-expressing tissue in the body. We propose to investigate lung and thyroid specific transcription factors and determine if they play role in canonical RAGE mRNA transcription.

Thyroid transcription factor 1 (TTF-1) has been shown to be expressed in lung and thyroid as early as 9 days of embryonic development in mice (141). We speculate that TTF-1 could induce canonical RAGE mRNA or protein expression *in vitro*. *In silico* studies of the mouse RAGE promoter confirmed the existence of two TTF-1 binding sites. In addition, TTF-1 is utilized in clinical applications for separating metastatic carcinoma from primary lung cancer (164). Therefore, we plan to transfect TTF-1 and see the effects on RAGE transcription. We know that when we transfect canonical RAGE cDNA into lung-derived cell lines they do not make RAGE protein. Thus, we will co-transfect RAGE and TTF-1 into the lung-derived cell line (A549) and look for RAGE expression. TTF-1 was shown not to be expressed in A549 cells; however other lung cancer cell lines express the protein (153). We are planning to screen other lung cancer cell lines for both RAGE and TTF-1 expression. We could also correlate TTF-1 and RAGE expression in lung and thyroid cell lines.

It is also possible that RAGE expression in the lung is driven by other transcription factors involved in lung morphogenesis. Other than TTF-1, this group includes β -catenin, Forkhead orthologs (FOX), GATA, SOX and ETS family members (165). Two approaches are possible. First, we can obtain expression plasmids of these factors, transfect them into A549 or any other lung-derived cell line together with the canonical RAGE plasmid and look for the canonical RAGE protein expression by Western blot. Second, we could assay those transcription factors in several available to us lung-derived cell lines, comparing it to the expression pattern of RAGE-expressing tissues (lung and thyroid). This way we could determine which factor(s) is permissive to express canonical RAGE.

6.1.5 Determine X-RAGE sequence

We identified a slightly bigger novel lung RAGE isoform which was initially induced in mice by LPS at 1 h *in vivo* and continued to be expressed for at least 48 h. We know that LPS-treated mice did not have an additional transcript on the Northern blot (unpublished observations), therefore x-RAGE should come from the same canonical RAGE transcript. We were able to confirm that it shares some similarities with the ‘canonical’ mouse RAGE with mass spectrometry sequence analysis but did not determine the exact difference. We are planning on continuing this work. First, we are going to repeat the procedure that we did initially, which include injecting mice with 2 mg/ml LPS and harvesting lungs in 24 h. We are going to purify x-RAGE and use methods described in Chapter 3 to sequence it. We would need to extend sequence coverage in comparison with the experiment we did before.

If it does not work we are planning to do an immunoaffinity capture of the mouse lung lysate with N-16 anti-RAGE antibody, fractionate the purified product on the 2D gel and perform Edman degradation coupled with mass spectroscopy. x-RAGE could play a role in the inflammatory response to LPS, or it could still contain pro-peptide in the sequence. Once the modification is established, its significance could be studied further.

6.2 RAGE SIGNALING

6.2.1 RAGE ligand signaling in cell lines

Exposing HMEC-1 cells to the RAGE ligands HMGB1 and S100B decreased and increased MCP-1 steady-state mRNA levels, respectively (135). S100B induced MCP-1 production was blocked by applying an anti-RAGE antibody (N-16). The same antibody was used in a paper previously published by our laboratory showing that it also blocked HMGB1-induced hyperpermeability in CaCo-2 cells (145). This particular antibody (N-16) was also used by other researchers with the similar effects: Ding et al. blocked O_2^- generation by mononuclear phagocytes in diabetes (166) and Bianchi et al. diminished pro-inflammatory effects of S100B in microglial cell line (167). Other antibodies against the N-terminus of RAGE were also successfully used to block RAGE signaling. In our previous studies we were not able to detect canonical RAGE protein in HMEC-1 cells. These cells appeared to express a different RAGE isoform (168). In our hands, HMGB1, a RAGE ligand, did not increase NF- κ B activation and this is important for increased iNOS expression and permeability. We wondered if anti-RAGE antibody was acting through another mechanism than blocking ligand binding to non-canonical RAGE.

When we blocked S100B and HMGB1 signaling in HMEC-1 cells with anti-RAGE antibody we also blocked responses to IL-1 β , which was used as a positive control for MCP1 induction. The question becomes whether N-16 works through RAGE or does it interfere with some signaling events that are shared between RAGE and IL-1 β signaling cascades. To test this possibility we performed a time course with HMEC-1 cells and N-16 antibody, using MCP1 as a readout. It turned out that N-16 anti-RAGE antibody stimulates MCP1 production in HMEC-1

cells as early as 2 h and the response was down-regulated by 24 h. We hypothesize that N-16 antibody could dimerize the non-canonical RAGE expressed in all cell lines and activate it that way. That impacts responses to other stimuli (like IL-1 β) through post-inductional repression.

To test this hypothesis we will use Fab fragments of N-16 antibody. We will digest the antibody with papain, a thiol-endopeptidase, to cleave whole IgG just above the hinge region and to create two separate Fab fragments and one Fc fragment per antibody molecule (kit from Pierce, IL). This way when the Fab fragment binds to RAGE it will not dimerize it. We hypothesize that if we use fragments instead of the whole antibody it will not activate HMEC-1 cells. The correct control will be performed by dimerizing Fab fragments back after they bind the receptor. Anti-goat Fab antibody could be used for this purpose. This will result in cross-linking of non-canonical RAGE which would induce a signal and post-induction repression as predicted.

To confirm that the same thing was happening in other publications including our own (145, 166, 167) we will first use N-16 anti-RAGE antibody in their models and try to block RAGE-dependent responses. If it works we'll try to perform experiments with the Fab fragments with and without cross linking. These experiments will be important for understanding the role of non-canonical RAGE and what steps should be taken to study RAGE signal transduction. It is also important to understand that N-16 blocking antibody does not work through canonical RAGE.

6.2.2 Canonical RAGE signaling in MLS

We established that canonical RAGE is only expressed in lung and thyroid. We also showed that none of our tested cell lines expressed canonical RAGE. Although non-lung cell lines are able to express canonical RAGE protein when transfected, they might not express

lung-specific factors that could be necessary for RAGE signal transduction (Chapter 3 and 168). MLS was the only tested *in vitro* system that permitted canonical RAGE expression in culture. We tested canonical RAGE expression for up to a week after harvest and levels of expression did not change.

We are planning on using MLS to study canonical RAGE ligands and signaling by comparing responses of wild-type and RAGE knockout mice. Preliminary studies showed that MLS from those mice do not respond differently to the known RAGE ligands (AGEs, S100B and HMGB1) but they exhibit weaker responses to IL-1 β and LPS (4.2.5 and 4.2.6). These findings suggest that RAGE might play a role in the amplifying of inflammatory response through secondary signaling components. Therefore we acquired mRNA samples from wild-type and RAGE knockout mice during 24 h time course. Conditions included responses to IL-1 β and LPS, with and without anti-RAGE blocking antibody (N-16). We hypothesize that N-16 will activate MLS from the wild-type mice impairing their respond to IL-1 β and LPS. RAGE knockout mice would not likely be effected by N-16 anti-RAGE antibody. When all the data is processed we can build a model for activation of different genes with and without RAGE.

We are also planning on performing a gene array in the MLS from wild-type and RAGE knockout mice at an early time point (2 h) and find new gene candidates for RAGE signaling. Then we are going to determine their role in inflammation. These genes could be new targets in the diseases that involve RAGE.

7.0 CHAPTER SEVEN - MATERIALS AND METHODS

7.1 REAGENTS

All reagents were purchased from Sigma unless stated otherwise. S100B expression plasmid provided by Dr. Gary S. Shaw (University of Western Ontario, Canada) was expressed in *E. coli* N99/pSS2 and purified as described (169). S100B tested negative for LPS.

7.2 CELL LINES

Human THP-1 (American Type Culture Collection #TIB-202) myeloid cells were maintained in RPMI 1640 supplemented with 10% FBS, 1mM of sodium pyruvate, and 1% penicillin-streptomycin. HMEC-1 cells, a human microvascular endothelial cell line immortalized with SV40 large T antigen, were provided by Dr. Edwin Ades (National Center for Infectious Diseases, Atlanta, Georgia, USA) (144). They were routinely maintained in MCDB 131 medium (Invitrogen Corporation, Carlsbad, CA) supplemented with 10% FBS, 10 ng/ml EGF, 1 µg/ml hydrocortisone, 10 mM L-glutamine, 1% penicillin-streptomycin. Caco-2 human enterocyte-like cells (ATCC #HTB-37) were cultured as described (145). Human A549 lung epithelial cell line was purchased from ATCC (ATCC #CCL-185) and maintained in F-12 Kaighn's medium (Invitrogen) supplemented with 10% FBS, 2 mM L-glutamine and 1% penicillin-streptomycin.

Human HEK 293 embryonic kidney cell line was purchased from ATCC (ATCC #CRL-1573) and maintained in minimal essential medium (Eagle) with 10% FBS, 0.1 mM non-essential amino acids, 1 mM sodium pyruvate and 1% penicillin-streptomycin. Rat type 1 alveolocytes (R3/1) were provided by Dr. Ronald Koslowski of Dresden University of Technology (Dresden, Germany) and maintained as described (163). Mouse cell lines CMT-93 (polyploid carcinoma, ATCC #CCL-223), LA-4 (lung adenoma, ATCC #CCL-196), MES-13 (mesangial cells, ATCC #CRL-1927), NIH 3T3 (fibroblasts, ATCC #CRL-1658), RAW 264.7 (macrophages, ATCC #TIB-71) and Y-1 (adrenal cortex, ATCC #CCL-79) were maintained exactly as described by ATCC. Mouse lung fibroblasts were created by immortalization as described (170).

All cell lines were passed once a week and grown at 37 °C in a humidified incubator maintained with 5% CO₂ and 95% air. C57BL/6 mice were obtained from the Jackson Laboratory (Bar Harbor, Maine). All cell culture lines were routinely tested on a monthly basis for *Mycoplasma* contamination using the Lonza MycoAlert® Mycoplasma Detection Kit (Rockland, ME).

RAW 264.7 mouse macrophage-like cells were plated in 6-well plates and were used the following day. They were stimulated by adding 100 ng/ml *Escherichia coli* LPS (serotype O111:B4) in the presence or absence of graded concentrations of the tested compounds. Nitrite and IL-6 concentrations were measured in 18 h in cell supernatants using commercially available Griess reaction kit (Oxis International, Portland, OR) and commercially available R&D Systems Quantikine Immunoassay Kit for IL-6. Cells were used for the real time reverse transcriptase PCR analysis.

7.3 CELL-BASED ASSAY FOR STUDYING THE RELATIVE PHARMACOLOGY OF THE ANTI-INFLAMMATORY DRUGS

Human astrocytoma cell line (U-373) expresses virtually no intracellular adhesion molecule-1 (ICAM-1, CD54) without pro-inflammatory stimulation (30). When stimulated with the pro-inflammatory stimuli (IL-1 β) 50-60% of the cells start expressing ICAM-1 (CD54). We decided to use this cell line for the cell-based pharmacological assessment of the potential anti-inflammatory drugs because of the simplicity of the assay (fluorescence activated cell sorting (FACS)). This way we were able to utilize endogenous reporter gene instead of the transfected one. First, we stimulated the cells with IL-1 β and used FACS to enrich the cell population for CD54-positive cells. Resulting bulk cell population was found to express CD54 in a higher percentage of cells (70-98%) compared to the parental population. We used the bulk cells as well as clonal cell lines (1-6). Clonal cell lines expressed different degrees of being CD-54-positive. To confirm that ICAM-1 was indeed NF- κ B-dependent gene we used a protease inhibitor N-tosyl-L-phenylalanine chloromethyl ketone (TPCK) to block proteasome activity and this almost completely blocked upregulation of CD54 expression on these cells. The percent of the CD-54 positive cells increased with the IL-1 β concentration used – dose-response curve (Fig. 7). We have used this endogenous NF- κ B reporter system to study the relative efficacy of several compounds that have similar chemical properties to ethyl pyruvate, a promising new candidate compound for treatment of a variety of systemic and localized inflammatory diseases.

7.4 TESTED COMPOUNDS

Tested compounds included ethyl pyruvate (EP), sodium pyruvate (SP), benzoyl formic acid (BF), and p-hydroxyphenylpyruvic acid (pHPP). They were purchased from Sigma-Aldrich Chemical Co. and their molecular structures are presented in Fig. 29.

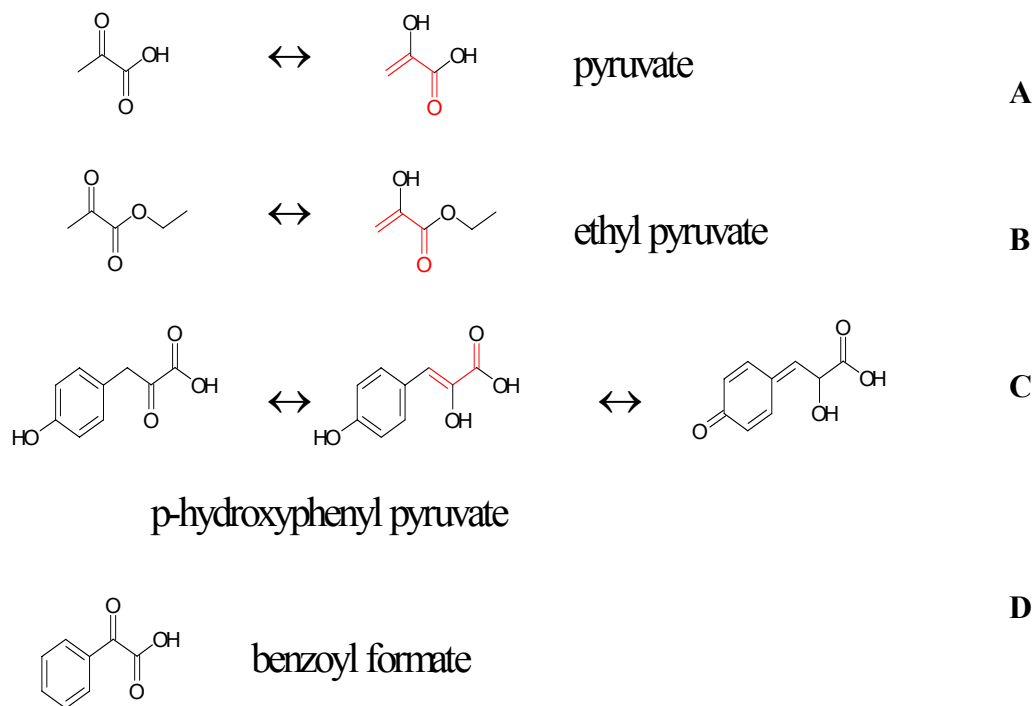


Figure 29. Molecular structure of the enone forming compounds (A,B,C) and one compound that does not isomerize to an enone (D).

Various isomers are shown for some molecules. The enone moiety is shown in red.

7.5 FLOW CYTOMETRY ANALYSIS

U373 astrocytoma clonal cells were cultured in the 6-well plates as described above in the presence or absence of IL-1 β (10 ng/ml) and in either the absence or presence of one of the test compounds. Cells were harvested with 10 mM EDTA in PBS, washed with DMEM and then

incubated either with a FITC-conjugated anti-human CD54 monoclonal antibody or a FITC-conjugated mouse IgG2a isotype control antibody (CALTAG lab., Burlingame, CA). Cells were fixed with 2% paraformaldehyde in PBS and analyzed by flow cytometry.

7.6 PHARMACOLOGIC ANALYSIS USING FACS ANALYSIS

Percent inhibition for each compound was determined by comparing mean channel fluorescence (MCF) of the cells stimulated with IL-1 β with the MCF of the cells which were pretreated with the drug of interest prior to treatment with IL-1 β , according to the formula: % inhibition = (MCF of the sample - MCF of unstimulated cells 1)/(MCF of IL-1 β -treated cells – MCF of unstimulated cells).

7.7 PROTEIN N-GLYCAN REMOVAL

Peptide: N-Glycosidase (PNGase) F (New England BioLabs) was used to remove N-linked glycans from protein according to the manufacturer's instructions. Briefly, we denatured equal amounts of protein (50 μ g) in Glycogen Denaturing Buffer, containing 5% SDS and 0.4 M DTT by heating at 100 °C for 10 m. After cooling the mixture the reaction buffer G7 (0.5 M sodium phosphate, pH 7.5) and 10% NP-40 were added at 1/10 volume each. 500 units of PNGase F were added and samples were incubated for 3 h at 37 °C. Control reactions contained the same buffer without enzyme. Proteins were analyzed using Western blot.

7.8 WESTERN BLOTTING

Equal amounts of total protein extract mixed in $1 \times$ Laemmli buffer were boiled for 5 min and centrifuged for 10 s. The supernatants were electrophoresed on reducing 8% or 10% SDS-polyacrylamide gels. The proteins were electroblotted onto Hybond-P polyvinylidene difluoride membranes (GE Healthcare, Piscataway, NJ) and blocked with Blotto ($1 \times$ Tris-buffered saline, 5% non-fat dry milk, 0.05% Tween-20, and 0.2% NaN_3) for 60 min. The filters were incubated at 4 °C overnight with primary anti-RAGE antibody (H-300 and N-16; (Santa Cruz Biotech, Santa Cruz, CA) or anti-esRAGE (Dr. Takuo Watanabe and Dr. Hiroshi Yamamoto) in fresh blocking buffer, washed 3 times in PBST and incubated with the appropriate secondary antibody. After three washes in PBST the membrane was impregnated with enhanced chemiluminescence substrate (GE Healthcare) and used to expose X-ray film (Blue Ultra Autorad Film, ISC BioExpress, Kaysville, UT).

We routinely run 20 μg of protein per lane for extracts prepared from cell lines, but only use 5 μg of mouse lung protein extract per lane to detect RAGE by Western. However, it was necessary to decrease the concentration of dry milk in the blotting solutions (1.5% vs. 5% final concentration) in order to reproducibly obtain a strong signal on Western analysis when probing cell line extracts. The N-16 antiserum was raised in goats using a peptide representing the amino-terminus of human pulmonary membrane RAGE. Anti-RAGE antibodies tested for recognition of RAGE isoform expression in cell lines included a rabbit polyclonal antibody generated against a fragment of the human pulmonary membrane RAGE isoform including amino acids 1-300 (H-300). Both antibodies were obtained from Santa Cruz Biotech (Santa Cruz, CA). Monoclonal anti-esRAGE antibody was provided by Dr. Takuo Watanabe and Dr.

Hiroshi Yamamoto of Kanazawa University Graduate School of Medical Science (Kanazawa, Japan).

7.9 ANIMAL AND HUMAN TISSUES

Human tissues were obtained postmortem from UPMC Presbyterian Hospital. The research described in this paper involving the use of human beings adheres to the principles of the Declaration of Helsinki and Title 45, U.S. Code of Federal Regulations, Part 46, Protection of Human Subjects, Revised November 13, 2001, effective December 13, 2001.

All study protocols using rats and mice followed the guidelines for the use of experimental animals of the U.S. National Institutes of Health and were approved by the Institutional Animal Care and Use Committee at the University of Pittsburgh. Male Sprague-Dawley rats (Charles River Laboratories, Wilmington, MA), weighing 150 to 250 g, and male C57BL/6J mice (Jackson Laboratories, Bar Harbor, ME) weighing 20–25 g were housed in a temperature-controlled environment with a 12-h light/dark cycle with free access to standard laboratory chow and water. Animals were not fasted prior to the experiments. To induce a systemic inflammatory response, mice were injected intraperitoneally with *E. coli* (strain 0111:B4) LPS, 2 mg/kg dissolved in 0.2 ml of phosphate-buffered saline (PBS). Control animals were injected with the same volume of PBS. Tissues were harvested from animals at the times indicated in the text following intraperitoneal injection with sodium pentobarbital (35 mg/kg). Tissues from RAGE knockout animals were obtained from the laboratory of Dr. Tim Oury at the University of Pittsburgh (32).

7.10 MOUSE LUNG SLICES

Mice were sacrificed by intraperitoneal injection with sodium pentobarbital (35 mg/kg). Lungs were perfused through the heart with the PBS. Lungs were removed using aseptic techniques and placed into PBS solution on ice. McIlwain tissue chopper (Mickle Laboratory Engineering Co. Ltd., United Kingdom) was used to cut the lungs transversely. The slice thickness was chosen to be 0.7 mm which is predicted by Warburg equation: $C_1 = C_0 - A/D * d^2/8$, where C_1 is the pO_2 in the deepest layer of the slice; C_0 is the pO_2 at the surface of the slice; A is oxygen uptake of the slice in ml/min/ml of tissue; D – diffusion coefficient in ml of oxygen/cm²/min; d – slice thickness in cm (171, 172). After being cut the slices were placed into the 10 mm dish filled with PBS and washed with agitation. Then 6 pieces were placed into each well of the 6-well plate. The slices were maintained in the RPMI-1640/Ham's- F12 medium (Lonza Group Ltd., Switzerland) (1:1) supplemented with 10% FBS and 1% penicillin-streptomycin. The tested reagents were applied in 1 h after seeding. The slices were harvested in TRI-Reagent as directed by the manufacturer (Molecular Research Center, Cincinnati, OH) at the time indicated and used for real time PCR. All experiments were performed in triplicate.

7.11 PRIMARY LUNG CELL CULTURE

Mouse lungs were extracted using aseptic techniques and placed in cold PBS on ice. They were cut into pieces with the sterile scalpel in a sterile tissue culture hood and placed in medium containing 1.0 mg/ml protease 14 (Sigma P-5147) plus 10 µg/ml DNase I (Sigma DN-25) in HAMs F12 medium (Invitrogen). The lung pieces were incubated overnight with gentle

agitation. The next morning the cells were spun down at approximately 800 ×g for 5 min and washed 4 times in RPMI-1640/Ham's-F12 (1:1) supplemented with 15% FBS, 10 mM L-glutamine, 1% penicillin-streptomycin. The cells were plated on collagen coated plates (Biocoat Plastics, Becton Dickinson, Framingham, MA) in the same medium. The medium was changed the next day to remove the dead cells.

7.12 NORTHERN BLOT ANALYSIS

Total RNA was isolated from cells and tissues using TRI-Reagent as directed by the manufacturer (Molecular Research Center, Cincinnati, OH). For Northern blot hybridization 2-10 µg of total RNA from each sample was separated on a 1% denaturing agarose gel containing 1% formaldehyde. RNA was transferred onto Hybond-N⁺ positive nylon membrane (GE Healthcare) overnight by capillary blot. The membrane was prehybridized for 30 min-1 h at 68 °C using Ultrahyb (Ambion, Austin, TX). Full-length human RAGE cDNA (GenBank Accession #NM_001136) served as a template to synthesize a complementary RNA probe for hybridization using [³²P]-UTP. The membrane was washed using the standard stringency conditions recommended by the manufacturer (Ambion) then used to expose X-ray film at -80 °C using an intensifying screen.

7.13 PURIFICATION AND MASS SPECTRAL ANALYSIS OF MOUSE LUNG RAGE ISOFORMS

Lungs were prepared from 10 mice 18 h after injection with 2 mg/ml of LPS. Total protein was isolated using RIPA buffer supplemented with 1% CHAPS, which increased RAGE protein yield when tested using Western blot. RAGE was captured on a 19.5 ml DEAE Sepharose CL4B column equilibrated with Buffer A (20 mM Tris, pH 7.5, 50 mM NaCl, 1% CHAPS, and 1 mM DTT). The column was washed with 1.5 column volumes (CV) of buffer A then eluted using 1.5 CV with 18% Buffer B (Buffer A with NaCl increased to 1 M), 1.5 CV of 43% Buffer B, followed by 100% Buffer B. RAGE was detected in different fractions was using Western blotting. Fractions from step two were enriched for pulmonary membrane and X-RAGE isoforms. Fractions were pooled and applied to a 10 ml column of concanavalin A Sepharose at 0.5 ml per h at 4 °C. The first flow through was collected and reapplied to the column before washing to baseline absorbance using 4 CV of Buffer A containing 250 mM NaCl. Proteins were eluted using wash buffer containing 0.5 M α D-methyl mannopyranoside. Buffer was exchanged to 20 mM Tris, pH 8.0, 50 mM NaCl, 0.2% CHAPS, and 1 mM DTT using a 50 ml G25 column. Proteins were captured and concentrated using a 1 ml Mono Q anion exchange column equilibrated with the same buffer. The column was developed using a linear gradient of 20 CV ending with 1 M NaCl in the start buffer. Fractions containing RAGE were pooled and concentrated using ultrafiltration. Samples were resolved on an 8% reducing SDS-PAGE gel which was stained with Coomassie to visualize the bands for excision with a glass micropipette. The gel plugs were digested with trypsin overnight at 37 °C. Eluted peptides were analyzed using a Applied Biosystems MALDI-TOF MS/MS running in reflection mode. The collection window was set to 799 to 4013 *m/z*. The mass spectrum was analyzed using Data Explorer

(Applied Biosystems), and calculated peptide mass to charge ratio was calculated and used to identify peptides using Aldente (173) (<http://www.expasy.org/tools/aldente/>).

7.14 REAL-TIME REVERSE TRANSCRIPTASE-PCR ANALYSIS

Cells were plated in 6-well plates and exposed to various treatments the following day. Cells were harvested in 1 ml of TRI-Reagent as directed by the manufacturer (Molecular Research Center, Cincinnati, OH). Bromochloropropane was used for the extraction. The final RNA pellet was dissolved in nuclease - free water and quantified using a GeneQuant pro UV spectrophotometer (GE Healthcare). Extracted RNA (1 μ g /reaction) was converted to single-stranded cDNA in a 20 μ l reaction using the Reverse Transcriptase System Kit (Promega) as directed by the manufacturer. The mixture was heated to 70 °C for 10 min, maintained at 42 °C for 30 min, and then heated to 95 °C for 5 min using a Gene Amp PCR System 9700 (Applied Biosystems, Foster City, CA). TaqMan Gene Expression Assays for MCP-1, iNOS and 18S RNA (endogenous control) and real-time PCR reagents were from Applied Biosystems (Foster City, CA). Reaction mixtures for PCR were assembled as follows: 10 μ l TaqMan Universal PCR Master Mix, 1 μ l of each Gene Expression Assay mix, 1 μ l cDNA template and 7 μ l of water. PCR reactions were performed in an Applied Biosystems thermocycler 7300 Real Time PCR System by incubating at 50 °C for 2 min, 95 °C for 10 min, 95 °C for 15 s, and 60 °C for 1 min; the two final steps were repeated for 40 cycles. Each sample was assayed in duplicate and the values were averaged. A $\Delta\Delta$ Ct relative quantification method was used to calculate mRNA levels for MCP-1 in the samples. Results were first normalized relative to 18S rRNA expression levels and then to the control (calibrator).

7.15 ANALYSIS OF MOUSE CYTOKINE MRNAS

Mouse lung slices were prepared and treated as described in 5.10. mRNA from mouse lung slices was extracted as described in 5.14. Mouse cytokines were detected using a Luminex™ 100 IS apparatus using the BioSource International Mouse 20-plex Luminex™ beadset. QuantiGene Plex 2.0 assays combine branched DNA (bDNA) signal amplification technology and xMAP® (multi-analyte profiling) beads to enable simultaneous quantification of multiple RNA targets directly from cultured cell or whole blood lysates; fresh, frozen or formalin-fixed, paraffin-embedded (FFPE) tissue homogenates; or purified RNA preparations. Branched DNA technology is a sandwich nucleic acid hybridization assay that provides a unique approach for RNA detection and quantification by amplifying the reporter signal rather than the sequence. By measuring the RNA at the sample source, the assay avoids variations or errors inherent to extraction and amplification of target sequences. The xMAP system, developed by Luminex Corp, combines flow cytometry, fluorescent-dyed microspheres (beads), lasers and digital signal processing to effectively allow multiplexing of up to 100 unique assays within a single sample.

7.16 ELECTROPHORETIC MOBILITY SHIFT ASSAY (EMSA)

The EMSA used to measure DNA-binding activity was carried out using a double stranded oligonucleotide (174). Briefly, the sequence of the double-stranded NF-κB oligonucleotide was as follows: sense, 5'-AGT TGA GGG GACTTT CCC AGG C-3'; antisense,

3'-TCA ACT CCC CTG AAA GGG TCC G-5' (NF- κ B DNA binding consensus sequence is underlined; Promega). The oligonucleotides were end-labeled with γ -[32 P]-ATP (PerkinElmer Life and Analytical Sciences, Boston, MA) using T4 polynucleotide kinase (Promega). Three micrograms of nuclear protein/reaction or 10 μ g of total cellular protein was incubated with radiolabeled NF- κ B probe in band shift buffer (10 mM Tris, pH 7.8, 40 mM KCl, and 1 mM EDTA) in the presence of 2 μ g of poly(dI·dC) for 20 min at room temperature. The binding reaction mixture was electrophoresed on 4% nondenaturing polyacrylamide gels, which were then dried and used to expose Kodak X-omat AR film (Eastman Kodak, Rochester, NY) at 80°C overnight using an intensifying screen.

APPENDIX A

ABBREVIATIONS

ET – ethyl pyruvate

SP – sodium pyruvate

pHPP – para-hydroxyphenyl pyruvate

BF – benzoyl formate

AGE – advanced glycation end-products

HMGB1 – high mobility group box-1

S100B – S100 calcium binding protein B

IL1- β – interleukin 1 β

NF- κ B – nuclear factor-kappa B

RAGE – receptor for advanced glycation end-products

sRAGE – soluble RAGE

CD54 – cluster of differentiation 54, the same as ICAM-1

ICAM-1 – inter-cellular adhesion molecule 1

MCP-1 – monocyte chemoattractant protein 1

APPENDIX B

PUBLICATIONS

B.1 PAPERS

Aneja RK, Tsung A, Sjodin H, **Gefter JV**, Delude RL, Billiar TR, Fink MP (2008) Preconditioning with high mobility group box 1 (HMGB1) induces lipopolysaccharide (LPS) tolerance. *J Leukoc Biol* 84:1326-1334

Gefter JV, Shaufli AL, Fink MP, Delude RL (2009) Comparison of distinct protein isoforms of the receptor for advanced glycation end-products expressed in murine tissues and cell lines. *Cell Tiss Res*, in press.

Gefter JV, Cotoia A, Englert JA, Delude RL. Treatment with p-hydroxyphenylpyruvate without resuscitation extends survival in a rat profound hemorrhagic shock model. (in preparation)

Macias CA, Killeen ME, Arora DS, **Gefter JV**, Sarumi O, Fink MP, Wipf P, and Delude RL. Nitroxyl-gramicidins block MAP kinase activation, NO⁻, HMGB1, and IL-10 release. (in preparation)

B.2 ABSTRACTS

- Macias CA, **Liachenko JV**, Delude RL, Fink MP (2005) Primary rat hepatocytes tolerate prolonged periods of oxygen/glucose deprivation (OGD) without losing viability. Lippincott Williams & Wilkins, pp A35-A35
- Gefter JV**, Shaufel AL, Fink MP, Delude RL (2006) Molecular analysis of receptor for advanced glycation end-products isoforms expressed in tissues and cell lines. Lippincott Williams & Wilkins, pp A29-A29
- Gefter JV**, Fink MP, Delude RL (2008a) Lung-specific isoforms of Receptor for Advanced Glycation End products (RAGE) are distinct from those expressed in other tissues and in cultured cell lines. Federation Amer Soc Exp Biol, pp A12-A12
- Gefter JV**, Fink MP, Delude RL (2008b) Assessment of distinct isoforms of the receptor for advanced glycation end-products expressed in tissues and cell lines. Shock 29:86-87
- Gefter JV**, Fink MP, Delude RL (2008c) RAGE isoforms International Shock Congress - 6th Congress of the International Federation of Shock Societies and 31st Annual Conference on Shock and 7th International Conference on Complexity in Acute Illness. Medimond Cologne, Germany
- Cotoia, A, **Gefter, JV**, Delude, RL (2008d) Treatment with p-hydroxyphenylpyruvate without resuscitation extends survival in a rat profound hemorrhagic shock model. Lippincott Williams & Wilkins, pp A18-A18

APPENDIX C

C.1.1 Gefter JV, Fink MP, Delude RL (2008) RAGE isoforms expressed in tissues and cell lines. International Shock Congress - 6th Congress of the International Federation of Shock Societies and 31st Annual Conference on Shock and 7th International Conference on Complexity in Acute Illness. Medimond Cologne, Germany

C.1.2 Gefter JV, Shaufli AL, Fink MP, Delude (2009) RL Comparison of distinct protein isoforms of the receptor for advanced glycation end-products expressed in murine tissues and cell lines. Cell and Tissue Research

BIBLIOGRAPHY

1. Galli SJ, Tsai M, Piliponsky AM. The development of allergic inflammation. *Nature* 2008;454:445-454.
2. Mantovani A, Allavena P, Sica A, Balkwill F. Cancer-related inflammation. *Nature* 2008;454:436-444.
3. Medzhitov R. Origin and physiological roles of inflammation. *Nature* 2008;454:428-435.
4. Kumar A, Takada Y, Boriek AM, Aggarwal BB. Nuclear factor-kappaB: its role in health and disease. *J Mol Med* 2004;82:434-448.
5. Sen R, Baltimore D. Inducibility of kappa immunoglobulin enhancer-binding protein Nf-kappa B by a posttranslational mechanism. *Cell* 1986;47:921-928.
6. Pahl HL. Activators and target genes of Rel/NF-kappaB transcription factors. *Oncogene* 1999;18:6853-6866.
7. Gilmore TD, Kalaitzidis D, Liang MC, Starczynowski DT. The c-Rel transcription factor and B-cell proliferation: a deal with the devil. *Oncogene* 2004;23:2275-2286.
8. Bowie AG, Moynagh PN, O'Neill LA. Lipid peroxidation is involved in the activation of NF-kappaB by tumor necrosis factor but not interleukin-1 in the human endothelial cell line ECV304. Lack of involvement of H₂O₂ in NF-kappaB activation by either cytokine in both primary and transformed endothelial cells. *J Biol Chem* 1997;272:25941-25950.
9. Alkalay I, Yaron A, Hatzubai A, Orian A, Ciechanover A, Ben-Neriah Y. Stimulation-dependent I kappa B alpha phosphorylation marks the NF-kappa B inhibitor for degradation via the ubiquitin-proteasome pathway. *Proc Natl Acad Sci U S A* 1995;92:10599-10603.
10. Gilmore TD. Introduction to NF-kappaB: players, pathways, perspectives. *Oncogene* 2006;25:6680-6684.
11. Wikipedia. NF-κB. 2009 April 1, 2009. Page last accessed April 24, 2009. Available from: <http://en.wikipedia.org/wiki/NF-%CE%BAB>.
12. Bunger R, Mallet RT, Hartman DA. Pyruvate-enhanced phosphorylation potential and inotropism in normoxic and postischemic isolated working heart. Near-complete prevention of reperfusion contractile failure. *Eur J Biochem* 1989;180:221-233.
13. Cicalese L, Lee K, Schraut W, Watkins S, Borle A, Stanko R. Pyruvate prevents ischemia-reperfusion mucosal injury of rat small intestine. *Am J Surg* 1996;171:97-100; discussion 100-101.
14. Salahudeen AK, Clark EC, Nath KA. Hydrogen peroxide-induced renal injury. A protective role for pyruvate in vitro and in vivo. *J Clin Invest* 1991;88:1886-1893.
15. Fink MP. Ethyl pyruvate. *Curr Opin Anaesthesiol* 2008;21:160-167.
16. Sims CA, Wattanasirichaigoon S, Menconi MJ, Ajami AM, Fink MP. Ringer's ethyl pyruvate solution ameliorates ischemia/reperfusion-induced intestinal mucosal injury in rats. *Crit Care Med* 2001;29:1513-1518.
17. Sappington PL, Fink ME, Yang R, Delude RL, Fink MP. Ethyl pyruvate provides durable protection against inflammation-induced intestinal epithelial barrier dysfunction. *Shock* 2003;20:521-528.
18. Morcillo EJ, Estrela J, Cortijo J. Oxidative stress and pulmonary inflammation: pharmacological intervention with antioxidants. *Pharmacol Res* 1999;40:393-404.
19. Rahman I. Regulation of nuclear factor-kappa B, activator protein-1, and glutathione levels by tumor necrosis factor-alpha and dexamethasone in alveolar epithelial cells. *Biochem Pharmacol* 2000;60:1041-1049.
20. Rahman I, Antonicelli F, MacNee W. Molecular mechanism of the regulation of glutathione synthesis by tumor necrosis factor-alpha and dexamethasone in human alveolar epithelial cells. *J Biol Chem* 1999;274:5088-5096.

21. Brennan P, O'Neill LA. Inhibition of nuclear factor kappaB by direct modification in whole cells--mechanism of action of nordihydroguaiaritic acid, curcumin and thiol modifiers. *Biochem Pharmacol* 1998;55:965-973.
22. Luduena RF, Roach MC, Epstein DL. Interaction of ethacrynic acid with bovine brain tubulin. *Biochem Pharmacol* 1994;47:1677-1681.
23. Xu S, Roychowdhury S, Gaskin F, Epstein DL. Ethacrynic acid inhibition of microtubule assembly in vitro. *Arch Biochem Biophys* 1992;296:462-467.
24. Brennan P, Bowie A, O'Neill LA. The effects of thiol modifiers on the activation of NF kappa B by interleukin-1. *Biochem Soc Trans* 1993;21:390S.
25. Garcia-Pineres AJ, Castro V, Mora G, Schmidt TJ, Strunck E, Pahl HL, Merfort I. Cysteine 38 in p65/NF-kappaB plays a crucial role in DNA binding inhibition by sesquiterpene lactones. *J Biol Chem* 2001;276:39713-39720.
26. Lyss G, Knorre A, Schmidt TJ, Pahl HL, Merfort I. The anti-inflammatory sesquiterpene lactone helenalin inhibits the transcription factor NF-kappaB by directly targeting p65. *J Biol Chem* 1998;273:33508-33516.
27. Schmidt TJ, Lyss G, Pahl HL, Merfort I. Helenanolide type sesquiterpene lactones. Part 5: the role of glutathione addition under physiological conditions. *Bioorg Med Chem* 1999;7:2849-2855.
28. Han Y, Englert JA, Yang R, Delude RL, Fink MP. Ethyl pyruvate inhibits nuclear factor-kappaB-dependent signaling by directly targeting p65. *J Pharmacol Exp Ther* 2005;312:1097-1105.
29. Han Y, Englert JA, Delude RL, Fink MP. Ethacrynic acid inhibits multiple steps in the NF-kappaB signaling pathway. *Shock* 2005;23:45-53.
30. Tapping RI, Orr SL, Lawson EM, Soldau K, Tobias PS. Membrane-anchored forms of lipopolysaccharide (LPS)-binding protein do not mediate cellular responses to LPS independently of CD14. *J Immunol* 1999;162:5483-5489.
31. Orlova VV, Choi EY, Xie C, Chavakis E, Bierhaus A, Ihanus E, Ballantyne CM, Gahmberg CG, Bianchi ME, Nawroth PP, et al. A novel pathway of HMGB1-mediated inflammatory cell recruitment that requires Mac-1-integrin. *Embo J* 2007;26:1129-1139.
32. Chavakis T, Bierhaus A, Al-Fakhri N, Schneider D, Witte S, Linn T, Nagashima M, Morser J, Arnold B, Preissner KT, et al. The pattern recognition receptor (RAGE) is a counterreceptor for leukocyte integrins: a novel pathway for inflammatory cell recruitment. *J Exp Med* 2003;198:1507-1515.
33. Demling N, Ehrhardt C, Kasper M, Laue M, Knels L, Rieber EP. Promotion of cell adherence and spreading: a novel function of RAGE, the highly selective differentiation marker of human alveolar epithelial type I cells. *Cell Tissue Res* 2006;323:475-488.
34. Huttunen HJ, Fages C, Kuja-Panula J, Ridley AJ, Rauvala H. Receptor for advanced glycation end products-binding COOH-terminal motif of amphoterin inhibits invasive migration and metastasis. *Cancer Res* 2002;62:4805-4811.
35. Huttunen HJ, Kuja-Panula J, Sorci G, Agneletti AL, Donato R, Rauvala H. Coregulation of neurite outgrowth and cell survival by amphoterin and S100 proteins through receptor for advanced glycation end products (RAGE) activation. *J Biol Chem* 2000;275:40096-40105.
36. Goova MT, Li J, Kislinger T, Qu W, Lu Y, Bucciarelli LG, Nowygrod S, Wolf BM, Caliste X, Yan SF, et al. Blockade of receptor for advanced glycation end-products restores effective wound healing in diabetic mice. *Am J Pathol* 2001;159:513-525.
37. Schmidt AM, Vianna M, Gerlach M, Brett J, Ryan J, Kao J, Esposito C, Hegarty H, Hurley W, Clauss M, et al. Isolation and characterization of two binding proteins for advanced glycosylation end products from bovine lung which are present on the endothelial cell surface. *J Biol Chem* 1992;267:14987-14997.
38. Yan SD, Chen X, Fu J, Chen M, Zhu H, Roher A, Slattery T, Zhao L, Nagashima M, Morser J, et al. RAGE and amyloid-beta peptide neurotoxicity in Alzheimer's disease. *Nature* 1996;382:685-691.
39. Hofmann MA, Drury S, Fu C, Qu W, Taguchi A, Lu Y, Avila C, Kambham N, Bierhaus A, Nawroth P, et al. RAGE mediates a novel proinflammatory axis: a central cell surface receptor for S100/calgranulin polypeptides. *Cell* 1999;97:889-901.
40. Taguchi A, Blood DC, del Toro G, Canet A, Lee DC, Qu W, Tanji N, Lu Y, Lalla E, Fu C, et al. Blockade of RAGE-amphoterin signalling suppresses tumour growth and metastases. *Nature* 2000;405:354-360.
41. Schmidt AM, Yan SD, Yan SF, Stern DM. The multiligand receptor RAGE as a progression factor amplifying immune and inflammatory responses. *Journal of Clinical Investigation* 2001;108:949-955.

42. Kislinger T, Fu C, Huber B, Qu W, Taguchi A, Du Yan S, Hofmann M, Yan SF, Pischetsrieder M, Stern D, et al. N(epsilon)-(carboxymethyl)lysine adducts of proteins are ligands for receptor for advanced glycation end products that activate cell signaling pathways and modulate gene expression. *J Biol Chem* 1999;274:31740-31749.
43. Bopp C, Bierhaus A, Hofer S, Bouchon A, Nawroth PP, Martin E, Weigand MA. Bench-to-bedside review: The inflammation-perpetuating pattern-recognition receptor RAGE as a therapeutic target in sepsis. *Crit Care* 2008;12:201.
44. Chavakis T, Bierhaus A, Nawroth PP. RAGE (receptor for advanced glycation end products): a central player in the inflammatory response. *Microbes Infect* 2004;6:1219-1225.
45. Hudson BI, Carter AM, Harja E, Kalea AZ, Arriero M, Yang H, Grant PJ, Schmidt AM. Identification, classification, and expression of RAGE gene splice variants. *Faseb J* 2007.
46. Bucciarelli LG, Wendt T, Rong L, Lalla E, Hofmann MA, Goova MT, Taguchi A, Yan SF, Yan SD, Stern DM, et al. RAGE is a multiligand receptor of the immunoglobulin superfamily: implications for homeostasis and chronic disease. *Cell Mol Life Sci* 2002;59:1117-1128.
47. Ramasamy R, Vannucci SJ, Yan SS, Herold K, Yan SF, Schmidt AM. Advanced glycation end products and RAGE: a common thread in aging, diabetes, neurodegeneration, and inflammation. *Glycobiology* 2005;15:16R-28R.
48. Schmidt AM, Vianna M, Gerlach M, Brett J, Ryan J, Kao J, Esposito C, Hegarty H, Hurley W, Clauss M, et al. Isolation and characterization of two binding proteins for advanced glycosylation end products from bovine lung which are present on the endothelial cell surface. *J Biol Chem* 1992;267:14987-14997.
49. Neeper M, Schmidt AM, Brett J, Yan SD, Wang F, Pan YC, Elliston K, Stern D, Shaw A. Cloning and expression of a cell surface receptor for advanced glycosylation end products of proteins. *J Biol Chem* 1992;267:14998-15004.
50. Katsuoka F, Kawakami Y, Arai T, Imuta H, Fujiwara M, Kanma H, Yamashita K. Type II alveolar epithelial cells in lung express receptor for advanced glycation end products (RAGE) gene. *Biochem Biophys Res Commun* 1997;238:512-516.
51. Shirasawa M, Fujiwara N, Hirabayashi S, Ohno H, Iida J, Makita K, Hata Y. Receptor for advanced glycation end-products is a marker of type I lung alveolar cells. *Genes Cells* 2004;9:165-174.
52. Uchida T, Shirasawa M, Ware LB, Kojima K, Hata Y, Makita K, Mednick G, Matthay ZA, Matthay MA. Receptor for advanced glycation end-products is a marker of type I cell injury in acute lung injury. *Am J Respir Crit Care Med* 2006;173:1008-1015.
53. Dahlin K, Mager EM, Allen L, Tigue Z, Goodglick L, Wadehra M, Dobbs L. Identification of genes differentially expressed in rat alveolar type I cells. *Am J Respir Cell Mol Biol* 2004;31:309-316.
54. Fehrenbach H, Kasper M, Tschernig T, Shearman MS, Schuh D, Muller M. Receptor for advanced glycation endproducts (RAGE) exhibits highly differential cellular and subcellular localisation in rat and human lung. *Cell Mol Biol (Noisy-le-grand)* 1998;44:1147-1157.
55. Li J, Schmidt AM. Characterization and functional analysis of the promoter of RAGE, the receptor for advanced glycation end products. *J Biol Chem* 1997;272:16498-16506.
56. Brett J, Schmidt AM, Yan SD, Zou YS, Weidman E, Pinsky D, Nowygrod R, Neeper M, Przysiecki C, Shaw A, et al. Survey of the distribution of a newly characterized receptor for advanced glycation end products in tissues. *Am J Pathol* 1993;143:1699-1712.
57. Lohwasser C, Neureiter D, Weigle B, Kirchner T, Schuppan D. The receptor for advanced glycation end products is highly expressed in the skin and upregulated by advanced glycation end products and tumor necrosis factor-alpha. *J Invest Dermatol* 2006;126:291-299.
58. Murua Escobar H, Meyer B, Richter A, Becker K, Flohr AM, Bullerdiek J, Nolte I. Molecular characterization of the canine HMGB1. *Cytogenetic & Genome Research* 2003;101:33-38.
59. Murua Escobar H, Soller JT, Sterenczak KA, Sperveslage JD, Schlueter C, Burchardt B, Eberle N, Fork M, Nimzyk R, Winkler S, et al. Cloning and characterization of the canine receptor for advanced glycation end products. *Gene* 2006;369:45-52.
60. Englert JM, Hanford LE, Kaminski N, Tobolewski JM, Tan RJ, Fattman CL, Ramsgaard L, Richards TJ, Loutaev I, Nawroth PP, et al. A role for the receptor for advanced glycation end products in idiopathic pulmonary fibrosis. *Am J Pathol* 2008;172:583-591.
61. Hanford LE, Enghild JJ, Valnickova Z, Petersen SV, Schaefer LM, Schaefer TM, Reinhart TA, Oury TD. Purification and characterization of mouse soluble receptor for advanced glycation end products (sRAGE). *J Biol Chem* 2004;279:50019-50024.

62. Simm A, Casselmann C, Schubert A, Hofmann S, Reimann A, Silber RE. Age associated changes of AGE-receptor expression: RAGE upregulation is associated with human heart dysfunction. *Exp Gerontol* 2004;39:407-413.
63. Hanford LE, Fattman CL, Shaefer LM, Enghild JJ, Valnickova Z, Oury TD. Regulation of receptor for advanced glycation end products during bleomycin-induced lung injury. *Am J Respir Cell Mol Biol* 2003;29:S77-81.
64. Hudson BI, Stickland MH, Grant PJ, Futers TS. Characterization of allelic and nucleotide variation between the RAGE gene on chromosome 6 and a homologous pseudogene sequence to its 5' regulatory region on chromosome 3: implications for polymorphic studies in diabetes. *Diabetes* 2001;50:2646-2651.
65. Schmidt AM, Yan SD, Yan SF, Stern DM. The multiligand receptor RAGE as a progression factor amplifying immune and inflammatory responses. *J Clin Invest* 2001;108:949-955.
66. Yan SF, Ramasamy R, Naka Y, Schmidt AM. Glycation, inflammation, and RAGE: a scaffold for the macrovascular complications of diabetes and beyond. *Circ Res* 2003;93:1159-1169.
67. Harashima A, Yamamoto Y, Cheng C, Tsuneyama K, Myint KM, Takeuchi A, Yoshimura K, Li H, Watanabe T, Takasawa S, et al. Identification of mouse orthologue of endogenous secretory receptor for advanced glycation end-products: structure, function and expression. *Biochem J* 2006;396:109-115.
68. Yonekura H, Yamamoto Y, Sakurai S, Petrova RG, Abedin MJ, Li H, Yasui K, Takeuchi M, Makita Z, Takasawa S, et al. Novel splice variants of the receptor for advanced glycation end-products expressed in human vascular endothelial cells and pericytes, and their putative roles in diabetes-induced vascular injury. *Biochemical Journal* 2003;370:1097-1109.
69. Galichet A, Weibel M, Heizmann CW. Calcium-regulated intramembrane proteolysis of the RAGE receptor. *Biochem Biophys Res Commun* 2008.
70. Raucci A, Cugusi S, Antonelli A, Barabino SM, Monti L, Bierhaus A, Reiss K, Saftig P, Bianchi ME. A soluble form of the receptor for advanced glycation endproducts (RAGE) is produced by proteolytic cleavage of the membrane-bound form by the sheddase a disintegrin and metalloprotease 10 (ADAM10). *Faseb J* 2008.
71. Ding Q, Keller JN. Splice variants of the receptor for advanced glycosylation end products (RAGE) in human brain. *Neurosci Lett* 2005;373:67-72.
72. Ding Q, Keller JN. Evaluation of rage isoforms, ligands, and signaling in the brain. *Biochim Biophys Acta* 2005;1746:18-27.
73. Schlueter C, Hauke S, Flohr AM, Rogalla P, Bullerdiek J. Tissue-specific expression patterns of the RAGE receptor and its soluble forms--a result of regulated alternative splicing? *Biochim Biophys Acta* 2003;1630:1-6.
74. Park IH, Yeon SI, Youn JH, Choi JE, Sasaki N, Choi IH, Shin JS. Expression of a novel secreted splice variant of the receptor for advanced glycation end products (RAGE) in human brain astrocytes and peripheral blood mononuclear cells. *Mol Immunol* 2004;40:1203-1211.
75. Malherbe P, Richards JG, Gaillard H, Thompson A, Diener C, Schuler A, Huber G. cDNA cloning of a novel secreted isoform of the human receptor for advanced glycation end products and characterization of cells co-expressing cell-surface scavenger receptors and Swedish mutant amyloid precursor protein. *Brain Res Mol Brain Res* 1999;71:159-170.
76. Hori O, Brett J, Slattery T, Cao R, Zhang J, Chen JX, Nagashima M, Lundh ER, Vijay S, Nitecki D, et al. The receptor for advanced glycation end products (RAGE) is a cellular binding site for amphotericin. Mediation of neurite outgrowth and co-expression of rage and amphotericin in the developing nervous system. *J Biol Chem* 1995;270:25752-25761.
77. Valencia JV, Mone M, Koehne C, Rediske J, Hughes TE. Binding of receptor for advanced glycation end products (RAGE) ligands is not sufficient to induce inflammatory signals: lack of activity of endotoxin-free albumin-derived advanced glycation end products. *Diabetologia* 2004;47:844-852.
78. Valencia JV, Mone M, Zhang J, Weetall M, Buxton FP, Hughes TE. Divergent pathways of gene expression are activated by the RAGE ligands S100b and AGE-BSA. *Diabetes* 2004;53:743-751.
79. Valencia JV, Weldon SC, Quinn D, Kiers GH, DeGroot J, TeKoppele JM, Hughes TE. Advanced glycation end product ligands for the receptor for advanced glycation end products: biochemical characterization and formation kinetics. *Anal Biochem* 2004;324:68-78.
80. Reznikov LL, Waksman J, Azam T, Kim SH, Bufler P, Niwa T, Werman A, Zhang X, Pischetsrieder M, Shaldon S, et al. Effect of advanced glycation end products on endotoxin-induced TNF- α , IL-1 β and IL-8 in human peripheral blood mononuclear cells. *Clin Nephrol* 2004;61:324-336.

81. Cai W, He JC, Zhu L, Lu C, Vlassara H. Advanced glycation end product (AGE) receptor 1 suppresses cell oxidant stress and activation signaling via EGF receptor. *Proc Natl Acad Sci U S A* 2006;103:13801-13806.
82. Lu C, He JC, Cai W, Liu H, Zhu L, Vlassara H. Advanced glycation endproduct (AGE) receptor 1 is a negative regulator of the inflammatory response to AGE in mesangial cells. *Proc Natl Acad Sci U S A* 2004;101:11767-11772.
83. Heizmann CW. The mechanism by which dietary AGEs are a risk to human health is via their interaction with RAGE: arguing against the motion. *Mol Nutr Food Res* 2007;51:1116-1119.
84. Chuyen Van N. Toxicity of the AGEs generated from the Maillard reaction: On the relationship of food-AGEs and biological-AGEs. *Molecular Nutrition & Food Research* 2006;50:1140-1149.
85. Huang JS, Guh JY, Chen HC, Hung WC, Lai YH, Chuang LY. Role of receptor for advanced glycation end-product (RAGE) and the JAK/STAT-signaling pathway in AGE-induced collagen production in NRK-49F cells. *J Cell Biochem* 2001;81:102-113.
86. Yeh CH, Sturgis L, Haidacher J, Zhang XN, Sherwood SJ, Bjercke RJ, Juhasz O, Crow MT, Tilton RG, Denner L. Requirement for p38 and p44/p42 mitogen-activated protein kinases in RAGE-mediated nuclear factor-kappaB transcriptional activation and cytokine secretion. *Diabetes* 2001;50:1495-1504.
87. Yan SD, Schmidt AM, Anderson GM, Zhang J, Brett J, Zou YS, Pinsky D, Stern D. Enhanced cellular oxidant stress by the interaction of advanced glycation end products with their receptors/binding proteins. *J Biol Chem* 1994;269:9889-9897.
88. Ishihara K, Tsutsumi K, Kawane S, Nakajima M, Kasaoka T. The receptor for advanced glycation end-products (RAGE) directly binds to ERK by a D-domain-like docking site. *FEBS Lett* 2003;550:107-113.
89. Nakano N, Fukuhara-Takaki K, Jono T, Nakajou K, Eto N, Horiuchi S, Takeya M, Nagai R. Association of advanced glycation end products with A549 cells, a human pulmonary epithelial cell line, is mediated by a receptor distinct from the scavenger receptor family and RAGE. *J Biochem* 2006;139:821-829.
90. Ohgami N, Nagai R, Ikemoto M, Arai H, Miyazaki A, Hakamata H, Horiuchi S, Nakayama H. CD36, serves as a receptor for advanced glycation endproducts (AGE). *J Diabetes Complications* 2002;16:56-59.
91. Sorci G, Riuzzi F, Agneletti AL, Marchetti C, Donato R. S100B inhibits myogenic differentiation and myotube formation in a RAGE-independent manner. *Molecular & Cellular Biology* 2003;23:4870-4881.
92. Sorci G, Riuzzi F, Agneletti AL, Marchetti C, Donato R. S100B causes apoptosis in a myoblast cell line in a RAGE-independent manner. *Journal of Cellular Physiology* 2004;199:274-283.
93. Liu Y, Dargusch R, Schubert D. Beta amyloid toxicity does not require RAGE protein. *Biochemical & Biophysical Research Communications* 1997;237:37-40.
94. Park JS, Gamboni-Robertson F, He Q, Svetkauskaite D, Kim JY, Strassheim D, Sohn JW, Yamada S, Maruyama I, Banerjee A, et al. High mobility group box 1 protein interacts with multiple Toll-like receptors. *American Journal of Physiology - Cell Physiology* 2006;290:C917-924.
95. Park JS, Svetkauskaite D, He Q, Kim JY, Strassheim D, Ishizaka A, Abraham E. Involvement of toll-like receptors 2 and 4 in cellular activation by high mobility group box 1 protein. *J Biol Chem* 2004;279:7370-7377.
96. Tian J, Avalos AM, Mao SY, Chen B, Senthil K, Wu H, Parroche P, Drabic S, Golenbock D, Sirois C, et al. Toll-like receptor 9-dependent activation by DNA-containing immune complexes is mediated by HMGB1 and RAGE. *Nat Immunol* 2007;8:487-496.
97. van Zoelen MA, van der Poll T. Targeting RAGE in sepsis. *Crit Care* 2008;12:103.
98. Tanaka N, Yonekura H, Yamagishi S, Fujimori H, Yamamoto Y, Yamamoto H. The receptor for advanced glycation end products is induced by the glycation products themselves and tumor necrosis factor-alpha through nuclear factor-kappa B, and by 17beta-estradiol through Sp-1 in human vascular endothelial cells. *J Biol Chem* 2000;275:25781-25790.
99. Schmidt AM, Hori O, Chen JX, Li JF, Crandall J, Zhang J, Cao R, Yan SD, Brett J, Stern D. Advanced glycation endproducts interacting with their endothelial receptor induce expression of vascular cell adhesion molecule-1 (VCAM-1) in cultured human endothelial cells and in mice. A potential mechanism for the accelerated vasculopathy of diabetes. *J Clin Invest* 1995;96:1395-1403.

100. Yan SF, Ramasamy R, Schmidt AM. Mechanisms of disease: advanced glycation end-products and their receptor in inflammation and diabetes complications. *Nat Clin Pract Endocrinol Metab* 2008;4:285-293.
101. Park L, Raman KG, Lee KJ, Lu Y, Ferran LJ, Jr., Chow WS, Stern D, Schmidt AM. Suppression of accelerated diabetic atherosclerosis by the soluble receptor for advanced glycation endproducts. *Nat Med* 1998;4:1025-1031.
102. Wear-Maggitti K, Lee J, Conejero A, Schmidt AM, Grant R, Breitbart A. Use of topical sRAGE in diabetic wounds increases neovascularization and granulation tissue formation. *Ann Plast Surg* 2004;52:519-521; discussion 522.
103. Aleshin A, Ananthkrishnan R, Li Q, Rosario R, Lu Y, Qu W, Song F, Bakr S, Szabolcs M, D'Agati V, et al. RAGE modulates myocardial injury consequent to LAD infarction via impact on JNK and STAT signaling in a murine model. *Am J Physiol Heart Circ Physiol* 2008;294:H1823-1832.
104. Raman KG, Sappington PL, Yang R, Levy RM, Prince JM, Liu S, Watkins SK, Schmidt AM, Billiar TR, Fink MP. The role of RAGE in the pathogenesis of intestinal barrier dysfunction after hemorrhagic shock. *Am J Physiol Gastrointest Liver Physiol* 2006;291:G556-565.
105. Liliensiek B, Weigand MA, Bierhaus A, Nicklas W, Kasper M, Hofer S, Plachky J, Grone HJ, Kurschus FC, Schmidt AM, et al. Receptor for advanced glycation end products (RAGE) regulates sepsis but not the adaptive immune response. *J Clin Invest* 2004;113:1641-1650.
106. Yonekura H, Yamamoto Y, Sakurai S, Petrova RG, Abedin MJ, Li H, Yasui K, Takeuchi M, Makita Z, Takasawa S, et al. Novel splice variants of the receptor for advanced glycation end-products expressed in human vascular endothelial cells and pericytes, and their putative roles in diabetes-induced vascular injury. *Biochem J* 2003;370:1097-1109.
107. Sakurai S, Yamamoto Y, Tamei H, Matsuki H, Obata K, Hui L, Miura J, Osawa M, Uchigata Y, Iwamoto Y, et al. Development of an ELISA for esRAGE and its application to type 1 diabetic patients. *Diabetes Research & Clinical Practice* 2006;73:158-165.
108. Koyama H, Shoji T, Yokoyama H, Motoyama K, Mori K, Fukumoto S, Emoto M, Shoji T, Tamei H, Matsuki H, et al. Plasma level of endogenous secretory RAGE is associated with components of the metabolic syndrome and atherosclerosis. *Arteriosclerosis, Thrombosis & Vascular Biology* 2005;25:2587-2593.
109. Koyama H, Shoji T, Fukumoto S, Shinohara K, Shoji T, Emoto M, Mori K, Tahara H, Ishimura E, Kakiya R, et al. Low circulating endogenous secretory receptor for AGEs predicts cardiovascular mortality in patients with end-stage renal disease. *Arteriosclerosis, Thrombosis & Vascular Biology* 2007;27:147-153.
110. Geroldi D, Falcone C, Emanuele E, D'Angelo A, Calcagnino M, Buzzi MP, Scioli GA, Fogari R. Decreased plasma levels of soluble receptor for advanced glycation end-products in patients with essential hypertension. *J Hypertens* 2005;23:1725-1729.
111. Emanuele E, D'Angelo A, Tomaino C, Binetti G, Ghidoni R, Politi P, Bernardi L, Maletta R, Bruni AC, Geroldi D. Circulating levels of soluble receptor for advanced glycation end products in Alzheimer disease and vascular dementia. *Arch Neurol* 2005;62:1734-1736.
112. Yamagishi S, Adachi H, Nakamura K, Matsui T, Jinnouchi Y, Takenaka K, Takeuchi M, Enomoto M, Furuki K, Hino A, et al. Positive association between serum levels of advanced glycation end products and the soluble form of receptor for advanced glycation end products in nondiabetic subjects. *Metabolism* 2006;55:1227-1231.
113. Tan KC, Shiu SW, Chow WS, Leng L, Bucala R, Betteridge DJ. Association between serum levels of soluble receptor for advanced glycation end products and circulating advanced glycation end products in type 2 diabetes. *Diabetologia* 2006;49:2756-2762.
114. Bopp C, Hofer S, Weitz J, Bierhaus A, Nawroth PP, Martin E, Buchler MW, Weigand MA. sRAGE is Elevated in Septic Patients and Associated with Patients Outcome. *J Surg Res* 2007.
115. Yamagishi S, Imaizumi T. Serum levels of soluble form of receptor for advanced glycation end products (sRAGE) may reflect tissue RAGE expression in diabetes. *Arterioscler Thromb Vasc Biol* 2007;27:e32; author reply e33-34.
116. Nawroth PP, Stern DM. Soluble forms of RAGE: an index of vascular stress? A commentary on "Soluble RAGE in type 2 diabetes: association with oxidative stress". *Free Radic Biol Med* 2007;43:506-510.
117. Griffiths MJ, McAuley DF. RAGE: a biomarker for acute lung injury. *Thorax* 2008;63:1034-1036.

118. Henkel T, Machleidt T, Alkalay I, Kronke M, Ben-Neriah Y, Baeuerle PA. Rapid proteolysis of I kappa B-alpha is necessary for activation of transcription factor NF-kappa B. *Nature* 1993;365:182-185.
119. Uchiyama T, Delude RL, Fink MP. Dose-dependent effects of ethyl pyruvate in mice subjected to mesenteric ischemia and reperfusion. *Intensive Care Med* 2003;29:2050-2058.
120. Yang R, Gallo DJ, Baust JJ, Uchiyama T, Watkins SK, Delude RL, Fink MP. Ethyl pyruvate modulates inflammatory gene expression in mice subjected to hemorrhagic shock. *Am J Physiol Gastrointest Liver Physiol* 2002;283:G212-221.
121. Yang R, Han X, Delude RL, Fink MP. Ethyl pyruvate ameliorates acute alcohol-induced liver injury and inflammation in mice. *J Lab Clin Med* 2003;142:322-331.
122. Yang R, Uchiyama T, Alber SM, Han X, Watkins SK, Delude RL, Fink MP. Ethyl pyruvate ameliorates distant organ injury in a murine model of acute necrotizing pancreatitis. *Crit Care Med* 2004;32:1453-1459.
123. Sappington PL, Cruz RJ, Jr., Harada T, Yang R, Han Y, Englert JA, Ajami AA, Killeen ME, Delude RL, Fink MP. The ethyl pyruvate analogues, diethyl oxalopropionate, 2-acetamidoacrylate, and methyl-2-acetamidoacrylate, exhibit anti-inflammatory properties in vivo and/or in vitro. *Biochem Pharmacol* 2005;70:1579-1592.
124. Brand K. Aerobic glycolysis by proliferating cells: protection against oxidative stress at the expense of energy yield. *J Bioenerg Biomembr* 1997;29:355-364.
125. Brand KA, Hermfisse U. Aerobic glycolysis by proliferating cells: a protective strategy against reactive oxygen species. *Faseb J* 1997;11:388-395.
126. Varma SD, Devamanoharan PS, Ali AH. Prevention of intracellular oxidative stress to lens by pyruvate and its ester. *Free Radic Res* 1998;28:131-135.
127. Song M, Kellum JA, Kaldas H, Fink MP. Evidence that glutathione depletion is a mechanism responsible for the anti-inflammatory effects of ethyl pyruvate in cultured lipopolysaccharide-stimulated RAW 264.7 cells. *J Pharmacol Exp Ther* 2004;308:307-316.
128. Tawadrous ZS, Delude RL, Fink MP. Resuscitation from hemorrhagic shock with Ringer's ethyl pyruvate solution improves survival and ameliorates intestinal mucosal hyperpermeability in rats. *Shock* 2002;17:473-477.
129. Barrett T, Troup DB, Wilhite SE, Ledoux P, Rudnev D, Evangelista C, Kim IF, Soboleva A, Tomashevsky M, Edgar R. NCBI GEO: mining tens of millions of expression profiles--database and tools update. *Nucleic Acids Res* 2007;35:D760-765.
130. Constien R, Forde A, Liliensiek B, Grone HJ, Nawroth P, Hammerling G, Arnold B. Characterization of a novel EGFP reporter mouse to monitor Cre recombination as demonstrated by a Tie2 Cre mouse line. *Genesis* 2001;30:36-44.
131. Schwenk F, Baron U, Rajewsky K. A cre-transgenic mouse strain for the ubiquitous deletion of loxP-flanked gene segments including deletion in germ cells. *Nucleic Acids Res* 1995;23:5080-5081.
132. Bierhaus A, Haslbeck KM, Humpert PM, Liliensiek B, Dehmer T, Morcos M, Sayed AA, Andrassy M, Schiekofler S, Schneider JG, et al. Loss of pain perception in diabetes is dependent on a receptor of the immunoglobulin superfamily. *J Clin Invest* 2004;114:1741-1751.
133. Zill H, Gunther R, Erbersdobler HF, Folsch UR, Faist V. RAGE expression and AGE-induced MAP kinase activation in Caco-2 cells. *Biochem Biophys Res Commun* 2001;288:1108-1111.
134. Thet LA, Law DJ. Changes in cell number and lung morphology during early postpneumectomy lung growth. *J Appl Physiol* 1984;56:975-978.
135. Geffter JV, Fink MP, Delude RL. RAGE isoforms 31st Annual Conference on Shock and 7th International Conference on Complexity in Acute Illness. Cologne, Germany: Medimond 2008.
136. Shenberger JS, Myers JL, Zimmer SG, Powell RJ, Barchowsky A. Hyperoxia alters the expression and phosphorylation of multiple factors regulating translation initiation. *Am J Physiol Lung Cell Mol Physiol* 2005;288:L442-449.
137. Hellqvist M, Mahlapuu M, Samuelsson L, Enerback S, Carlsson P. Differential activation of lung-specific genes by two forkhead proteins, FREAC-1 and FREAC-2. *J Biol Chem* 1996;271:4482-4490.
138. Cheng C, Tsuneyama K, Kominami R, Shinohara H, Sakurai S, Yonekura H, Watanabe T, Takano Y, Yamamoto H, Yamamoto Y. Expression profiling of endogenous secretory receptor for advanced glycation end products in human organs. *Mod Pathol* 2005;18:1385-1396.
139. Sakurai S, Yamamoto Y, Tamei H, Matsuki H, Obata K, Hui L, Miura J, Osawa M, Uchigata Y, Iwamoto Y, et al. Development of an ELISA for esRAGE and its application to type 1 diabetic patients. *Diabetes Res Clin Pract* 2006;73:158-165.

140. Srikrishna G, Huttunen HJ, Johansson L, Weigle B, Yamaguchi Y, Rauvala H, Freeze HH. N - Glycans on the receptor for advanced glycation end products influence amphotericin binding and neurite outgrowth. *J Neurochem* 2002;80:998-1008.
141. Cardoso WV, Lu J. Regulation of early lung morphogenesis: questions, facts and controversies. *Development* 2006;133:1611-1624.
142. Minoo P, Su G, Drum H, Bringas P, Kimura S. Defects in tracheoesophageal and lung morphogenesis in Nkx2.1(-/-) mouse embryos. *Dev Biol* 1999;209:60-71.
143. Yuan B, Li C, Kimura S, Engelhardt RT, Smith BR, Minoo P. Inhibition of distal lung morphogenesis in Nkx2.1(-/-) embryos. *Dev Dyn* 2000;217:180-190.
144. Ades EW, Candal FJ, Swerlick RA, George VG, Summers S, Bosse DC, Lawley TJ. HMEC-1: establishment of an immortalized human microvascular endothelial cell line. *J Invest Dermatol* 1992;99:683-690.
145. Sappington PL, Yang R, Yang H, Tracey KJ, Delude RL, Fink MP. HMGB1 B box increases the permeability of Caco-2 enterocytic monolayers and impairs intestinal barrier function in mice. *Gastroenterology* 2002;123:790-802.
146. Uchida M, Fukazawa T, Yamazaki Y, Hashimoto H, Miyamoto Y. A modified fast (4 day) 96-well plate Caco-2 permeability assay. *J Pharmacol Toxicol Methods* 2009;59:39-43.
147. Warboys CM, Toh HB, Fraser PA. Role of NADPH oxidase in retinal microvascular permeability increase by RAGE activation. *Invest Ophthalmol Vis Sci* 2009;50:1319-1328.
148. Cataldegirmen G, Zeng S, Feirt N, Ippagunta N, Dun H, Qu W, Lu Y, Rong LL, Hofmann MA, Kislinger T, et al. RAGE limits regeneration after massive liver injury by coordinated suppression of TNF-alpha and NF-kappaB. *J Exp Med* 2005;201:473-484.
149. Gebhardt C, Riehl A, Durchdewald M, Nemeth J, Furstenberger G, Muller-Decker K, Enk A, Arnold B, Bierhaus A, Nawroth PP, et al. RAGE signaling sustains inflammation and promotes tumor development. *J Exp Med* 2008;205:275-285.
150. Liliensiek B, Weigand MA, Bierhaus A, Nicklas W, Kasper M, Hofer S, Plachky J, Grone HJ, Kurschus FC, Schmidt AM, et al. Receptor for advanced glycation end products (RAGE) regulates sepsis but not the adaptive immune response. *Journal of Clinical Investigation* 2004;113:1641-1650.
151. Lutterloh EC, Opal SM. Antibodies against RAGE in sepsis and inflammation: implications for therapy. *Expert Opin Pharmacother* 2007;8:1193-1196.
152. Bingle CD. Thyroid transcription factor-1. *Int J Biochem Cell Biol* 1997;29:1471-1473.
153. Fujita J, Ohtsuki Y, Bandoh S, Ueda Y, Kubo A, Tojo Y, Yamaji Y, Ishida T. Expression of thyroid transcription factor-1 in 16 human lung cancer cell lines. *Lung Cancer* 2003;39:31-36.
154. Behm-Ansmant I, Rehwinkel J, Izaurralde E. MicroRNAs silence gene expression by repressing protein expression and/or by promoting mRNA decay. *Cold Spring Harb Symp Quant Biol* 2006;71:523-530.
155. Palakurthi SS, Fluckiger R, Aktas H, Changolkar AK, Shahsafaei A, Harneit S, Kilic E, Halperin JA. Inhibition of translation initiation mediates the anticancer effect of the n-3 polyunsaturated fatty acid eicosapentaenoic acid. *Cancer Res* 2000;60:2919-2925.
156. Nagan N, Hajra AK, Das AK, Moser HW, Moser A, Lazarow P, Purdue PE, Zoeller RA. A fibroblast cell line defective in alkyl-dihydroxyacetone phosphate synthase: a novel defect in plasmalogen biosynthesis. *Proc Natl Acad Sci U S A* 1997;94:4475-4480.
157. Laffly E, Pelat T, Cedrone F, Blesa S, Bedouelle H, Thullier P. Improvement of an antibody neutralizing the anthrax toxin by simultaneous mutagenesis of its six hypervariable loops. *J Mol Biol* 2008;378:1094-1103.
158. Baker EK, Tozer EC, Pfaff M, Shattil SJ, Loftus JC, Ginsberg MH. A genetic analysis of integrin function: Glanzmann thrombasthenia in vitro. *Proc Natl Acad Sci U S A* 1997;94:1973-1978.
159. Morris SM, Domon OE, McGarrity LJ, Kodell RL, Casciano DA. Flow cytometric evaluation of cell-cycle progression in ethyl methanesulfonate and methyl methanesulfonate-exposed P3 cells: relationship to the induction of sister-chromatid exchanges and cellular toxicity. *Environ Mol Mutagen* 1991;18:139-149.
160. Seed B, Aruffo A. Molecular cloning of the CD2 antigen, the T-cell erythrocyte receptor, by a rapid immunoselection procedure. *Proc Natl Acad Sci U S A* 1987;84:3365-3369.
161. Dobbs LG, Gonzalez R, Matthay MA, Carter EP, Allen L, Verkman AS. Highly water-permeable type I alveolar epithelial cells confer high water permeability between the airspace and vasculature in rat lung. *Proc Natl Acad Sci U S A* 1998;95:2991-2996.

162. Kheolamai P, Dickson AJ. Liver-enriched transcription factors are critical for the expression of hepatocyte marker genes in mES-derived hepatocyte-lineage cells. *BMC Mol Biol* 2009;10:35.
163. Koslowski R, Barth K, Augstein A, Tschernig T, Bargsten G, Aufderheide M, Kasper M. A new rat type I-like alveolar epithelial cell line R3/1: bleomycin effects on caveolin expression. *Histochem Cell Biol* 2004;121:509-519.
164. Chang YL, Lee YC, Liao WY, Wu CT. The utility and limitation of thyroid transcription factor-1 protein in primary and metastatic pulmonary neoplasms. *Lung Cancer* 2004;44:149-157.
165. Maeda Y, Dave V, Whitsett JA. Transcriptional control of lung morphogenesis. *Physiol Rev* 2007;87:219-244.
166. Ding Y, Kantarci A, Hasturk H, Trackman PC, Malabanan A, Van Dyke TE. Activation of RAGE induces elevated O₂- generation by mononuclear phagocytes in diabetes. *J Leukoc Biol* 2007;81:520-527.
167. Bianchi R, Giambanco I, Donato R. S100B/RAGE-dependent activation of microglia via NF-kappaB and AP-1 Co-regulation of COX-2 expression by S100B, IL-1beta and TNF-alpha. *Neurobiol Aging* 2008.
168. Geffer JV, Shaufel AL, Fink MP, Delude RL. Comparison of distinct protein isoforms of the receptor for advanced glycation end-products expressed in murine tissues and cell lines. *Cell Tissue Res* 2009;337:79-89.
169. Smith SP, Barber KR, Dunn SD, Shaw GS. Structural influence of cation binding to recombinant human brain S100b: evidence for calcium-induced exposure of a hydrophobic surface. *Biochemistry* 1996;35:8805-8814.
170. Wang ZQ, Auer B, Stingl L, Berghammer H, Haidacher D, Schweiger M, Wagner EF. Mice lacking ADPRT and poly(ADP-ribosyl)ation develop normally but are susceptible to skin disease. *Genes Dev* 1995;9:509-520.
171. Freeman BA, O'Neil JJ. Tissue slices in the study of lung metabolism and toxicology. *Environ Health Perspect* 1984;56:51-60.
172. Talcott RE, Shu H, Wei ET. Dissociation of microsomal oxygen reduction and lipid peroxidation with the electron acceptors, paraquat and menadione. *Biochem Pharmacol* 1979;28:665-671.
173. Tuloup M, Hernandez C, Coro I, Hoogland C, Binz P-A, Appel RD. Protein Identification and Analysis Tools on the ExpASY Server. In: Walker JM, editor. *The Proteomics Protocols Handbook*. Totowa, NJ: Humana Press;2005.
174. Delude RL, Fenton MJ, Savedra R, Jr., Perera PY, Vogel SN, Thieringer R, Golenbock DT. CD14-mediated translocation of nuclear factor-kappa B induced by lipopolysaccharide does not require tyrosine kinase activity. *J Biol Chem* 1994;269:22253-22260.